The innate immune response against RNA viruses in bat cell lines

Ronald Tarigan

Laboratory of Animal Morphology
Department of Animal Sciences
Graduate School of Bioagricultural Sciences
Nagoya University

September, 2020

Table of Contents

List of abbreviations:

AQP1 - Aquaporin-1
BHK-21 - Baby hamster kidney-21
COVID19 – Coronavirus disease 2019
CPE - Cytopathic effect
DMEM - Dulbecco's modified eagle medium
Dpi - Days post infection
EMCV - Encephalomyocarditis virus
FBS - Fetal bovine serum
GAPDH - Glyceraldehyde-3-phosphate
HEK293T - Human embryonic kidney 293T
IFN - Interferon
IKKε - Inhibitor of nuclear factor kappa-beta kinase subunit epsilon
IRF3 - IFN regulatory factor 3
IRF7 - IFN regulatory factor 7
ISGs - Interferon-stimulated genes
JAK - Janus kinase
JEV - Japanese encephalitis virus
LGP2 - Laboratory of genetics and physiology 2
MAVS - Mitochondrial antiviral signaling protein
MERS-CoV - Middle East respiratory syndrome coronaviruses
MDA5 - Melanoma differentiation associated protein 5
MOI- multiplicity of infection
MUC-1 - Mucin-1
NF-κβ - Nuclear factor kappa-light-chain-enhancer of activated B cells
NS1 – Non-structural protein 1
ORF - Open reading frame
PKR - Protein kinase R
PRRs - Pattern recognition receptors
PRV - Pteropine orthoreovirus
RIG-I - Retinoic acid-inducible gene I
RLRs - RIG-I-like receptors
RNaseL - Ribonuclease L
SARS - Severe acute respiratory syndrome
STAT - Signal transducer and activator of transcription
TBK1 - TANK-binding kinase 1
TLRs - Toll-like receptors
TNF-α -Tumor necrosis factor alpha
TRIF - TIR-domain-containing adapter-inducing interferon-β
UTR - Untranslated region
VSV - Vesicular stomatitis virus
WHO - World Health Organization
WNV- West Nile virus

General Introduction

In the last two decades, bats have attracted attention for their role as reservoirs of viruses. Some of the biggest outbreak of emerging infectious diseases, such as SARS-CoV outbreak in 2003 – 2004, ebola virus outbreak in 2014 – 2015, the recent Nipah virus outbreak in 2018, and the current COVID19 pandemic have been suspected to be originated from bats [1–4]. Bats are also believed to be the natural host of other highly pathogenic viruses, such as Marburg virus [5], MERS-CoV [3], and Hendra virus [6]. Many novel viral sequences have been identified in bats, now a total of 5,629 viral genome sequences from 24 virus families have been detected in bats and most of them (88.8%) are RNA viruses [7]. This high viral diversity in bats can cause serious problems for public health.

In the past, the circulation of the bat-borne virus must have been restricted inside the bat habitats. However, human activities allow the viruses to enter the human population. Reduction of bat habitats by deforestation for agriculture and animal breeding could attract the migration of bats to the human settlement for food supply and can trigger the emergence of bat-borne viruses in the human population. In addition, the development of global transportation can accelerate the human to human transmission of bat-borne viruses and possibly cause an outbreak or pandemic in the future. *"Initially, new infectious diseases could spread only as fast and far as people could walk, then as fast and far as horses could gallop and ships could sail"*—Arno Karlen [8].

In contrast to the high viral diversity in bats, there have been few report of illness or deaths of wild bats caused by viruses that have spread to human and domestic mammals with high virulence, except Australian bat lyssavirus, the closely related rabies virus [9–11]. Experimental infection of some highly pathogenic, such as Marburg virus, Nipah virus, and MERS-CoV in bats showed that the viral replication was present at a

low level without developing little clinical symptom that were observed in susceptible hosts [12–14]. These findings attract many scientists to elucidate how "unique" or "special" bats are so that bats can host viruses without developing significant diseases. The first hypothesis is that the lack of clinical symptoms after viral infection in bats is related to bats as the only mammals capable of sustainable flight.

During flight, the body temperature in bats can rise above 40^{o}C, that reaches the range of core temperatures typical of fever in domestic mammals. This high body temperature consequently will increase metabolic rate and production of reactive oxygen species (ROS) in bats [9]. Fever is one of the general signs of infection in domestic mammals and becomes an integral part of host defense by activating innate and adaptive immune response [15]. High body temperature generated by flight might arm bats to control viral infection. To minimize the effect of oxidative stress generated by flight, heat shock proteins (HSPs), a chaperone that are produced by heat stress, is highly expressed in bats [16].

Another hypothesis is that bats have a more robust innate immune response against viruses than other mammals that enable them to prevent a high level of viral replication in the early stage of infection [17]. Unique immune system in pteropoid bats is in their IFNs system that is constitutively active without the presence of viruses [18]. During RNA virus infection, the innate immune response is initiated by viral RNA recognition by pattern recognition receptors (PRRs) that rapidly induce interferons (IFNs) production. The IFNs response is one of the first and very important line of defense against viral infection and is responsible for the activation of adaptive immune system for long-last protection against recurrent infection [19]. The author speculates that bat

cells express a higher amount of antiviral proteins than other mammals that can limit viral replication and cause limited diseases in bats.

The author hypothesizes that bats can control viral infection by their innate immune response, especially IFNs response. This hypothesis is introducing the research questions of the present thesis:

(1) How does the innate immune response protect bats from RNA virus infection? In Chapter 1, the author compared the resistance against several RNA viruses (EMCV, JEV, and PRV) between several bats and other mammalian cell lines; and compared the expression of some immune genes as candidates of anti-viral factor. Our study demonstrated that most bat cell lines are resistant against EMCV, JEV, and PRV infection with a limited viral replication and a higher expression IFNs in bat cell lines.

(2) How are the IFNs stimulated in bat cell lines after RNA virus infection? In Chapter 2, the author performed knockdown of PRRs in bat cell lines to confirm the role of PRRs to stimulate IFNs expression in bat cells.

Overall, the present thesis provides some information about how bat cells can control viral replication through IFNs response. The thesis also raises several questions that will allow other researchers to develop future plans to improve our understanding of bats-viruses interaction to prevent the outbreak of bat-borne viruses.

Chapter 1: **Comparison of viability and immune genes expression between bat and non-bat cell lines**

Introduction

Several RNA viruses, such as encephalomyocarditis virus (EMCV), Japanese encephalitis virus (JEV), and pteropine orthoreovirus (PRV) that have previously been detected or isolated from bats [20–24], are used as the model of bats - viruses interaction. EMCV, a potential omnipresent zoonotic agent, has a broad host range with rodents as its natural reservoir [25]. In humans, EMCV has been isolated from serum obtained from two febrile patients in Peru with urinary tract infection [26] and clinical symptoms consistent with those observed in mice and hamster [27, 28]. As yet, there has been no report of EMCV isolation from bats, however the eastern bent-wing bat (*Miniopterus fuliginosus*) is supposed to be one of the natural hosts of EMCV due to the detection of a genome fragment of the virus in the bat's fecal guano [20].

The Japanese encephalitis virus is a mosquito-transmitted flavivirus with humans as the definitive hosts and pigs as the amplification hosts [29]. JEV is the main cause of human encephalitis in Asia [30], approximately 20-30% of JE cases are fatal and 30-50% of survivors have significant neurologic sequelae [31]. JEV has been isolated from multiple species of fruit and insectivorous bats in Asia [21, 22]. The author used some cell lines derived from those species of bats, such as Leschenault's rousette (*Rousettus leschenaultii*), flying foxes (*Pteropus* sp), the eastern bent-wing bats (*Miniopterus fuliginosus*), and horseshoe bats (*Rhinolophus* sp).

The pteropine orthoreovirus is a bat-origin zoonotic virus that has been isolated from multiple fruit bats in South-east Asia [23, 24, 32], Australia [33], and China [34]. Virus spillover from bats to humans might already occurred, based on viral isolation from peoples living near the bat roosts in Malaysia [35]; and serological studies in Malaysia [36], Vietnam [37], and Singapore [38]. Imported cases of PRV have been reported in

Japan [39] and Hong Kong [40] from patients with acute respiratory syndrome who had traveled to Bali, Indonesia without any fatal case. Notably, the virulence of PRV may be altered by the appearance of reassortant of PRV because of its segmented genome like influenza virus [41].

Some bats have different innate immune system than other mammals, called "always on" interferon system. The constitutive expression of interferon-alpha (IFN-α) genes [18] and broad tissue distribution of interferon regulatory factor 7 (IRF7) and type III IFN receptors allowed a constitutive expression of IFN-stimulated genes (ISGs) in the black flying foxes (*Pteropus alecto*). The antiviral effector, 2-5A–dependent endoribonuclease, RNaseL which was not IFN-inducible in human is highly induced by IFNs in *P.alecto* [42]. The STAT1 (signal transducer and activator of transcription) protein was constitutively phosphorylated in primary kidney cell from the Jamaican fruit bats (*Artibeus jamaicensis*) [43]. However, there might be a high species dependency of bats in their innate immune system. Similar to human and mice, the constitutive IFN- α expression was absent in another mega bat, Egyptian fruit bats (*Rousettus aegyptiacus*) and a microbat, Daubenton's bats (*Myotis daubentonii*) [44, 45]. In addition, a limited viral-mediated inflammatory response occurred in bats [46, 47], while the same viral infection in human is associated with excessive inflammation pathology caused by a massive cytokines activation [25, 48].

Innate immune response is initiated through recognition of viral pathogens by the pattern recognition receptors (PRRs). The main double-stranded RNA (dsRNA) virus-sensing PRRs are toll-like receptors-3 (TLR3), which are expressed in endosomes and retinoic acid-inducible gene-I-like receptors (RLRs), which are expressed in the cytoplasm. The members of RLRs are retinoic acid-inducible gene-I (RIG-I), melanoma

differentiation associated protein 5 (MDA5), and laboratory of genetics and physiology 2 (LGP2) [49]. TLRs and RLRs activation by RNA viruses will activate downstream adaptor proteins, such as TIR-domain-containing adapter-inducing interferon-β (TRIF) and mitochondrial antiviral signaling protein (MAVS). These adaptor proteins will activate cellular kinases for phosphorylation of IFN regulatory factor 3 and 7 (IRF3 and IRF7) and NFκβ to initiate production of IFNs and pro-inflammatory cytokines. The IFNs then bind with IFNs receptors in infected neighboring cells to activate the JAK-STAT signaling pathway to induce expression of ISGs for antiviral response (Figure 1-1).

The outcome of viral infection depends on the ability of virus to counteract the host immune system and the ability of host immune system to inhibit viral replication [45]. As the first line of defense against RNA viruses, TLR3, RIG-I, and MDA5 signaling is critical for IFNs production and susceptibility against EMCV, JEV, and PRV infection in human and murine cells [50–55]. However, viruses also developed strategies to antagonize IFNs response to promote viral replication. EMCV can antagonize multiple stages in IFNs pathway, such as by interacting with MDA5 protein [56], RIG-I protein degradation [57], and disruption of TBK1-IKKε-IRF3 complex [58]. JEV is also reported to antagonize the production of IFN-β and ISGs by the NS1 protein of JEV [59]. Other closely related flavivirus with JEV, West Nile virus (WNV) can antagonize IFNs production by targeting RIG-I and MDA5 [60]. Other reovirus, mammalian orthoreovirus can antagonize IFNs by disruption of interferon regulatory factor-9 (IRF9) to repress interferon-stimulated genes (ISGs) expression, and prevent activation of antiviral effector protein, the IFN-induced double-stranded RNA-dependent protein kinase (PKR) [61].

As the possible natural hosts of EMCV, JEV, and PRV, bats might control replication of EMCV, JEV, and PRV because of their special innate immune response.

However, there is limited information available about the innate immune response against those viruses in bats. Bats might use IFNs as the antiviral response [62] or using other unidentified mechanisms, not via IFN response [63] to control EMCV, JEV, and PRV infection. In this study, the author investigated the innate immune response against EMCV, JEV, and PRV using several bat and non-bat cell lines as model of bats-viruses interaction.

Materials and Methods

Cells and viruses

BHK-21 (Syrian hamster, *Mesocricetus auratus*, kidney), HEK293T (human, kidney), FBKT1 (Ryukyu flying fox, *Pteropus dasymallus*, kidney), DEMKT1 (Leschenault's rousette, *Rousettus leschenaultii*, kidney), BKT1 (Greater horseshoe bat, *Rhinolophus ferrumequinum*, kidney), and YUBFKT1 (Eastern bent-wing bats, *Miniopterus fuliginosus*, kidney) cell lines were maintained in Dulbecco's modified eagle medium (DMEM; Nissui, Tokyo, Japan) supplemented with 10% fetal bovine serum (FBS; HyClone, Logan, USA), 2% L-Glutamine (Sigma, Milwaukee, Wisconsin, USA), 0.14% Sodium hydrogen carbonate ($NaHCO_3$; Sigma, Milwaukee, USA), and penicillin-streptomycin (Meiji, Tokyo, Japan) at final concentration of 100 U/mL (penicillin) and 0.1 μg/mL (streptomycin). The bat kidney cell lines were established as previously described [64, 65] and were derived from proximal epithelial tubules cells based on the presence or absence of Aquaporin-1 (AQP1) and Mucin-1 (MUC-1), specific markers for proximal and distal epithelial cells, respectively (Figure 1-2). Partial DNA sequence of AQP1 and MUC-1 from all cell lines can be found in Figure 1-3, and 1-4; and Table 1-1.

The viruses used in this study, the encephalomyocarditis virus (EMCV, NIID-NU1), the Japanese encephalitis virus (JEV, JEV/sw/Chiba/88/2002), and the pteropine orthoreovirus (PRV, Garut-50) were previously isolated from swine for JEV [66] and large flying fox (*Pteropus vampyrus*) for PRV. Both EMCV and JEV were propagated in BHK-21 cells, while the PRV was propagated in Vero 9013 cells (JCRB number; JCRB9013).

Molecular identification of EMCV

Viral genomic RNA and DNA were extracted from supernatant of infected cell culture using High Pure Viral Nucleic Acid Kit (Roche, Basel, Switzerland) and were subjected to first strand cDNA synthesis using ReverTra Ace (Toyobo, Osaka, Japan). RNA region corresponding to the whole ORF of EMCV was amplified using a set of degenerate EMCV-specific primers (Table 1-3). The primers were designed based on ORF of EMCV strains available from GenBank nucleotide database using the Primer3 plus software (https://primer3plus.com). Oligo dT-anchor primers were used as reverse primers to synthesize the first strand during cDNA synthesis, which was used as the template for amplification of 3′-UTR. PCR products were extracted using QIAquick gel extraction kit (Qiagen, Hilden, Germany) and subjected to direct sequencing. Sequence assembly was carried out using the SeqMan program included in the DNASTAR software package (Madison, USA). Phylogenetic analysis was performed using the full ORF sequence of identified EMCV by the neighbor-joining (NJ) method in the MEGA7 software package.

Plaque assay for viral titration

The viruses were serially diluted in DMEM medium containing 2% FBS and were inoculated to ~ 900,000 BHK-21 cells in 6-well plates. The viruses were allowed to adsorb for 2 hours then suspension of 2.4% agarose in DMEM medium containing 2% FBS was overlaid on the monolayers (SeaPlaque, Lonza, Rockland, ME, USA) in DMEM with 2% FBS medium was added to the monolayers. After 30 minutes incubation at room temperature, the plates were incubated at 37°C and 5% CO_2. After 1 day for EMCV, 2

days for PRV, and 3 days for JEV, 1 ml of 10% formaldehyde was added per well and incubated for 2 hours at room temperature. Then the wells were washed with PBS (pH 7.2) to remove the gel, and cells were stained with 0.5% crystal violet for 1 min. The excess stain was washed off with PBS (pH 7.2), air-dried, and the number of plaques were counted.

Virus infection

The cells were seeded at a concentration of 1×10^5 cells/well in DMEM medium containing 10% FBS in a 12-well plate to obtain 80% confluency in 24 hours. The viral infection was carried out in a biosafety level 2 laboratory. The cells were infected with EMCV and JEV at a multiplicity of infection (MOI) of 1.0, and a MOI of 0.1 for PRV. The viruses were allowed to adsorb into the cells for 2 hours in DMEM medium containing 2% FBS. The inoculum was removed, the cells were rinsed twice with DMEM medium containing 2% FBS to remove the residual inoculum, and then fresh DMEM medium containing 2% FBS was added.

Cell growth analysis

The cells were seeded at a concentration of 5×10^4 cells/well in a 24-well plate and were infected with EMCV and JEV at MOI of 1.0 and 0.01; and with PRV at MOI of 0.1 and 0.001. Both mock (not infected) and viruses-infected cells were washed with PBS (pH 7.2) and were harvested using 0.25% Trypsin-EDTA at 1 – 7 days post infection (dpi) (Gibco, Ontario, Canada). Assessment of cell growth (cell viability and total live cell numbers) was carried out by trypan blue dye exclusion test. Cell suspensions were mixed with an equal volume of 0.4% trypan blue solution (Chroma-Gesellschaft Schmid,

Stuttgart, Germany). Unstained or live cells and stained or died cells were counted using an automated cell counter (model R1, Olympus, Tokyo, Japan).

Quantitative Real-time PCR

RNA extraction was performed using ISOGEN II (Nippon Gene, Japan) and RNA cleanup were performed using RNeasy Mini kit (QIAGEN, Hilden, Germany). First strand cDNA synthesis was carried out using SuperScript IV First-Strand Synthesis System (Invitrogen, Carlsbad, USA).

The expression levels of TLR3, RIG-I, MDA5, TNF-α, IFN-β, IFN-λ_1, and Glyceraldehyde-3-phosphate (GAPDH, housekeeping gene) in mock (without viral infection), EMCV, JEV, and PRV-infected cells were determined by qRT-PCR. The primer sequences are listed in Table 1-2 and were designed based on partial sequences of TLR3, RIG-I, and MDA5 that previously have been determined (Figure 1-5, 1-6, and 1-7). Roche LightCycler 96 system was used in conjunction with Thunderbird SYBR qPCR Mix (Toyobo, Osaka, Japan) as per the manufacturer's instructions. For qRT-PCR, after the pre-denaturation step (95ºC, 60 seconds), three-step cycling for 40 cycles was performed at 95ºC/60 s, 55ºC/30 s, and 72ºC/30 s. The melting curve analysis was performed at 95ºC/10 s, 60ºC/60 s, and 97ºC/1 s to generate the dissociation curve. mRNA expression level is expressed as reciprocal of ΔCt (the PCR cycle at which the product is measurable and normalized to Ct for GAPDH).

For comparative quantitative analysis of viral genome titers, absolute quantification was performed i.e. a known number of PCR-amplified fragments was 10-fold serially diluted and used to generate standard curves. The exact number of copies of EMCV, JEV, and PRV genes was calculated using the standard curve.

Knockdown of TNF-α in HEK293T

Phosphorothioate antisense RNA oligonucleotide (s-oligo) against human TNF-α were synthesized at FASMAC Co., Ltd., Kanagawa, Japan. The sequence of s-oligo used in this study were as follows: 5'-GGCGUGGAGCUGAGAGAUA-3'[67]. HEK293T were transfected with the antisense RNA oligonucleotides (120 pmol) using polyethylenimine [68]. The knockdown was verified by measuring the expression level of TNF-α by qRT-PCR. The knockdown cells were then infected with EMCV at a MOI of 1.0 and PRV at a MOI of 0.1. RNA extraction and first strand cDNA synthesis using 500 ng of total RNA were performed at 12 hours post infection. The viral genome titers of EMCV and PRV in cells knocked down for TNF-α and cells without gene knockdown were determined by qRT-PCR. The cell growth (live cell numbers and cell viability) were measured using trypan blue dye exclusion test.

Statistical Analysis

Data were presented as the mean ± S.D. Differences between means were analyzed by Student's t-test or one-way analysis of variance (ANOVA) and followed by Tukey HSD test, with $p < 0.01$ is considered statistically significant.

Results

Sequence comparison and phylogenetic analysis of EMCV

Genome sequence of EMCV isolate, identified as EMCV strain NIID-NU1, which has 7,263 nucleotides (nt) in length with a partial 5′-UTR of 254 nt, a 3′-UTR of 130 nt, and an ORF of 6,879 nt was determined (GenBank accession number LC508268, NIID-NU1 strain). The deduced amino acid sequence of the encoding region revealed that the ORF encodes for a polyprotein of 2,292 amino acids with no insertions or deletions, coding for 12 proteins (Protein L, VP4, VP3, VP2, VP1, 2A, 2B, 2C, 3A, 3B 3C, and 3D). Pairwise comparison of the nucleotide sequences was performed to examine the degree of sequence identity between the sequence of NIID-NU1 strain and sequences of 18 EMCV reference strains obtained from GenBank nucleotide database (Table 1-3). Phylogenetic analysis of the ORF sequence showed that all EMCV strains could be divided into two main groups (groups 1A and 1B) (Figure 1-8). The isolated EMCV NIID-NU1 strain shared the highest sequence similarity (99.49-99.77%) with EMCV strains of the group 1A. However, it shared a lower identity with EMCV strains of group 1B (82.35-82.54%) (Table 1-4). EMCV NIID-NU1 strain was clustered into group 1A and most closely related to EMCV GS01 and PV21 strains, which were isolated from pigs. Most of the EMCV strains from group 1A were isolated from pigs, except EMCV C15 and Ruckert (EMC-R) strains that were isolated from dogs and chimpanzees, respectively.

Viral replication in bat and non-bat cell lines

Most of bat cell lines showed a different viral replication levels than non-bat cell lines. Three bat cell lines (BKT1, DEMKT1, and YUBFKT1) showed a significantly

lower viral replication of EMCV, JEV, and PRV than non-bat cell lines (HEK293T and BHK-21). One bat cell line (FBKT1) showed a higher viral replication than other bat cell lines but the viral replication of EMCV and PRV was lower than non-bat cell lines.

The total destruction cytopathic effect (CPE) after EMCV infection with MOI of 1.0 and 0.01 was observed in non-bat cell lines (BHK-21 and HEK293T) at 1 dpi. The total destruction CPE was also observed in FBKT1 at 1 dpi with MOI of 1.0 and at 2 dpi with MOI of 0.01, whereas the other bat cell lines (DEMKT1, BKT1, and YUBFKT1) showed a more delayed CPE. In BKT1, the total destruction CPE appeared at 4 and 5 dpi for MOI of 1.0 and 0.01, respectively. Remarkably, in YUBFKT1 and DEMKT1, the CPE was delayed to 7 dpi for MOI of 1.0 and 0.01 without total destruction CPE was observed (Figure 1-10). The cell growth of non-bat cell lines and FBKT1 rapidly decreased within 1 – 2 dpi (Figure 1-11a–c) while the cell growth in two bat cell lines (DEMKT1 and YUBFKT1) declined slowly with a higher total live cell numbers than other cell lines until 7 dpi (Figure 1-11e –f).

In JEV-infected non-bat cell lines and FBKT1, CPE appeared earlier than in other bat cell lines. The total destruction CPE was observed at 3 dpi in FBKT1 and HEK293T, and at 4 dpi in BHK-21 for MOI of 1.0, and at 4 dpi in FBKT1 and BHK-21, and 5 dpi in HEK293T for MOI of 0.01. Other bat cell lines (DEMKT1, BKT1, and YUBFKT1) showed a more delayed CPE at 7 dpi for MOI of 1.0 and 0.01, but total destruction CPE was not observed (Figure 1-12). The cell growth of non-bat cell lines and FBKT1 was rapidly decrease within 2 – 4 dpi (Figure 1-13a–c) while the cell growth in three bat cell lines (BKT1, DEMKT1 and YUBFKT1) declined slowly with a higher total live cell numbers than other cell lines until 7 dpi (Figure 1-13d –f).

The syncytial CPE after PRV infection with MOI of 0.1 and 0.001 was observed in non-bat cell lines (BHK-21 and HEK293T) at 1 dpi. The syncytial CPE was also observed in FBKT1 at 2 dpi with MOI of 0.1 and at 3 dpi with MOI of 0.001. No syncytial formation was observed in other bat cells (BKT1, DEMKT1, YUBFKT1) after PRV infection. After PRV infection with MOI of 0.1, the subtotal destruction CPE was observed at 4 dpi in BKT1 and at 5 dpi in DEMKT1 and YUBFKT1. The subtotal destruction CPE appearance was delayed to 7 dpi after PRV infection with MOI of 0.01 in BKT1, DEMKT1, and YUBFKT1 (Figure 1-14). The cell growth was rapidly decreased at 1-2 dpi in non-bat cell lines (HEK293T and BHK-21) and FBKT1 (Figure 1-15a–c). However, the significant decrease of cell growth in other bat cell lines (BKT1, DEMKT1, and YUBFKT1) was observed at 4 – 5 dpi (Figure 1-15d–f).

The basal expression level of Pattern Recognition Receptors and IFN-β

The basal expression level of PRRs (TLR3, RIG-I, and MDA5) and IFNs (β and λ_1) in bat cell lines was measured. Almost all bat cell lines had a higher basal expression level of TLR3, RIG-I, and MDA5 than other mammalian cell lines (Figure 1-16a). Among the bat cell lines, BKT1 and YUBFKT1 had the highest basal expression level of TLR3 and RIG-I. In contrast, FBKT1 had the lowest basal expression level of TLR3 and RIG-I among bat cell lines and had an expression level of RIG-I comparable to other mammalian cell lines. The basal expression of MDA5 was comparable among all bat cell lines. The pattern of basal expression level of IFNs was different than that of PRRs. Only one bat cell line (YUBFKT1) had a significantly higher basal expression level of IFN-β (Figure 1-16b) and IFN-λ_1 (Figure 1-16c) than human cell line, while other bat cell lines did not show any difference in the expression level of IFN-β and IFN- λ_1 (Fig. 1-156–c). The

basal expression level of IFN-β and IFN-λ_1 in BHK-21 could not be measured because BHK-21 cell line is known to be deficient in IFN-α and -β production [69] and IFN-λ_1 is a pseudogene in rodents [70]. The basal expression level of IFN-λ_1 also could not be measured in two bat cell lines (BKT1 and DEMKT1).

PRRs and IFNs expression level with viral-infected cell lines

After EMCV infection, it was observed that all bat cell lines with low replication level of EMCV (BKT1, DEMKT1, and YUBFKT1) showed an up-regulation of TLR3, RIG-I, and MDA5 (Figure 1-17). RIG-I and MDA5 were highly up-regulated, especially in BKT1 and DEMKT1 (Figure 1-17b–c), whereas TLR3 was also up-regulated in those cell lines with a fold change lower than that of RIG-I and MDA5 (Figure 1-17a). In the cell lines with high EMCV replication level (BHK-21, HEK293T, and FBKT1), down-regulation of all PRRs in BHK-21 (Figure 1-17a–c) and RIG-I in FBKT1 (Figure 1-17b) was observed. Conversely, RIG-I and MDA5 were up-regulated in HEK293T but their expression level was still lower than that in the bat cell lines.

Expression profile of IFNs was different from that of PRRs. IFN-β was highly up-regulated in BKT1 and DEMKT1, and also in HEK293T but with a lower fold change. Surprisingly, IFN-β and IFN-λ_1 was not up-regulated in YUBFKT1 that showed resistance against EMCV infection (Figure 1-18a–b).

Similar to EMCV infection, JEV infection also resulted in a higher expression level of PRRs in bat cell lines with a lower JEV replication level (DEMKT1, BKT1, and YUBFKT1) (Figure 1-17a–c). However, JEV infection showed a different pattern of expression profile than EMCV infection wherein only RIG-I and MDA5 were up-regulated in DEMKT1 and YUBFKT1 (Figure 1-17b–c). The MDA5 was up-regulated

in other cell lines too (Figure 1-17c) but TLR3 and RIG-I were down-regulated in FBKT1 cells (Figure 1-17a–b). Moreover, no change in expression level of TLR3 and RIG-I was observed in BKT1 and HEK293T (Figure 1-17a–b). All PRRs were up-regulated in BHK-21 but their expression level was lower than that in bat cell lines that showed resistance against JEV infection.

The cell lines with a lower JEV replication level showed a different IFNs expression profile than other cells. The BKT1, DEMKT1, and YUBFKT1 showed a higher expression level of IFN-β, while the cell lines with high JEV replication level (FBKT1 and BHK-21) showed no change in IFN-β expression (Figure 1-18a). IFN-$\lambda_1$was highly up-regulated in YUBFKT1, and also in FBKT1 but with a lower fold change (Figure 1-18b).

After PRV infection, it was observed that all bat cell lines with a low replication level of PRV (BKT1, DEMKT1, and YUBFKT1) showed an up-regulation of RIG-I, and MDA5. RIG-I and MDA5 were highly up-regulated, especially in BKT1 and YUBFKT1 (Figure 1-17b–c), whereas TLR3 was only up-regulated in YUBFKT1 (Figure 1-17a). In the cell lines with high PRV replication level (BHK-21, HEK293T, and FBKT1), down-regulation of RIG-I and MDA5 was observed in BHK-21 (Figure 1-17b–c) Conversely, lower up-regulation of TLR3 in HEK293T (Figure 1-17a) and MDA5 in HEK293T and FBKT1 (Figure 1-17c) was observed but their expression level was still lower than that in the bat cell lines.

IFN-β was highly up-regulated in BKT1 and YUBFKT1, and also in HEK293T but with a lower fold change. Surprisingly, IFN-β was not up-regulated in DEMKT1 that showed lower PRV replication (Figure 1-18a). IFN-λ_1 was up-regulated in YUBFKT1

that had lower PRV replication. In contrast, other cell lines with higher PRV replication (FBKT1 and HEK293T) also showed up-regulation of IFN-λ_1 (Figure 1-18b).

TNF-α expression level with viral-infected cell lines and knockdown of TNF-α in HEK293T cell lines.

Infection of all viruses, especially EMCV and PRV caused a high up-regulation of TNF-α, a pro-inflammatory cytokine in HEK293T. In contrast, all viral infection did not cause up-regulation of TNF-α in bat cell lines, except limited increase of TNF-α in BKT1 and DEMKT1 after EMCV infection and FBKT1 after PRV infection (Figure 1-19).

Knockdown of TNF-α was performed in HEK293T using antisense RNA oligonucleotide to determine the role of TNF-α in supporting viral replication. The knockdown was confirmed by qRT-PCR in which the expression level of TNF-α was significantly reduced in HEK293T (Figure 1-20a). The knockdown of TNF-α reduced the viral genome titer of EMCV and PRV but the viral genome titer was not significantly different (Figure 1-20b). The infection of EMCV and PRV to the cells knocked down for TNF-α caused a similar CPE without significant difference of live cell numbers than cells without knockdown of TNF-α at 12 hours post infection (Figure 1-21a–b).

Discussion

EMCV infection in several primary cells and cell lines derived from human and hamster clearly demonstrates their susceptibility to EMCV [25, 71, 72]. In this study, EMCV infection in non-bat mammalian cell lines (BHK-21 and HEK293T) resulted in a massive cell death at 1-day post infection. EMCV is a lytic virus that causes necrotic cell

death within 7 to 10 hours post infection in BHK-21 cells [25]. In this study, the bat cell lines derived from Leschenault's rousette (DEMKT1), the greater horseshoe bats (BKT1), and the eastern-bent wing bats (YUBFKT1) showed resistance against EMCV infection while massive cell death was observed in bat cell line derived from Ryukyu flying foxes (FBKT1). To our knowledge, this is the first report on resistance against EMCV in bat cell line since the lung cell line derived from Mexican free-tailed bats, *Tadarida brasiliensis* (Tb1.Lu) did not show resistance against EMCV infection [73].

JEV can propagate in many different human and hamster cell lines and shows a complete CPE within 4-5 dpi [74]. The appearance of CPE in JEV-infected cell lines is more delayed compared to that in EMCV-infected cell lines because JEV appears to trigger apoptosis at a rather late stage of infection in order to achieve efficient propagation [75, 76]. The resistance against JEV infection has been reported in Tb1.Lu cell line and primary kidney cells derived from Leschenault's rousette (*Rousettus leschenaultii*), which did not develop CPE until 7 dpi [77]. Similar to EMCV infection, the resistance against JEV infection was most notable in DEMKT1, BKT1, and YUBFKT1, while FBKT1 showed susceptibility in this study. Leschenault's rousette (*Rousettus leschenaultii*), the eastern-bent wing bats (*Miniopterus fuliginosus*), and the greater horseshoe bats (*Rhinolophus ferrumequinum*) might be the natural hosts of JEV because JEV isolation and anti-JEV antibodies detection have been reported from those bats [21, 78]. JEV infection in bat cell line derived from Ryukyu flying foxes (FBKT1) had a different result than experimental infection to other flying fox, the black flying fox (*Pteropus alecto*). Experimental JEV infection to *P.alecto* only led to a low-level viremia without any significant clinical symptoms [79]. The susceptibility of FBKT1 against JEV

indicates the Ryukyu flying foxes might have a different antiviral response than other flying foxes.

PRV is capable to infect and replicate in several mammalian cell lines derived from human, rodents, and non-human primates; and induce syncytia formation within 1 day post infection [23, 24, 34, 80]. The absence of syncytia formation as characteristic of fusogenic orthoreovirus in three bat cell lines (BKT1, DEMKT1, and YUBFKT1) suggests that those bat cell lines are resistant against PRV. This is the first report on resistance against PRV in bat cell lines since kidney cell line derived from the black flying foxes (*Pteropus alecto*) was susceptible to PRV [54].

In this study, DEMKT1, YUBFKT1, and BKT1 showed a limited CPE, a lower replication level of EMCV, JEV, and PRV with a higher basal expression level of PRRs than other cell lines. PRRs, the first line of defense against invading pathogens, induce IFNs expression to enter the antiviral state. The high basal expression level of PRRs (TLR3, RIG-I, and MDA5) has been observed in several bats species, including Leschenault's rousette (*Rousettus leschenaultii*) [81], the intermediate horseshoe bats (*Rhinolophus affinis*) [82], and the common vampire bats (*Desmodus rotundus*) [83]. In embryonic cells and splenocytes from *R.sinicus*, IFN-β expression was induced to a significantly higher level than that in mouse cells after poly(I:C) transfection and vesicular stomatitis virus (VSV) infection [82]. Similar expression patterns of TLR3, RIG-I, and MDA5 after infection with EMCV, JEV, and PRV have been recognized in three bat kidney cell lines used in this study (BKT1, DEMKT1, and YUBFKT1); hence, the high basal expression level of PRRs in the above three species of bats enables quick elimination of EMCV, JEV, and PRV through stimulation of IFNs production. Conversely, the FBKT1 showed a low basal expression of PRRs. This is consistent with

previous study wherein the expression level of TLR3, RIG-I, and MDA5 in other flying fox (*P.alecto*) kidney was very low compared to that in other tissues [84, 85]; however, the kidneys of other bats (*R.leschenaultii* and *R.sinicus*) had an expression level of TLR3, RIG-I and MDA5 comparable to other tissues [81, 82]. There seems to be high species dependency of bats in innate immune system [83].

After EMCV and PRV infection, the expression of RIG-I and MDA5 in DEMKT1, BKT1, and YUBFKT1 was highly up-regulated, which possibly led to up-regulation of IFN-β to reach antiviral state, and consequently resulted in a limited EMCV replication. Inability of FBKT1 and HEK293T to limit EMCV and PRV replication might be due to their inability to increase the expression of PRRs and IFNs as high as those in DEMKT1, BKT1, and YUBFKT1. Surprisingly, high induction of IFNs was absent in YUBFKT1 after EMCV infection and DEMKT1 after PRV infection. YUBFKT1 had a high basal expression level of IFNs before infection. The basal IFNs expression is important for predisposing cells to antiviral response, which includes amplification of virus-induced IFNs production through triggering of the positive-feedback loop [86]. Absence of EMCV-induced IFNs production in YUBFKT1 might be due to an early suppression of EMCV replication by IFNs produced initially, which diminished the EMCV-induced IFNs production. Nevertheless, there is a probability that eastern-bent wing bats use an antiviral pathway other than IFNs for controlling EMCV replication.

Similar to other flaviviruses, JEV also antagonizes IFNs production to evade antiviral immunity and benefit viral replication [59]. The West Nile virus (WNV) inhibits type I IFNs production through suppression of RIG-I and MDA5 [60]. The suppression of RIG-I and TLR3 observed in FBKT1 should have caused limited increase in IFNs production. In contrast, JEV failed to suppress the PRRs in BKT1, DEMKT1, and

YUBFKT1. The expression of RIG-I and MDA5 was up-regulated in DEMKT1 and YUBFKT1, and should have caused increased expression of IFNs leading to a limited replication of JEV in BKT1, DEMKT1, and YUBFKT1.

In this study, limited excessive inflammation might occurred in bat cell lines after EMCV, JEV, and PRV infection because of the limited increased of TNF-α. The limited increased of TNF-α have been reported in bat cell line derived from the big brown bats (*Eptesicus fuscus*) after MERS-CoV infection [62] and it is caused by the presence of functional c-Rel binding site in the promoter region of TNF-α [47]. c-Rel is a NF-κβ family member that act as transcriptional repressor of proinflammatory genes [87]. In contrast, strong inflammatory response might occur in HEK293T because of the high up-regulation of TNF-α, especially after EMCV and PRV infection. Previous studies showed that EMCV, JEV, and orthoreovirus infection to several cell lines derived from human and rodents caused a high increase of TNF-α [25, 88, 89]. The role of TNF-α in the pathogenesis of EMCV and PRV cannot be elucidated because of no significant viral genome titers and cell growth between cells knocked down for TNF-α and cells without gene knockdown. Inhibition of NFκβ, the regulator of pro-inflammatory cytokines also did not have any significant effect on EMCV replication even though increased the survival rate in mice [90].

In conclusion, most of the bat cell lines had a different innate immune response than non-bat cell lines against EMCV, JEV, and PRV infection. Most of the bat cell lines had a higher expression of pattern recognition higher IFNs response in most bat cell lines might be responsible for antiviral response against EMCV, JEV, and PRV in most bat cell lines. In addition, the limited viral-mediated inflammation might occur in all bat cell lines because of a limited increased of pro-inflammatory cytokine (TNF-α). This

special innate immune response might explain the asymptomatic viral infection of EMCV, JEV, and PRV in bats.

Figures and Tables

Figure 1-1

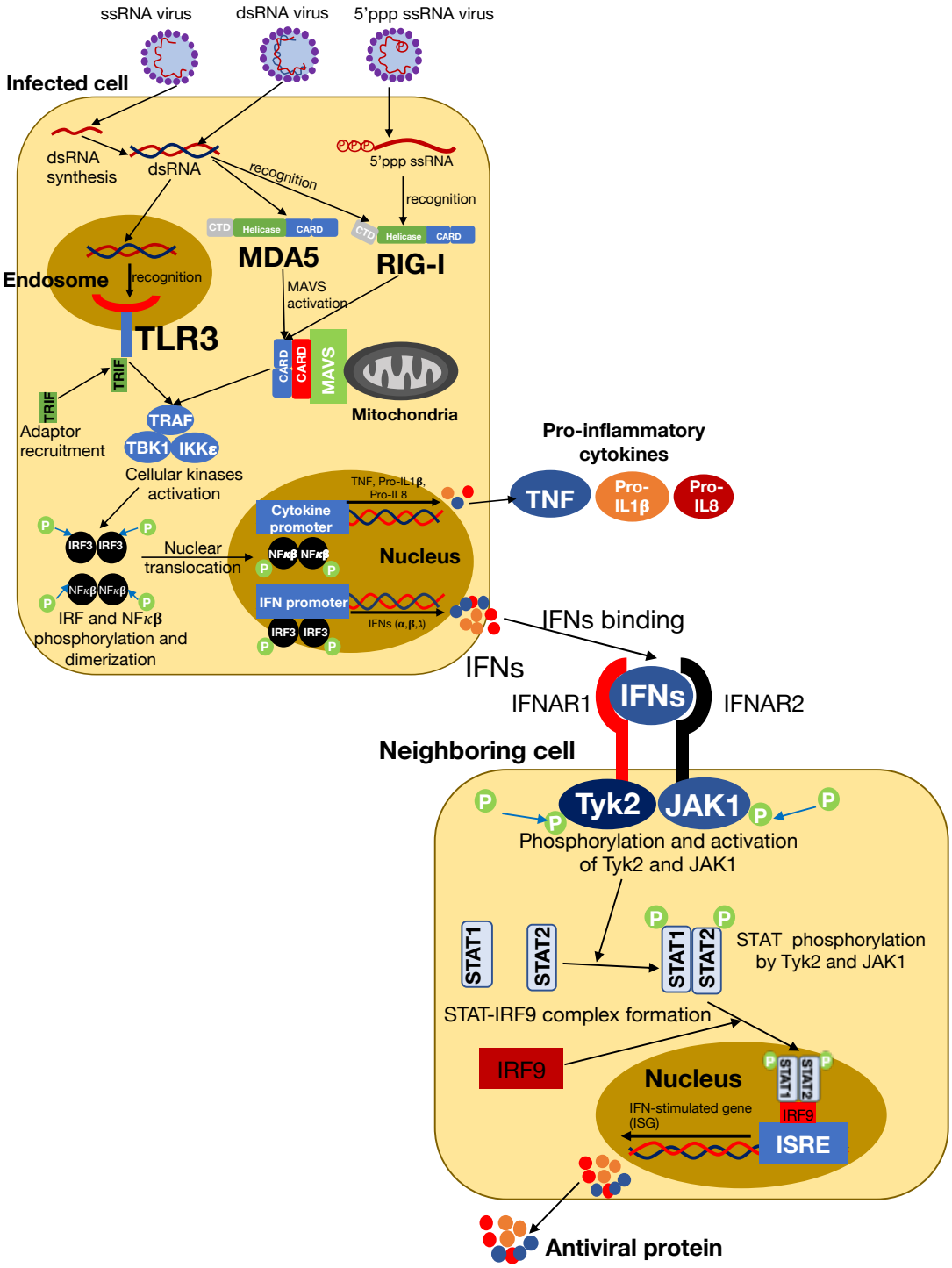

Continue…

Continued…

Innate immune response against RNA virus infection. The illustration is the signaling cascade of innate immune response compiled from domestic mammals. Question marks (?) showed pathways that have not been characterized or identified in bats. *TRIF*: TIR-domain-containing adapter-inducing interferon-β, *TRAF*: Tumor necrosis factor receptor-associated factor, *TBK1*: TANK-binding kinase 1, *IKK-ε*: Inhibitor of nuclear kappa beta kinase subunit epsilon, *CTD*: C-terminal domain, *CARD*: Caspase activation and recruitment domain, *MAVS*: Mitochondrial antiviral signaling protein, *Tyk2*: Tyrosine kinase 2, *JAK1*: Janus kinase 1, *STAT*: Signal transducer and activator of transcription, *ISRE*: Interferon-stimulated response element.

Figure 1-2

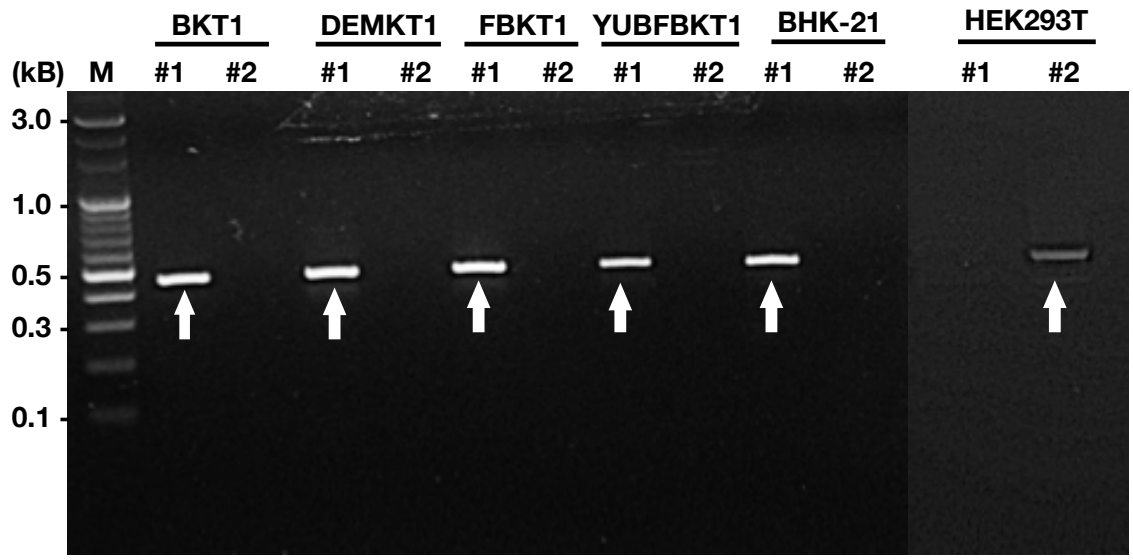

Electrophoresis results of cell genotyping in bat and non-bat cell lines. PCR was performed for proximal tubule epithelial cell marker (AQP1) and distal tubule epithelial cell marker (MUC-1) in bat and non-bat kidney cell lines using specific primers listed in Table 1-1. (a) Electrophoresis result of AQP1 and MUC-1 in BKT1, DEMKT1, FBKT1, YUBFKT1, and BHK-21 cells, Positive PCR-fragment for AQP1 after Sanger sequencing is indicated by arrow. The result of Sanger sequencing can be found in Figure 1-2. (b) Electrophoresis result of AQP1 and MUC-1 in HEK293T. Positive PCR-fragment for MUC-1 after Sanger sequencing is indicated by arrow. The result of Sanger sequencing can be found in Figure 1-3.

Figure 1-3

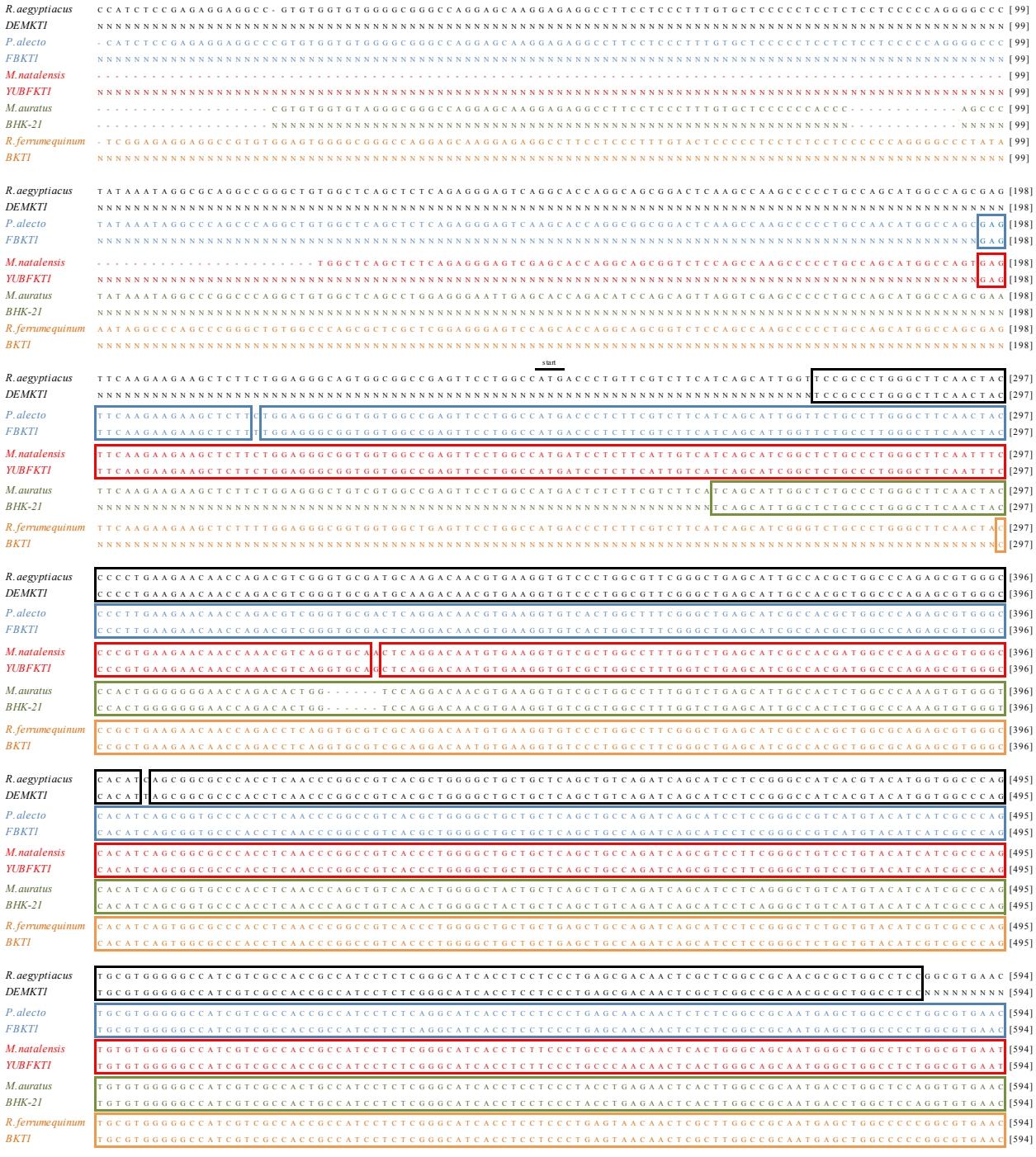

Continue…

Continued…

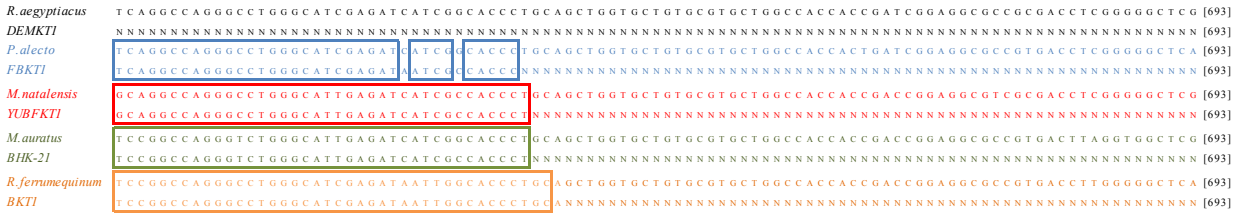

Partial sequences of aquaporin-1 (AQP1) isolated from kidney cells. AQP1 partial sequences from same genus are written in the same color and the conserved nucleotides among related species are highlighted. AQP1 partial sequences that have not been determined are denoted as N.

Figure 1-4

```
                                                                        start codon
Human    ACCTCTCAAGCAGCCAGCGCCTGCCTGAATCTGTTCTGCCCCCTCCCCACCCATTTCACCACCACCATGACACCGGGCACCCAGTCTCCT [ 90]
HEK293T  NNNNNNNNNNNNNNNNNNNNNNNNNNNNNNNNNNNNNNNNNNNNNNNNNNNNNNNNNNNNNNNNNNNNNNNNNNNNNNNNNNNNNNNNNNNNNN [ 90]

Human    TTCTTCCTGCTGCTGCTCCTCACAGTGCTTACAGTTGTTACGGGTTCTGGTCATGCAAGCTCTACCCCAGGTGGAGAAAAGGAGACTTCG [180]
HEK293T  NNNNNNNNNNNNNNNNNNNNNNNNNNNNNNNNNNNNNNNNNNNNNNNNNNNNNNNNNNNNNNNNNNNNNNNNNNNNNNNNNNNNNNNNNNNNNN [180]

Human    GCTACCCAGAGAAGTTCAGTGCCCAGCTCTACTGAGAAGAATGCTTTGTCTACTGGGGTCTCTTTCTTTTTCCTGTCTTTTCACATTTCA [270]
HEK293T  NNNNNNNNNNNNNNNNNNNNNNNNNNNNNNNNNNNNNNNNNNNNNNNNNNNNNNNNNNNNNNNNNNNNNNNNNNNNNNNNNNNNNNNNNNNNNN [270]

Human    AACCTCCAGTTTAATTCCTCTCTGGAAGATCCCAGCACCGACTACTACCAAGAGCTGCAGAGAGACATTTCTGAAATGTTTTTGCAGATT [360]
HEK293T  NNNNNNNNNNNNNNNNNNNNNNNNNNNNNNNNNNNNNNNNNNNNNNNNCAAGAGCTGCAGAGAGACATTTCTGAAATGTTTTTGCAGATT [360]

Human    TATAAACAAGGGGGTTTTCTGGGCCTCTCCAATATTAAGTTCAGGCCAGGATCTGTGGTGGTACAATTGACTCTGGCCTTCCGAGAAGGT [450]
HEK293T  TATAAACAAGGGGGTTTTCTGGGCCTCTCCAATATTAAGTTCAGGCCAGGATCTGTGGTGGTACAATTGACTCTGGCCTTCCGAGAAGGT [450]

Human    ACCATCAATGTCCACGACGTGGAGACACAGTTCAATCAGTATAAAACGGAAGCAGCCTCTCGATATAACCTGACGATCTCAGACGTCAGC [540]
HEK293T  ACCATCAATGTCCACGACGTGGAGACACAGTTCAATCAGTATAAAACGGAAGCAGCCTCTCGATATAACCTGACGATCTCAGACGTCAGC [540]

Human    GTGAGTGATGTGCCATTTCCTTTCTCTGCCCAGTCTGGGGCTGGGGTGCCAGGCTGGGGCATCGCGCTGCTGGTGCTGGTCTGTGTTCTG [630]
HEK293T  GTGAGTGATGTGCCATTTCCTTTCTCTGCCCAGTCTGGGGCTGGGGTGCCAGGCTGGGGCATCGCGCTGCTGGTGCTGGTCTGTGTTCTG [630]

Human    GTTGCGCTGGCCATTGTCTATCTCATTGCCTTGGCTGTCTGTCAGTGCCGCCGAAAGAACTACGGGCAGCTGGACATCTTTCCAGCCCGG [720]
HEK293T  GTTGCGCTGGCCATTGTCTATCTCATTGCCTTGGCTGTCTGTCAGTGCCGCCGAAAGAACTACGGGCAGCTGGACATCTTTCCAGCCCGG [720]

Human    GATACCTACCATCCTATGAGCGAGTACCCCACCTACCACACCCATGGGCGCTATGTGCCCCCTAGCAGTACCGATCGTAGCCCCTATGAG [810]
HEK293T  GATACCTACCATCCTATGAGCGAGTACCCCACCTACCACACCCATGGGCGCTATGTGCCCCCTAGCAGTACCGATCGTAGCCCCTATGAG [810]

                                                                                    stop codon
Human    AAGGTTTCTGCAGGTAATGGTGGCAGCAGCCTCTCTTACACAAACCCAGCAGTGGCAGCCACTTCTGCCAACTTGTAGGGGCACGTCGCC [900]
HEK293T  AAGGTTTCTGCAGGTAATGGTGGCAGCAGCCTCTCTTACACAAACCCAGCAGTGGCAGCCACTTCTGCCAACTTGTAGNNNNNNNNNNNN [900]
```

Partial sequences of mucin-1 (MUC-1) isolated from HEK293T cell line. Conserved nucleotides between human MUC-1 sequences obtained from database and HEK293T are highlighted in yellow. MUC-1 partial sequences that have not been determined are denoted as N.

Figure 1-5

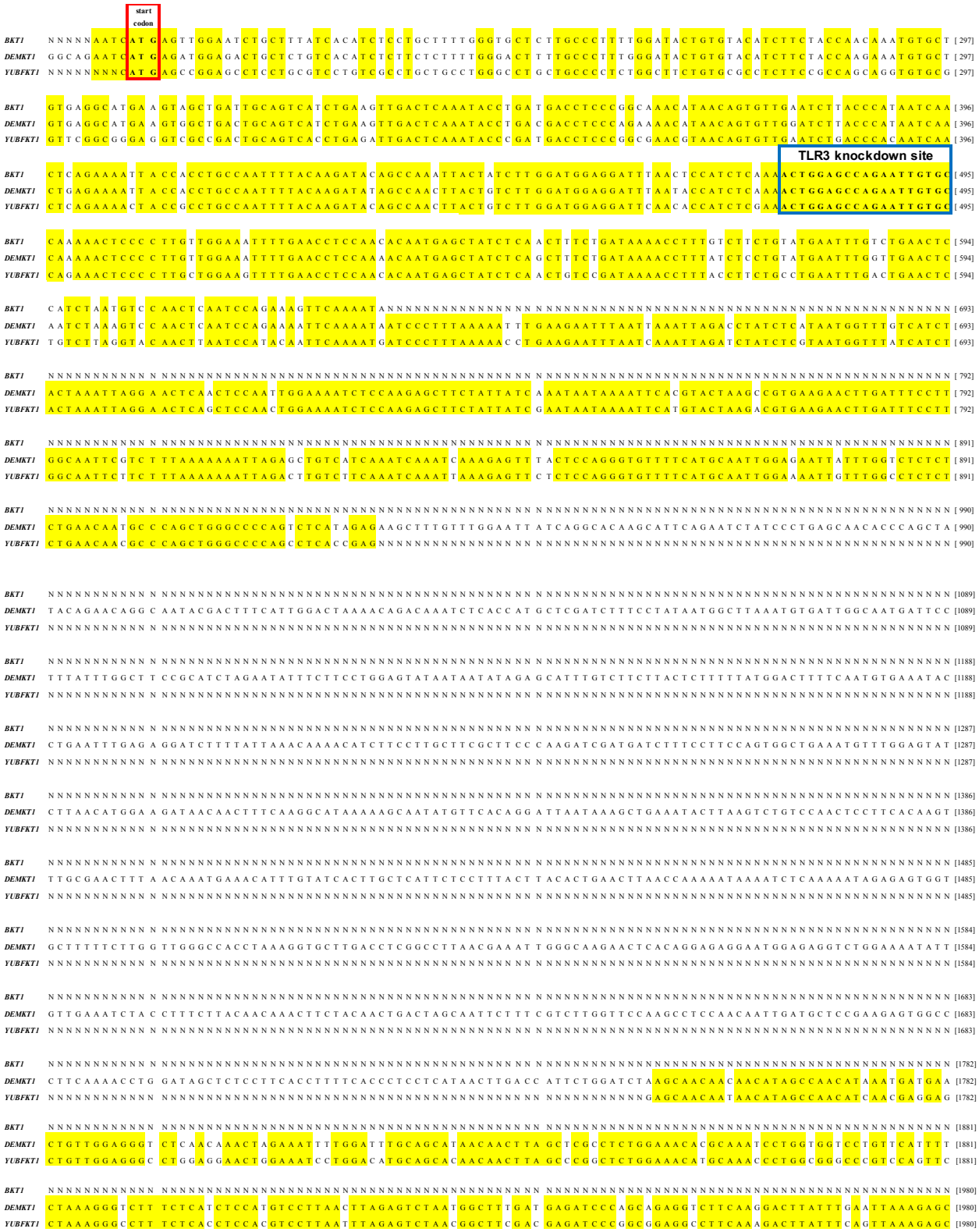

Continue…

Continued…

Comparison of TLR3 partial sequences from bat cell lines used in this study. Conserved nucleotides and targeted site for TLR3 mRNA knockdown among bat species are highlighted in yellow and blue, respectively. TLR3 partial sequences that have not been determined are denoted as N.

Figure 1-6

Continue…

Continued…

```
DEMKT1   NNNNNNNNNNNNNNNNNNNNNNNNNNNNNNNNNNNNNNNNNNNNNNNNNNNNNNNNNNNNNNNNNNNNNNNN N N NNNNNNNNNNNNNNNNNNNNNNNNN [1287]
BKT1     TGCCTCAGATCGTTGGGCTGACTGCCTCGGTCGGTGTTGGGGATGCCAAAAGCACAACTGAAGCCATGGAAT A T ATCTGCAAACTGTGTGCGTCTCTTG [1287]
YUBFKT1  TGCCCCAGGTTATTGGGCTGACTGCCTCAGTCGGCGTTGGGGATGCCAAAAACACAGCCGAAGCCACGGAAC A T ATCTGCAGGCTGTGTGCTTCTCTTG [1287]
FBKT1    NNNNNNNNNNNNNNNNNNNNNNNNNNNNNNNNNNNNNNNNNNNNNNNNNNNNNNNNNNNNNNNNNNNNNNNN N N NNNNNNNNNNNNNNNNNNNNNNNNN [1287]

DEMKT1   NNNNNNNNNNNNNNNNNNNNNNNNNNNNNNNNNNNNNNNNNNNNNNNNNNNNNNNNNNNNNNNNNNNNNNNN N N NNNNNNNNNNNNNNNNNNNNNNNNN [1386]
BKT1     ACATATCAGTGATAGCAACAGTCAAAGACAACTTAGAGGAACTGGAAGAAATTGTTTATAAGCCCCAGAAGT T T TTCAGGAAAGTGGAATTACGGACTA [1386]
YUBFKT1  ACACATCAGTGCTGGCAACAGTCAAAGACAACTTGGAGGAACTGGAGGAAATTGTCTATAAGCCCCAGAAGT A T TTCAGGAAAGTGGAGTCGCGGGCCA [1386]
FBKT1    NNNNNNNNNNNNNNNNNNNNNNNNNNNNNNNNNNNNNNNNNNNNNNNNNNNNNNNNNNTAAGCCCCAGAAGT T T TTCAGGAAAGTGGAATCACGGACTA [1386]

DEMKT1   NNNNNNNNNNNNNNNNNNNNNNNNNNNNNNNNNNNNNNNNNNNNNNNNNNNNNNNNNNNNNNNNNNNNNNNN N N NNNNNNNNNNNNNNNNNNNNNNNNN [1485]
BKT1     ACGACAGATTTAAATATATTATCTCTCAGTTAATGAGGGAGACAGAGAGTCTGGCAAAGAGTGTCTTTGGCG A A CTGGGTACCGTAACTCTCGAAAACT [1485]
YUBFKT1  CCGACAGATTTAAATGCATCATCTCTCAGCTGATGAGGGACACAGAGAGTCTGGCAGAGAGCGTCTTTGGTG A A CTCGGGACCGGAAGTCTCGAAAACT [1485]
FBKT1    CTGACAGATTTAAATGCATCATCTCTCAGCTGATGAAGGAGACAGAGAGTCTAGCAAAGAGTATCTTTGACA A A CTTGGTACCATAACTCTCGGAGACT [1485]

DEMKT1   NNNNNNNNNNNNNNNNNNNNNNNNNNNNNNNNNNNNNNNNNNNNNNNNNNNNNNNNNNNNNNNNNNNNNNNN N N NNNNNNNNNNNNNNNNNNNNNNNNN [1584]
BKT1     TATCTGAAATTCAAAACAGGAATTTTGGAACACAGAAATACGAACAATGGATTGTTGCAGTTCAGAAAAAGT G C ATGGTGTTACACATGGCAGACAAAG [1584]
YUBFKT1  TATCTCAGATTCAAAACAGGAATTTTGGAACTCAGAAATATGAACAGTGGATCGTTACAGTTCAGAAGAAGT G C AAGCTGTTACAGATGCCAGACAAAG [1584]
FBKT1    TCTCTCAAATTCAAAACAGGAATTTTGGCACACAGAAATATGAACAGTGGATTGTTGCAGTTCAGAAAAAGT G C ATGGTGTTAAAGATGCCAGATAAAG [1584]

DEMKT1   NNNNNNNNNNNNNNNNNNNNNNNNNNNNNNNNNNNNNNNNNNNNNNNNNNNNNNNNNNNNNNNNNNNNNNNN N N NNNNNNNNNNNNNNNNNNNNNNNNN [1683]
BKT1     ATGAAGAGAGCAGGATTTGTAAAGCACTGTTTTTGTACACTTCACATTTGCGGAAATTGAATGATGCCCTCG T T ATCAATGAGCATGCGCGGATGAAAG [1683]
YUBFKT1  ACAAAGAGAGCAGGATTTGTAAAGCACTGTTCTTGTACACTTCACATTTGCGGAAATTTAATGATGCCCTCA T T ATCAATGAGGACGCGCGGACGAAAG [1683]
FBKT1    ATGAAGAGAGCAGAATTTGTAAAGCACTGTTTTTGTACACTTCACATTTGCGGAAATTTAATGATGCCCTCA T C ATCAGTGAGCATGCACGGATGAAAG [1683]

DEMKT1   NNNNNNNNNNNNNNNNNNNNNNNNNNNNNNNNNNNNNNNNNNNNNNNNNNNNNNNNNNNNNNNNNNNNNNNN N N NNNNNNNNNNNNNNNNNNNNNNNNN [1782]
BKT1     ATGCGCTGGATTACTTGAAAGACTTCTTCACTAATGTCCGATCAGCAGGATTTGATGAGATAGAGCAAGATC T T ACTCGGAGATTTGAAGAAAAGTTGC [1782]
YUBFKT1  ATGCTCTGGATTACTTGAAAAACTTCTTCAGTAATGTCCGAGCAGCAGGATTTGATGAGATTGAGCAGGATC T C ACTCGGAGATTTGAAGAAAAGCTGC [1782]
FBKT1    ATGCTCTGGATTACTTGAAAGACTTCTTCCGTAATGTCCGAACAGCAGGCTTTGATGAGACTGAGCAAGATC T C ACTCGGAGATTTGAAGAAAAGCTGC [1782]

DEMKT1   NNNNNNNNNNNNNNNNNNNNNNNNNNNNNNNNNNNNNNNNNNNNNNNNNNNNNNNNNNNNNNNNNNNNNNNN N N NNNNNNNNNNNNNNNNNNNNNNNNN [1881]
BKT1     AAGAACTAGAAAGCATTTCCATGGATCCCAGCAATGAGAATCCTGAACTCAAAGACCTCTGCTTCATCTTGC A A GAGGAGTACCATTTTAATCCGGACA [1881]
YUBFKT1  AAGAATTAGAGAGCATTTCCAAGGATCCCAGCAATGAGAACCCTAAACTCAAAGACCTCTGCTTCATCTTGC A A GAGGAGTACCACTAAACCCGGAGAC [1881]
FBKT1    AAGAACTAGAAAGAATTTCCATGGATCCCAGCAACGAGAACCCTAAACTCAAAGACCTCTGCTTCGTCTTGA A A GAGGAGTACCACTNNNNNNNNNNNN [1881]

DEMKT1   NNNNNNNN [1889]
BKT1     CTAGAACC [1889]
YUBFKT1  CAGAACCN [1889]
FBKT1    NNNNNNNN [1889]
```

Comparison of RIG-I partial sequences from bat cell lines used in this study. Conserved nucleotides and targeted site for RIG-I mRNA knockdown among bat species are highlighted in yellow and blue, respectively. RIG-I partial sequences that have not been determined are denoted as N.

Figure 1-7

Continue…

Continued…

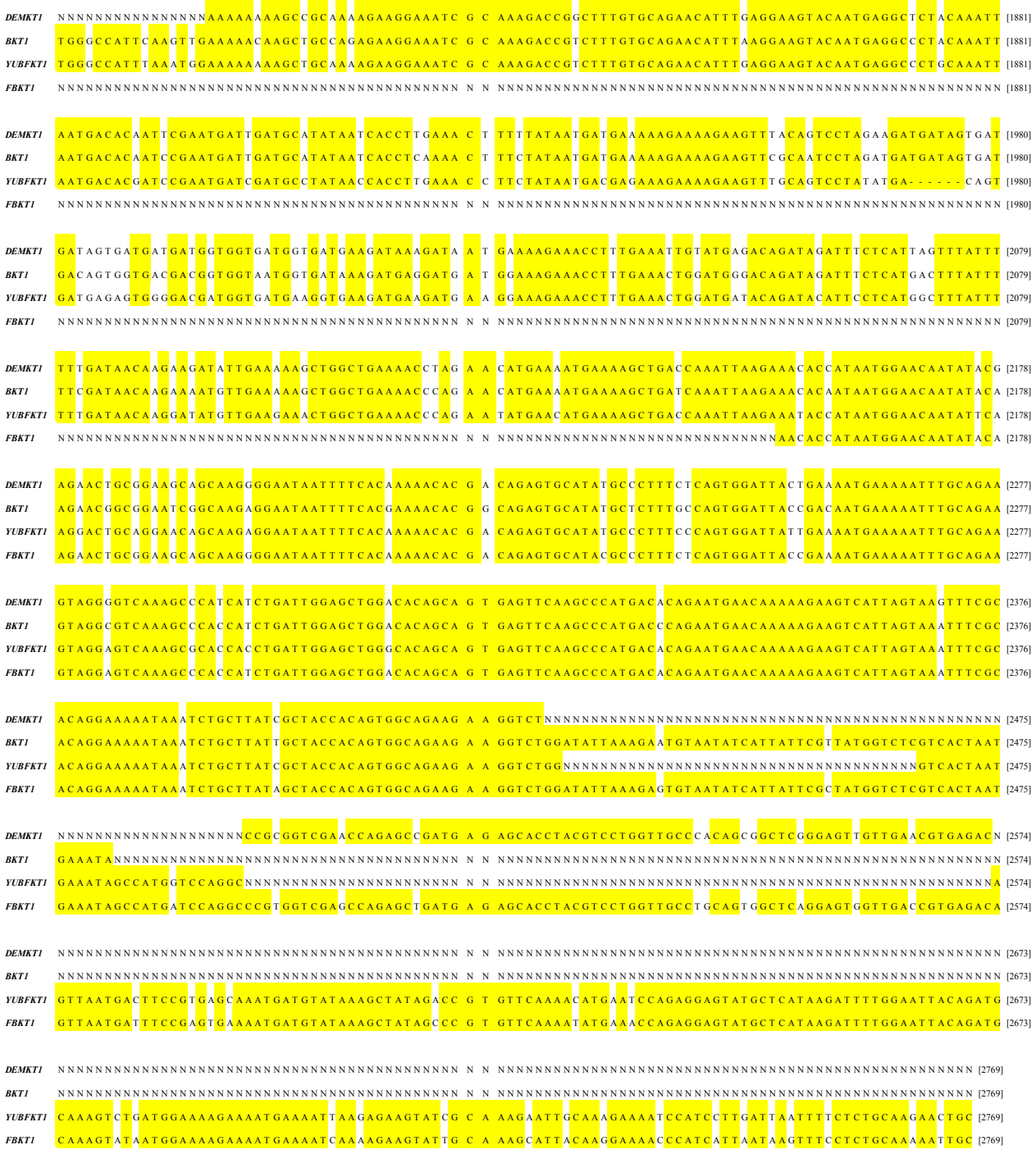

Comparison of MDA5 partial sequences from bat cell lines used in this study. Conserved nucleotides and targeted site for MDA5 mRNA knockdown among bat species are highlighted in yellow and blue, respectively. MDA5 partial sequences that have not been determined are denoted as N.

Figure 1-8

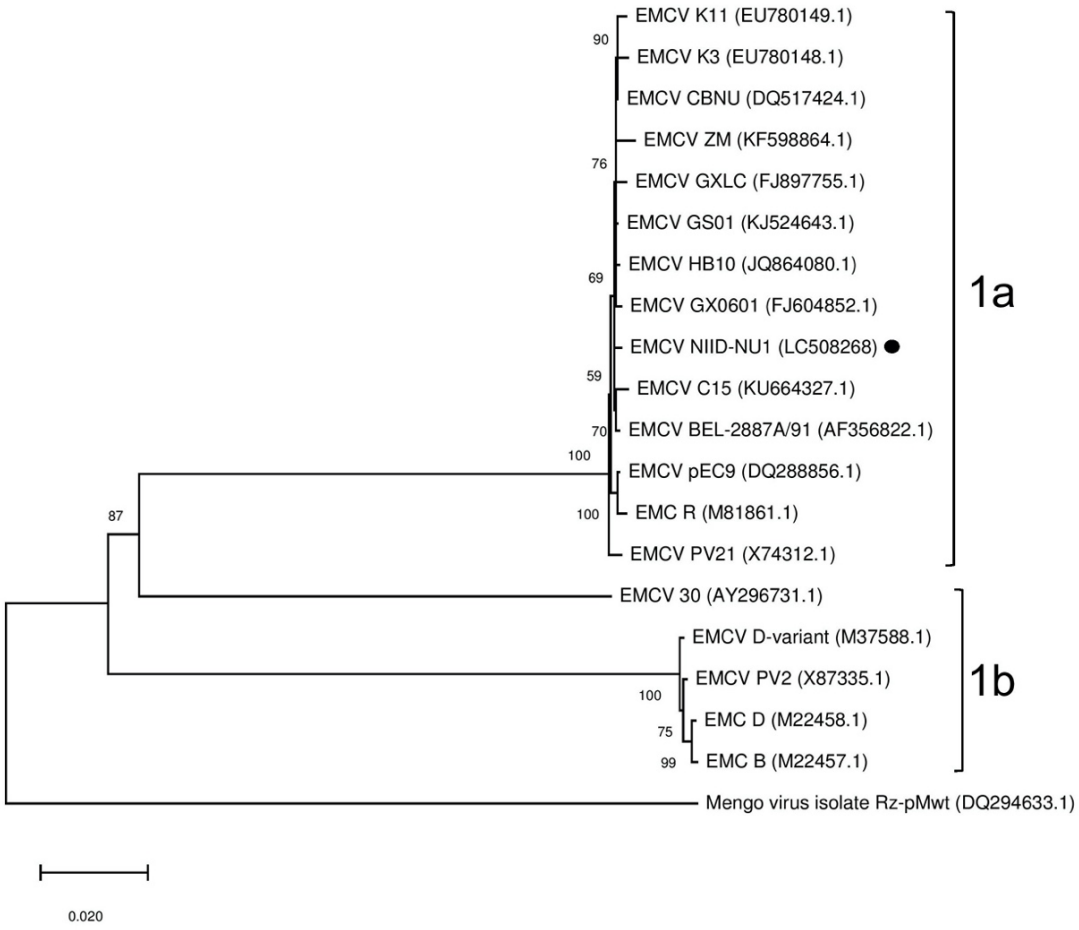

Phylogenetic analysis of isolate EMCV NIID-NU1 based on the complete ORF of 6879 nt. A phylogenetic tree was constructed using MEGA7 software. Mengovirus served as an outgroup. Bootstrap values obtained from 1,000 replicates are shown at the major nodes. The isolate identified in this study is indicated with a solid dot.

Figure 1-9

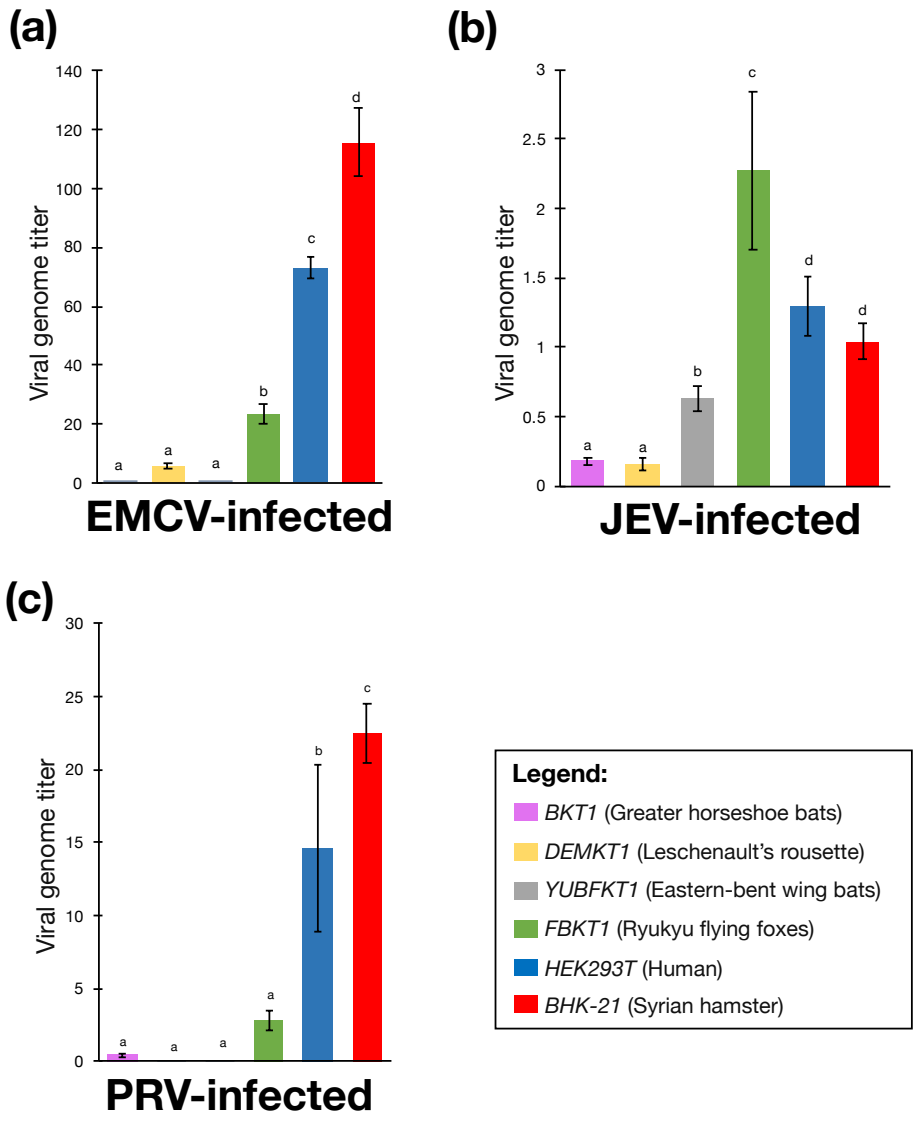

Viral genome titers in bats and non-bat cell lines. The cell lines were infected by EMCV and JEV with a multiplicity of infection (MOI) of 1.0; and PRV with a MOI of 0.1. Viral genome of EMCV (a), JEV (b), and PRV (c) was measured 1-day post-infection (mean ± SD, n = 3). Viral genome titer is expressed as: $x10^9$ copy numbers/µg total RNA for EMCV and JEV; and $x10^6$ copy numbers/µg total RNA for PRV. Differences between cell lines were analyzed by one-way ANOVA, followed by Tukey's test. Values that do not share a common letter are significantly different ($p<0.05$).

Figure 1-10

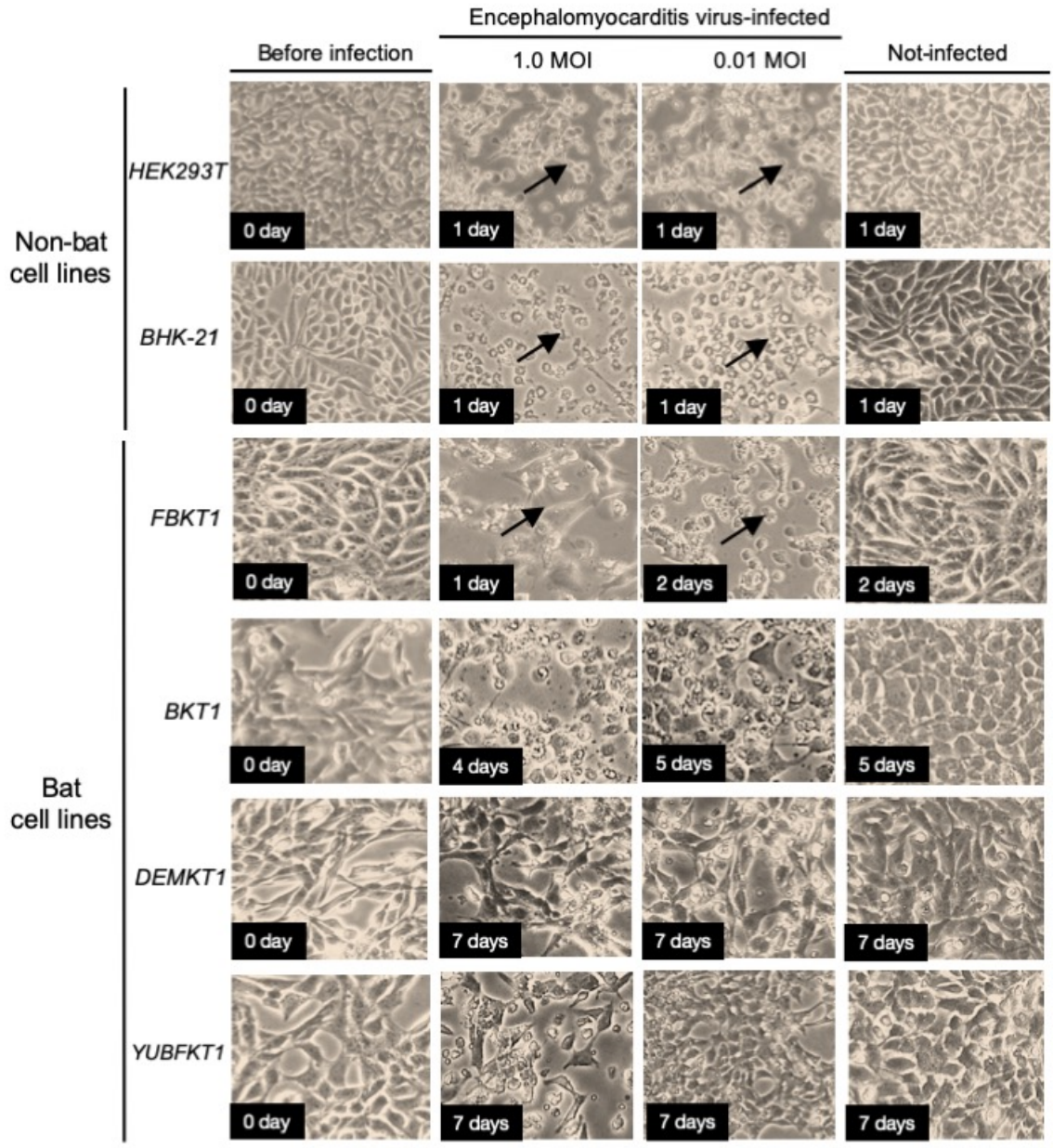

Cytopathic effect (CPE) after EMCV infection. EMCV infection caused total destruction CPE in non-bat cell lines (HEK293T and BHK-21) and one bat cell line (FBKT1) in 1-day post infection (dpi). The CPE after EMCV infection was delayed to 4 dpi in BKT and 7 dpi in DEMKT1, and YUBFKT1. The total destruction CPE after EMCV infection is indicated by arrow.

Figure 1-11

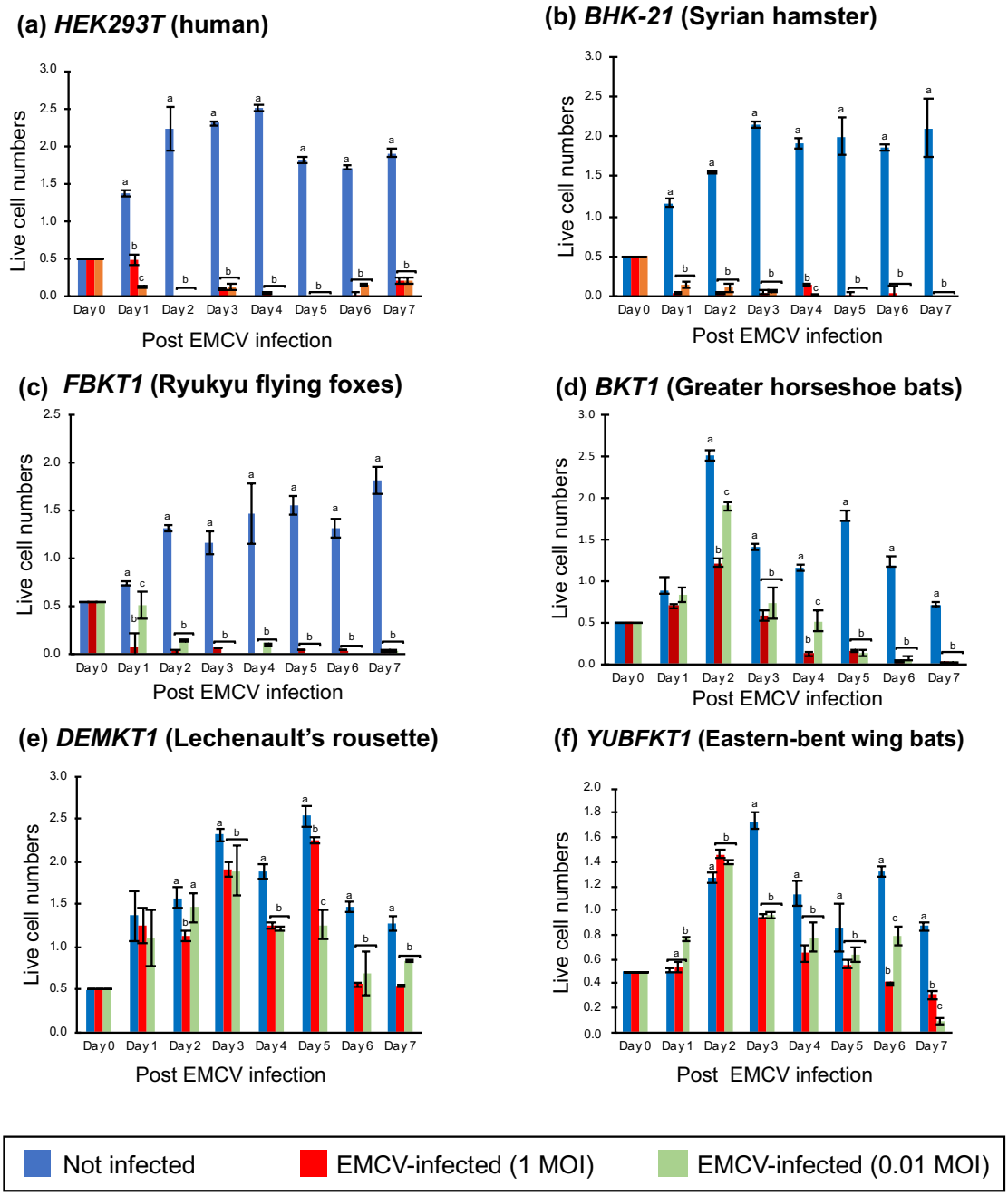

Cell growth after EMCV infection. Live cell numbers in HEK293T (a), BHK-21 (b), FBKT1 (c), BKT1 (d), DEMKT1 (e), and YUBFKT1 (f) after EMCV infection at multiplicity of infection (MOI) of 1.0 and 0.01 until 7 days post infection (dpi) (mean ± SD, n = 3). Live cell numbers are expressed as $x10^5$ cells/mm^3.Differences between cell lines were analyzed by one-way ANOVA, followed by Tukey's test. Values that do not share a common letter are significantly different ($p<0.05$).

Figure 1-12

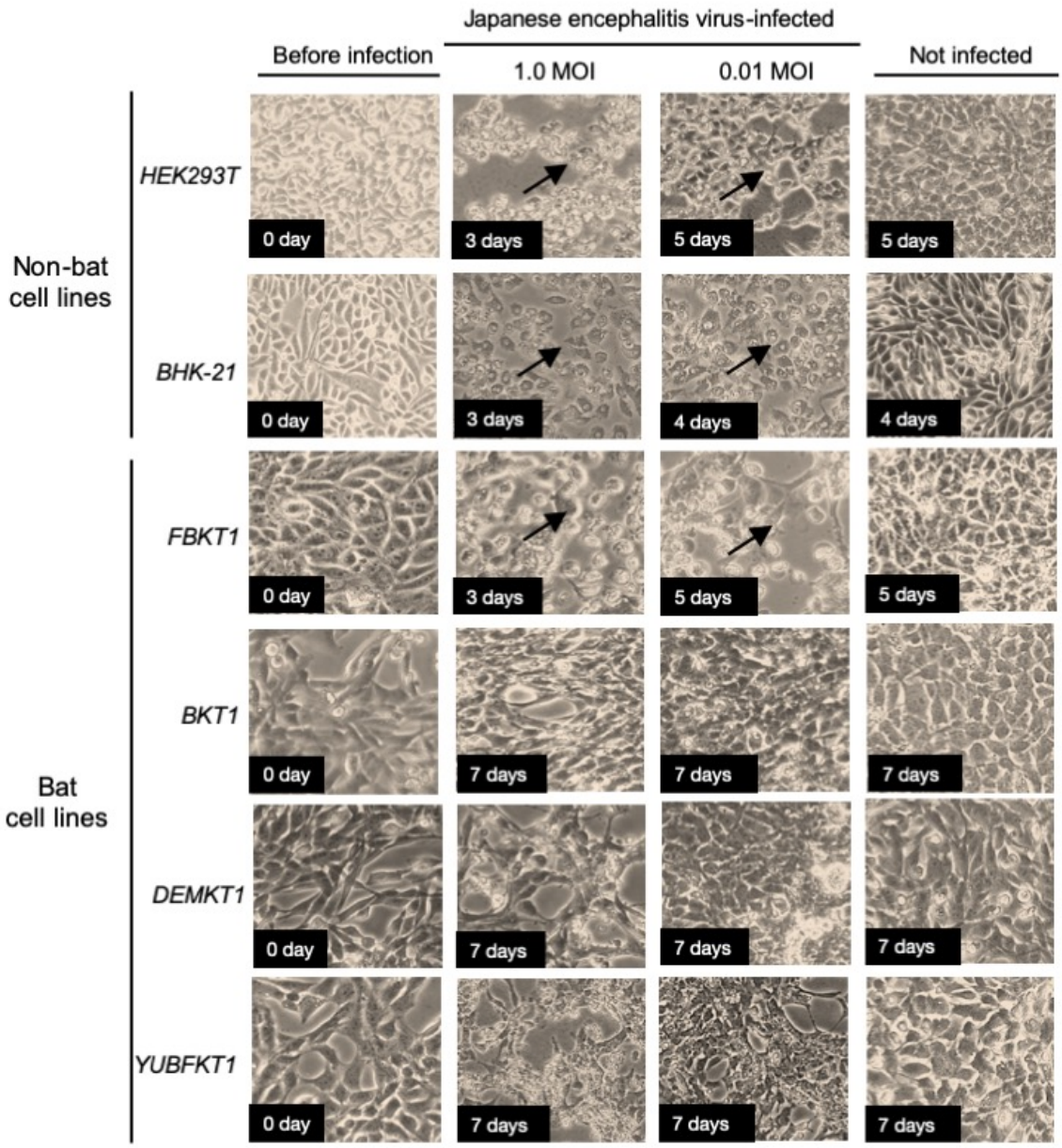

Cytopathic effect (CPE) after JEV infection. JEV infection caused total destruction CPE in non-bat cell lines (HEK293T and BHK-21) and one bat cell line (FBKT1) in 3 – 5 days post infection (dpi). The CPE after JEV infection was delayed to 7 dpi in BKT1, DEMKT1, and YUBFKT1. The total destruction CPE after JEV infection is indicated by arrow.

Figure 1-13

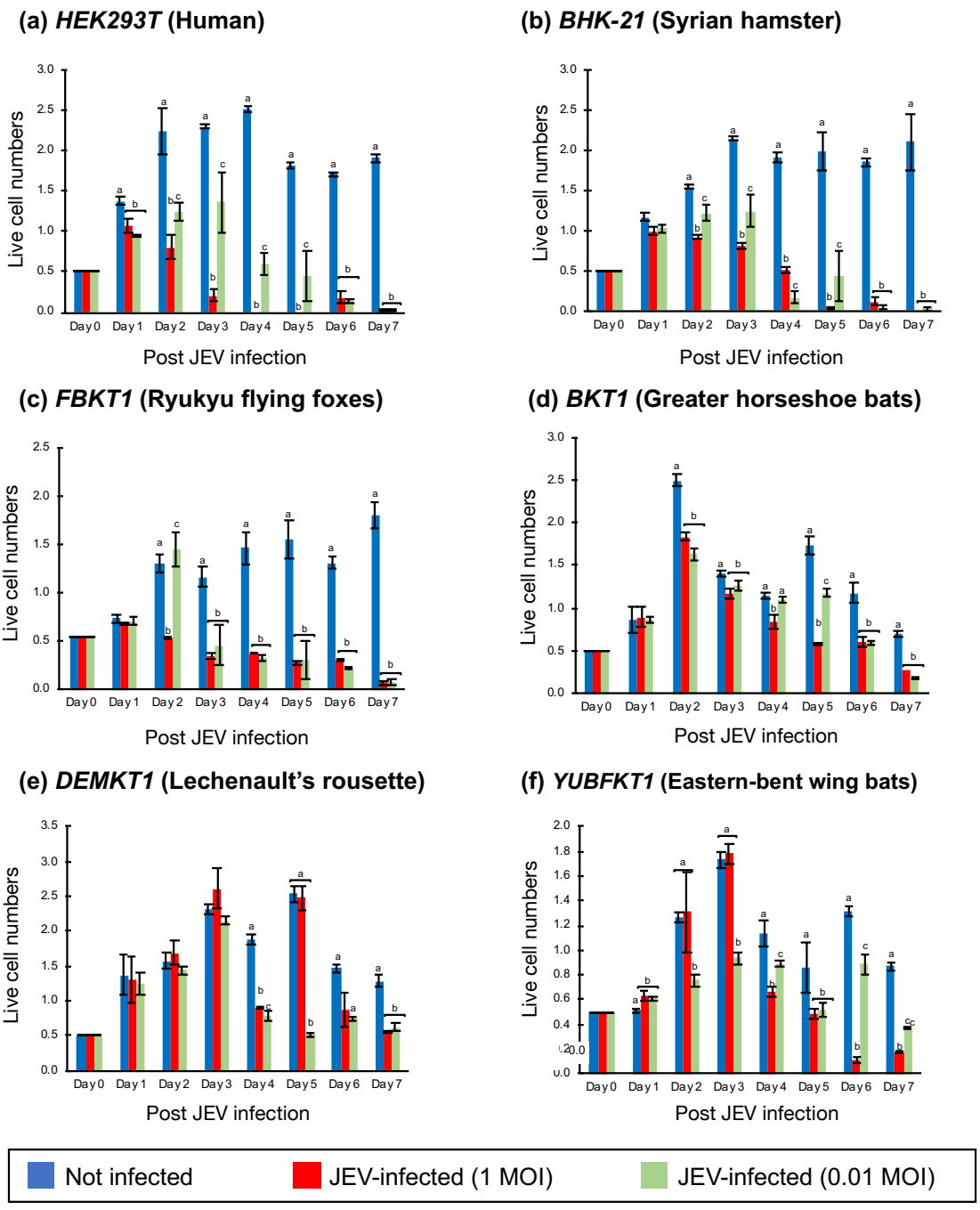

Cell growth after JEV infection. Live cell numbers in HEK293T (a), BHK-21 (b), FBKT1 (c), BKT1 (d), DEMKT1 (e), and YUBFKT1 (f) after JEV infection at multiplicity of infection (MOI) of 1.0 and 0.01 until 7 days post infection (dpi) (mean ± SD, n = 3). Live cell numbers are expressed as $x10^5$ cells/mm^3. Differences between cell lines were analyzed by one-way ANOVA, followed by Tukey's test. Values that do not share a common letter are significantly different ($p<0.05$).

Figure 1-14

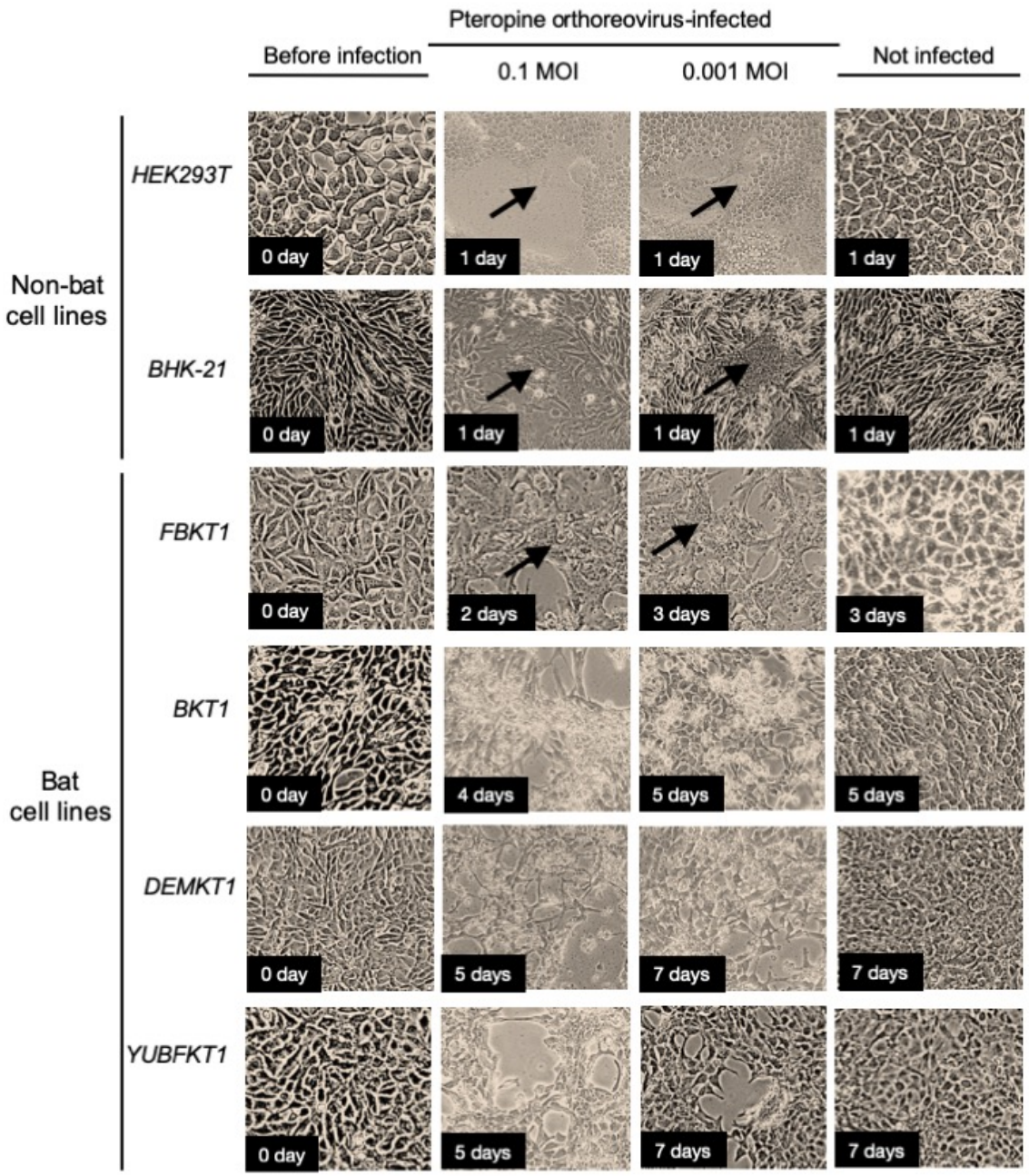

Cytopathic effect (CPE) after PRV infection. JEV infection caused fast syncytial CPE in non-bat cell lines (HEK293T and BHK-21) and one bat cell line (FBKT1) in 1 – 2 days post infection (dpi). The CPE was delayed to 4 – 7 dpi in BKT1, DEMKT1, and YUBFKT1 but not syncytial CPE was observed in DEMKT1 and YUBFKT1. The syncytial CPE after PRV infection is indicated by arrow.

Figure 1-15

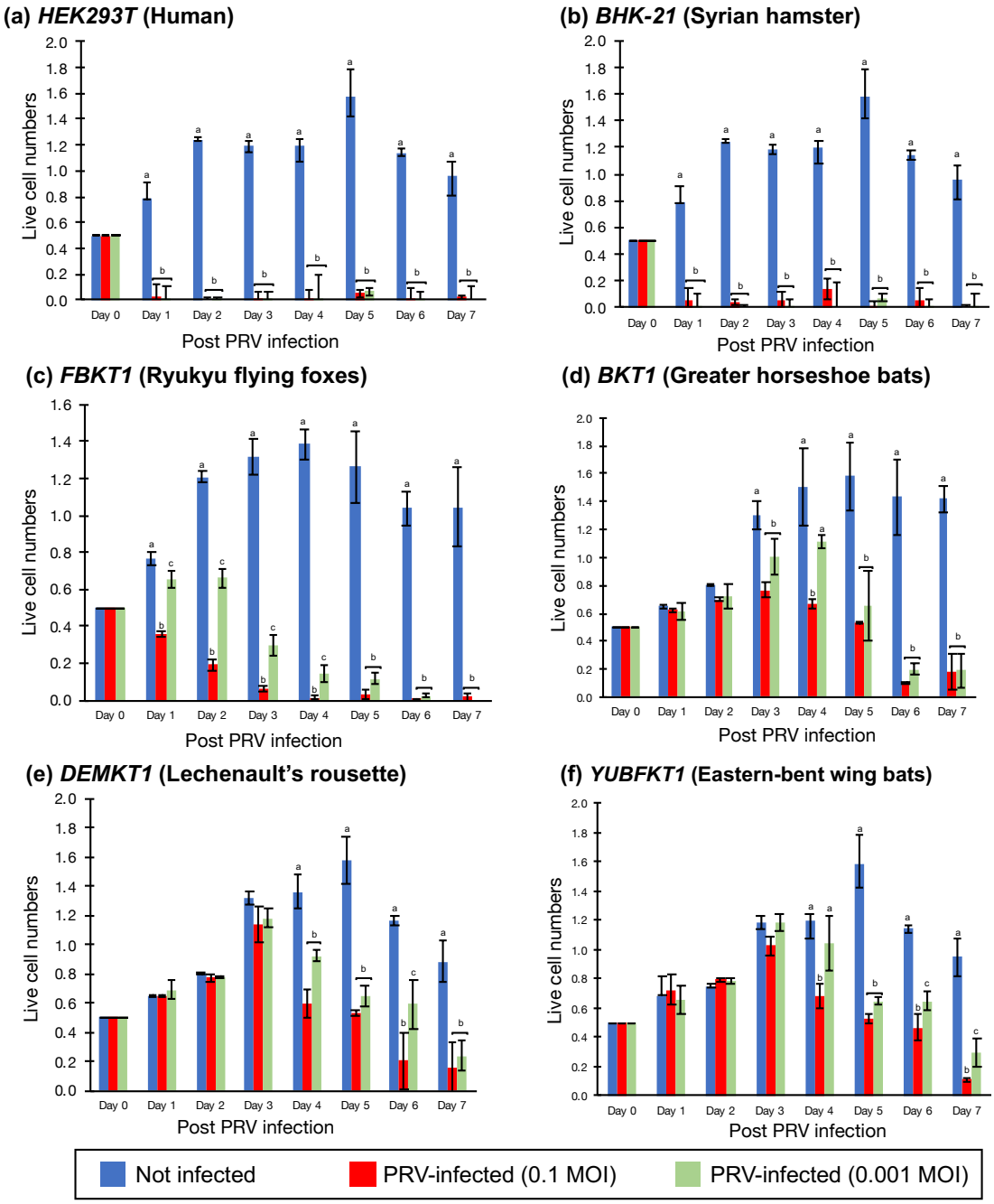

Cell growth after PRV infection. Live cell numbers in HEK293T (a), BHK-21 (b), FBKT1 (c), BKT1 (d), DEMKT1 (e), and YUBFKT1 (f) after PRV infection at multiplicity of infection (MOI) of 0.1 and 0.001 until 7 days post infection (dpi) (mean ± SD, n = 3). Differences between cell lines were analyzed by one-way ANOVA, followed by Tukey's test. Values that do not share a common letter are significantly different ($p<0.05$).

Figure 1-16

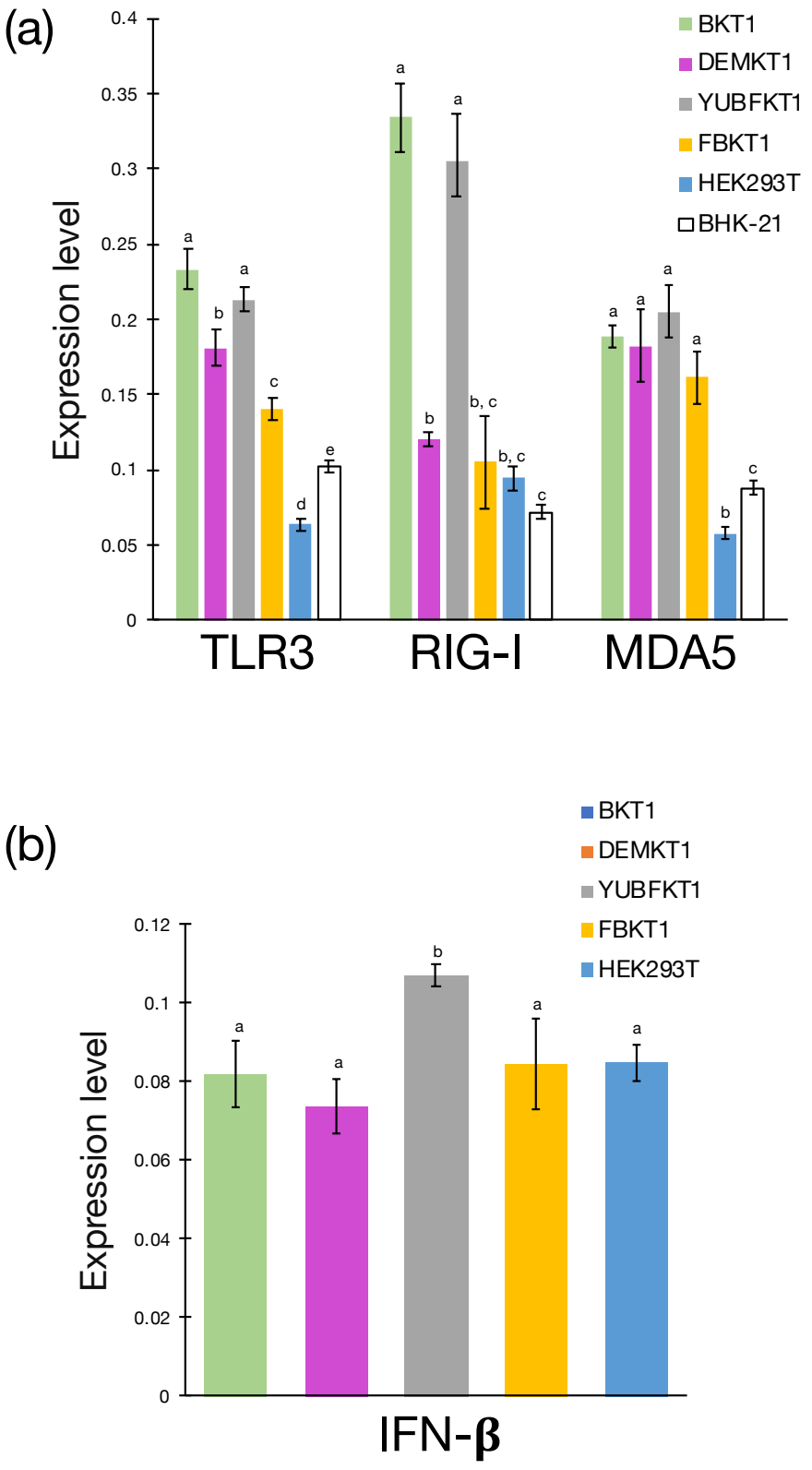

Continue…

Continued…

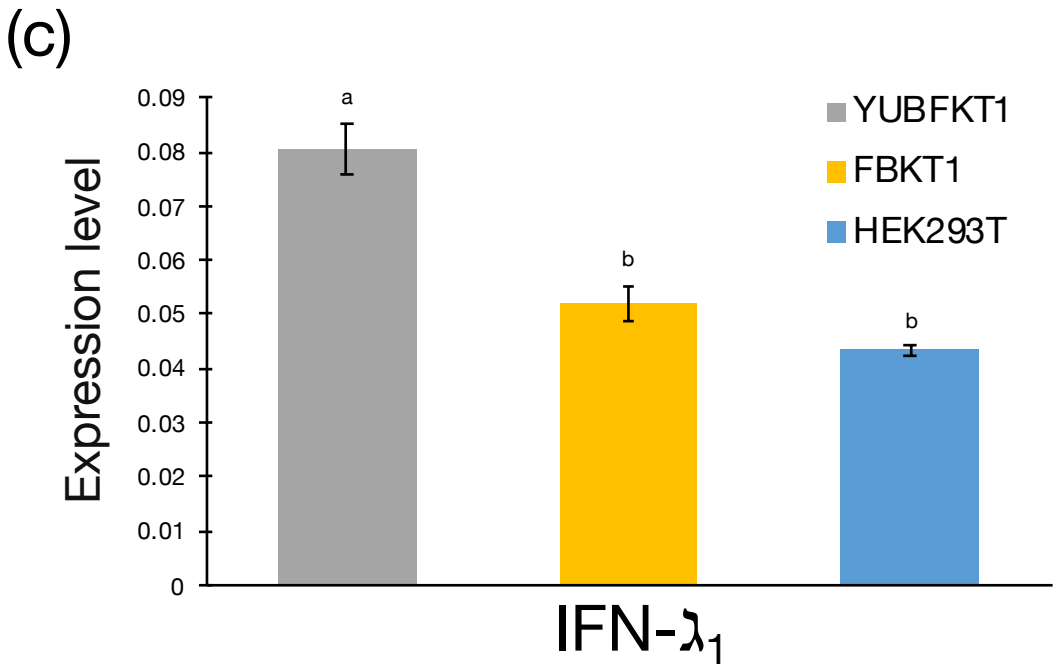

The basal expression level of pattern recognition receptors and interferons. The basal expression level of TLR3, RIG-I, and MDA5 (a); IFN-β (b); and IFN-λ_1 was measured in bat cell lines (BKT1, DEMKT1, YUBFKT1, and FBKT1) and non-bat cell lines (HEK293T and BHK-21) (mean ± SD, n = 3). Basal expression level of IFN-β for BHK-21 and IFN-λ_1 for BHK-21, BKT1 and DEMKT1 could not be measured. Differences between cell lines were analyzed by one-way ANOVA, followed by Tukey's test. Values that do not share a common letter are significantly different ($p<0.05$).

Figure 1-17

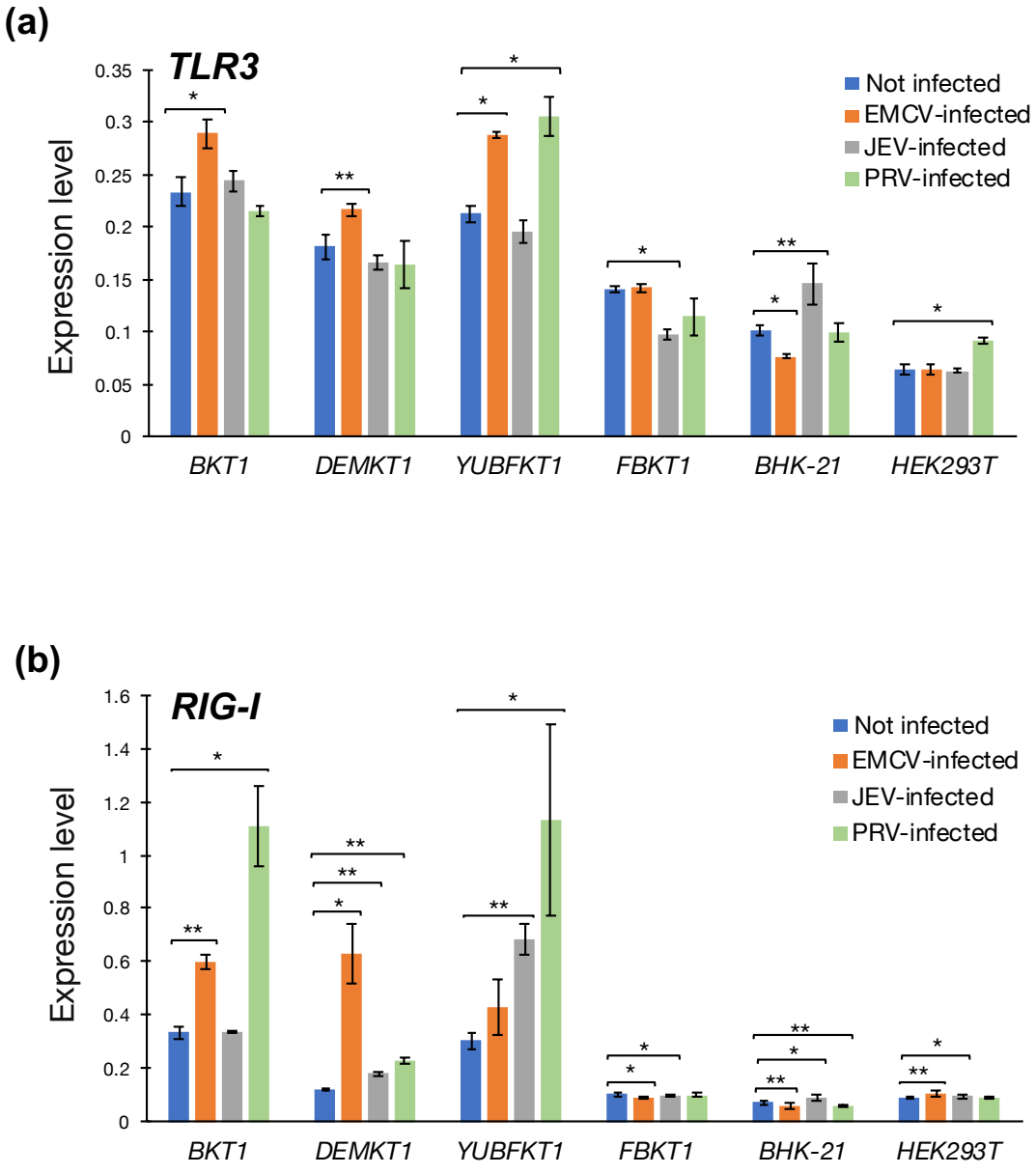

Continue…

Continued…

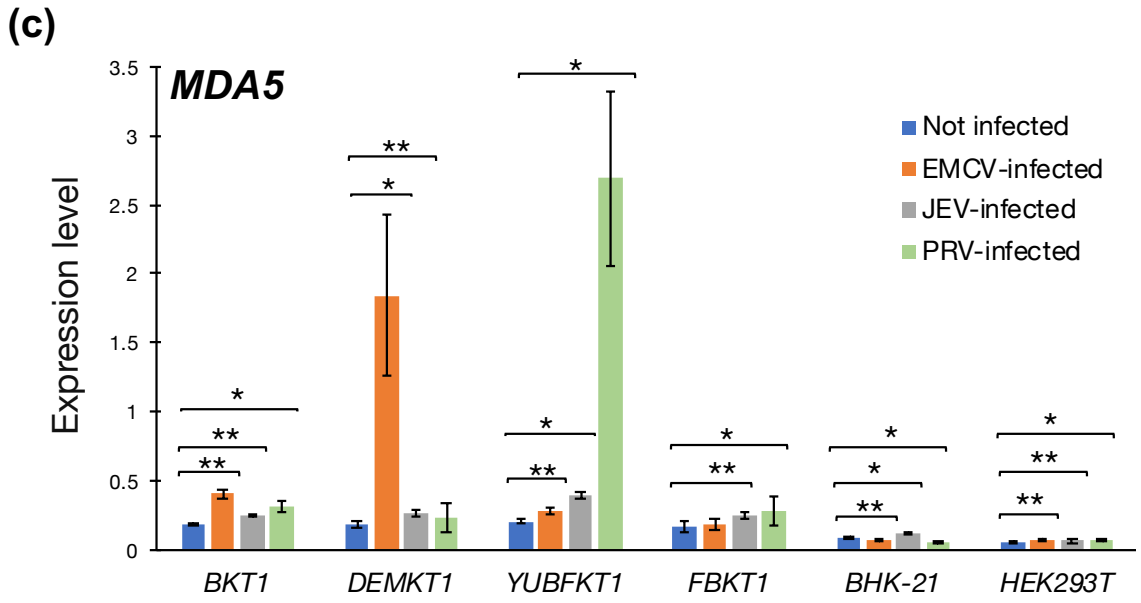

The expression level of pattern recognition receptors after viral infection. The expression of TLR3 (a), RIG-I (b), and MDA5 (c) were measured in bat cell lines (BKT1, DEMKT1, YUBFKT1, and FBKT1) and non-bat cell lines (HEK293T and BHK-21) after viral infection of EMCV (MOI of 1.0), JEV (MOI of 1.0), and PRV (MOI of 0.1) at 1-day post infection (mean ± SD, n = 3). *p < 0.01 vs Not infected, **p < 0.001 vs Not infected.

Figure 1-18

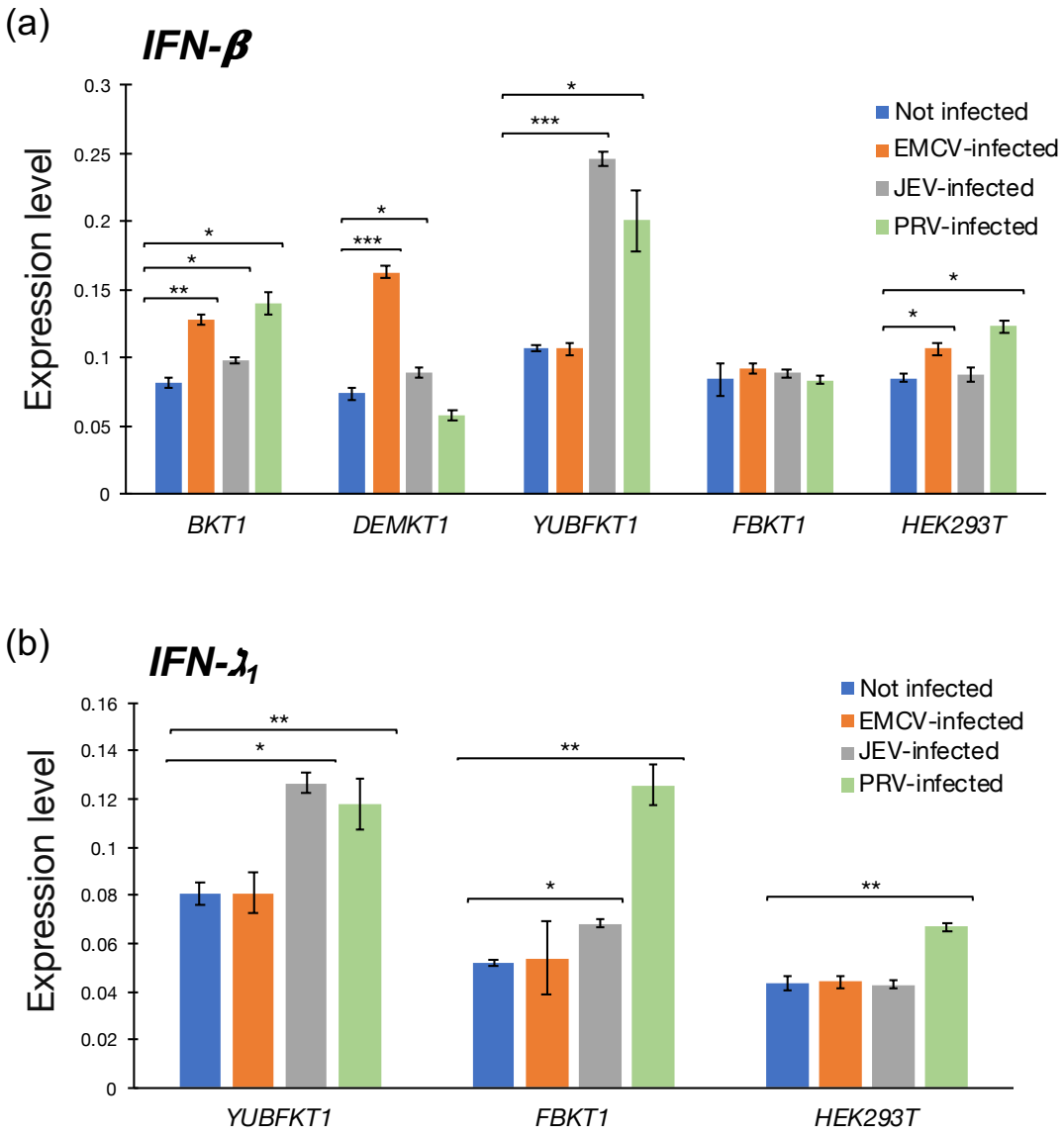

The expression level of interferons after viral infection. The expression of IFN-β (a), and IFN-λ_1 (b) were measured in bat and non-bat cell lines after viral infection of EMCV (MOI of 1.0), JEV (MOI of 1.0), and PRV (MOI of 0.1) at 1-day post infection (mean ± SD, n = 3). *$p < 0.01$ vs Not infected, **$p < 0.001$ vs Not infected.

Figure 1-19

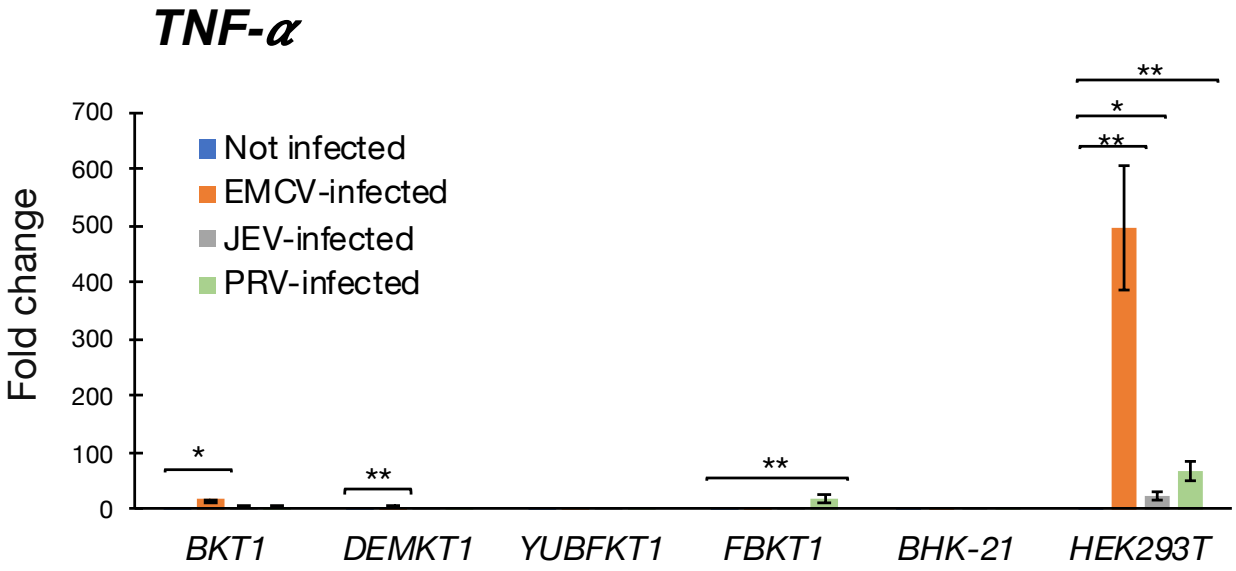

The expression level of TNF-α after viral infection. The expression of TNF-α were measured in bat cell lines (BKT1, DEMKT1, YUBFKT1, and FBKT1) and non-bat cell lines (HEK293T and BHK-21) after viral infection of EMCV (MOI of 1.0), JEV (MOI of 1.0), and PRV (MOI of 0.1) at 1-day post infection (mean ± SD, n = 3). Expression level is expressed as fold change than not infected (mock). *$p < 0.01$ vs Not infected, **$p < 0.001$ vs Not infected.

Figure 1-20

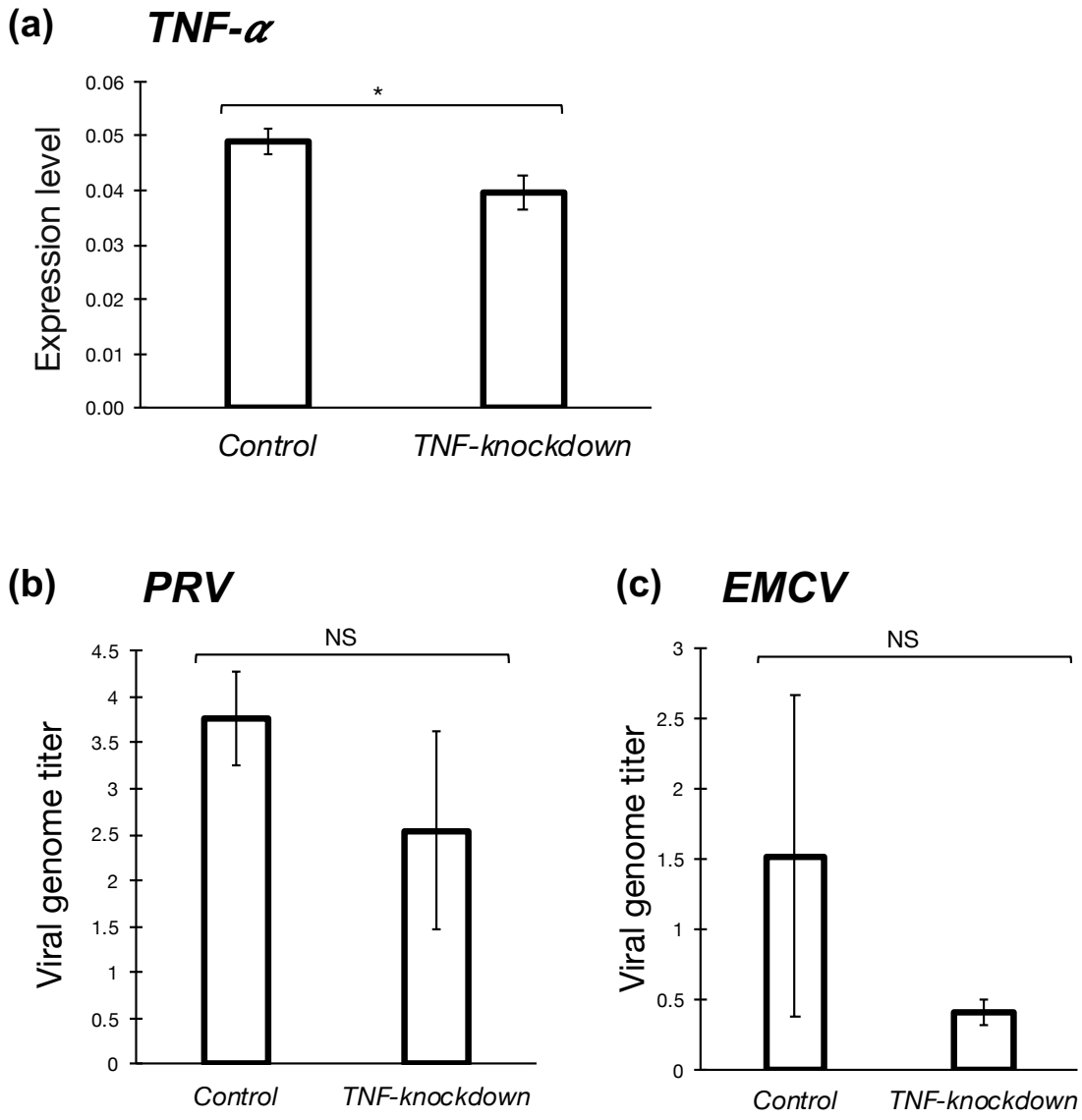

Knockdown of TNF-α in HEK293T. The expression of TNF-α (a) were significantly reduced after knockdown of TNF-α mRNA in HEK293T. The viral genome titer of PRV (b) and EMCV (c) 12 hours after viral infection was not significantly different between cells knocked down for TNF-α and cells without gene knockdown (mean ± SD, n = 3). *$p < 0.05$ vs No knockdown. NS: Not significant

Figure 1-21

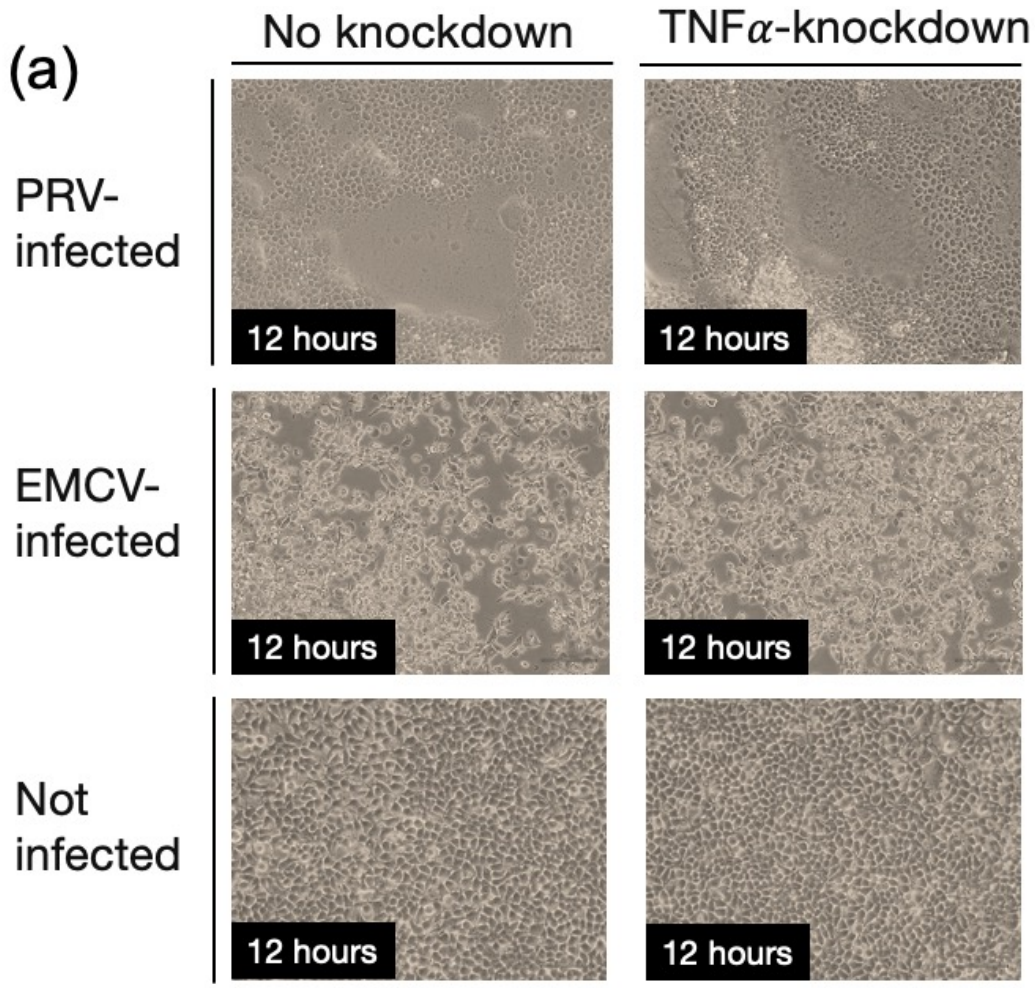

Continue…

Continued…

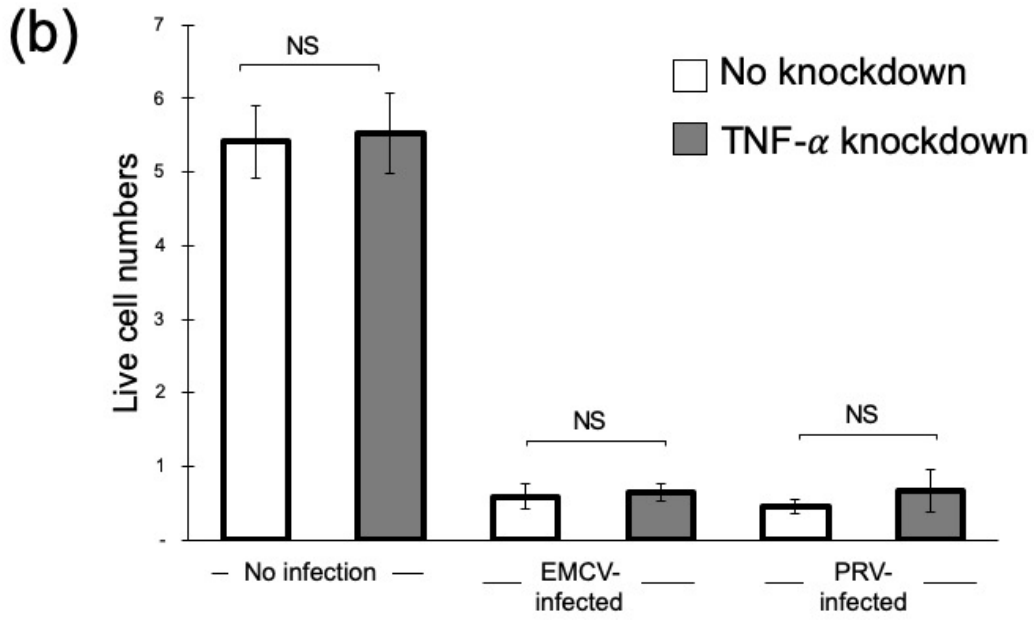

Knockdown of TNF-α in HEK293T. The syncytial and total destruction CPE was appeared 12 hours post PRV and EMCV infection, respectively (a). No significant difference of live cell numbers between cells knocked down for TNF-α and cells without gene knockdown (mean ± SD, n = 3) (b). NS: Not significant.

Tables

Table 1-1. Nucleotides partial sequences identity of renal marker (AQP1 and MUC-1) from cell lines used in this study. Multiple sequence alignment with available AQP1 and MUC-1 sequences available from the GenBank nucleotide database was completed using the Clustal X program.

Cell lines/species origin	Gene	Nucleotides (bp)	Nucleotides identity (*)				
			P.alecto	*R.aegypticus*	*M.natalensis*	*M.auratus*	*H.sapiens*
FBKT1/ *P.dasymallus*	AQP1	436	99.87%	93.53%	91.10%	86.54%	90.07%
DEMKT1/ *R.leschenaultii*	AQP1	309	93.24%	99.33%	87.16%	83.45%	87.50%
YUBFKT1/ *M.fuliginosus*	AQP1	437	90.55%	87.48%	99.58%	85.27%	86.87%
BKT1/ *R.ferrumeguinum*	AQP1	339	91.93%	90.99%	89.94%	87.32%	89.06%
BHK-21/ *M.auratus*	AQP1	361	85.48%	83.92%	72.55%	100%	88.37%
HEK293T/ H.*sapiens*	MUC-1	571	85.90%	82.81%	84.58%	84.70%	100%

Table 1-2 Primers used in this study.

Gene	Cells		Primers sequence (5'→ 3')	Application
Aqp1	FBKT1, DEMKT1, YUBFKT1, BHK-21, HEK293T	F	ATGGCCAGYGARTTCAAGAA	Cell marker amplification
		R	ATGGCCAGYGARTTCAAGAA	
	BKT1	F	ATGGCCAGCGAGTTCAAGAA	
		R	AGCTGCAGGGTGCCAATTAT	
MUC1	FBKT1, BKT1, DEMKT1, YUBFKT1	F	TYTKAACCTYCMRTTYAACTC	Cell marker amplification
		R	ACTCGCTCATAGGATGGTAG	
	BHK-21, HEK293T	F	TGGAAGATCCCAGCWCCRAC	
		R	CTACAAGTTGGCMGAAGTGG	
TLR3	BKT1	F	GYTACTYTRATTMTCTCYRC	Partial sequence cloning
		R	ARYTCGATGCACTRAAACRT	
	YUBFKT1	F	GYTACTYTRATTMTCTCYRC	
		R	CGTTCTTTCTGAASTGGCCA	
		F	TTAGGAACTCAGCTCCAACTG	qPCR
		R	ACACCCTGGAGAGAACTCTT	
	FBKT1	F	TTAGGAACTCAGCTCCAACTG	
		R	ACACCCTGGAGAGAACTCTT	
	BKT1	F	CCAGCTTTCCAGAACCTGAGT	
		R	TGAGGCGGAGTATTACAGAGGTA	
	DEMKT1	F	CCGAAGAGTGGCCCTTCAAA	
		R	GTGTTTCCAGAGGCGAGCTA	
	HEK293T	F	CACCATTCCAGCCTCTTCGT	
		R	CAGGGTTTGCGTGTTTCCAG	
	BHK-21	F	GAGCCAGAACTGTGCCAAAC	
		R	GGTCCCTGCAGAAGACGAAA	
RIG-I	DEMKT1	F	CTCTGTGCTGGAACCATTTT	Partial sequence cloning
		R	TCCCTCATCAGCTGAGAGAT	
	BKT1	F	TGCTTTTAARGCGTTTGCAR	
		R	TCTTTAAAGCATCCACAAGT	
	FBKT1	F	TGCTTTTAARGCGTTTGCAR	
		R	TCTTTAAAGCATCCACAAGT	
	YUBFKT1	F	AGCGGCGGAACCTGCTGGCC	
		R	TCTTTAAAGCATCCACAAGT	
	BKT1	F	CTCTGTGCTGGAACCATTTT	qPCR
		R	TCCCTCATCAGCTGAGAGAT	
	YUBFKT1	F	TGCTTTTAARGCGTTTGCAR	
		R	TCTTTAAAGCATCCACAAGT	
	DEMKT1, FBKT1	F	TGCTTTTAARGCGTTTGCAR	
		R	TCTTTAAAGCATCCACAAGT	
	HEK293T	F	AGCGGCGGAACCTGCTGGCC	
		R	TCTTTAAAGCATCCACAAGT	
	BHK-21	F	GCATGCGCGGATGAAAGATG	
		R	GCTGGGATCCATGGAAATGC	
MDA5	DEMKT1	F	GAGAACAGMMRCCTGTCC	Partial sequence cloning
		R	ACCAGGACGTAGGTGCTYTCAT	
	BKT1	F	GAGAACAGMMRCCTGACC	
		R	ACCAGGACGTAGGTGCTYTCAT	
	YUBFKT1	F	TGAAAAKGTAYATCCAGGT	
		R	ACCAGGACGTAGGTGCTYTCAT	
		R	TCACCATTTGTTTGATAGTC	
	FBKT1	F	TGAAAAKGTAYATCCAGGT	
		R	TGTYTCCARCTRCTGAACCT	
		R	TCACCATTTGTTTGATAGTC	

Gene	Cells		Primers sequence (5'→ 3')	Application
	YUBFKT1,	F	TCTGATTGGAGCTGGACACA	qPCR
	DEMKT1	R	CCACTGTGGTAGCGATAAGCA	
	BKT1	F	GCGGAATCGGCAAGAGGAAT	
		R	GGTGCGCTTTGACTCCTACT	
	FBKT1	F	GTGGCAGAAGAAGGTCTGGAT	
		R	CCAGGACGTAGGTGCTCTCA	
	HEK293T	F	GAGCAACTTCTTTCAACCACAG	
		R	CACTTCCTTCTGCCAAACTTG	
	BHK-21	F	TGGTGTGCAGCTGTCAGATT	
		R	ATCTGCGGCAGGTGAACTAC	
IFN-**β**	BKT1	F	AACCACAGCAGTTCCAGAAG	qPCR
		R	ATGGTCTCATTCCAGCCAGTG	
	FBKT1	F	TCCCTGCGGAGATTAAACAACC	
		R	ATGGTTTCATTCCAGCCAGTG	
	DEMKT1,	F	TCCCTGCGGAGATTAAACAACC	
		R	ATGGTCTCATTCCAGCCAGTG	
	YUBFKT1	F	AGAAGGAGAAAGCCGTGCTG	
		R	ATGGTCTCATTCCAGCCAGTG	
	HEK293T	F	CTTGGATTCCTACAAAGAAGCAGC	
		R	TCCTCCTTCTGGAACTGCTGCA	
IFN-λ_1	FBKT1	F	GCCCCAAAGAAAGTGTCTCAAG	qPCR
		R	GGCGGAAGAGGTGAATGTG	
	YUBFKT1	F	GACTGTGGCTGACTCATCCC	
		R	TGCTGTGGGCTGAGTTGAAA	
	HEK293T	F	GGACGCCTTGGAAGAGTCACT	
		R	AGAAGCCTCAGGTCCCAATTC	
TNF-α	BHK-21	F	CTCCTGTCCGCCATCAAGAG	qPCR
		R	AGTAGACCTGCCCGGATTCT	
	HEK293T	F	CTCCTGTCCGCCATCAAGAG	
		R	AGATGATCTGACTGCCTGGG	
	FBKT1, BKT1	F	CGACTGGCCTCCCACTAATC	
		R	TCTAATGGCACCACCAGCTG	
	DEMKT1	F	CAGCTGGTGGTGCCATTAGA	
		R	TCCTGGTAGGAGTCAGCGAA	
	YUBFKT1	F	GGCAGAACAAGATCGCCAAC	
		R	CCTTGTCCTGGTAGGAAGCG	
GAPDH	BKT1, DEMKT1,	F	TCACCAGGGCTGCTTTTAAC	qPCR
	FBKT1, YUBFKT	R	GTGCCTTTGAACTTGCCATG	
	HEK293T	F	GTCTCCTCTGACTTCAACAGCG	
		R	ACCACCCTGTTGCTGTAGCCAA	
	BHK-21	F	GAAGGTCGGAGTGAACGGAT	
		R	CTCAGCCTTGACTGTGCCTT	
EMCV		F	ATTCCACCTCCTCAGACAAGA	qPCR
		R	AGCTAGCAATGGAAGCATAT	
JEV		F	TCGCCCATCACCAGTGCGAG	
		R	CAAGTGGATGTTATCGG	
PRV		F	TTG GAT CGA ATG GTG CTG CT	
		R	TCG GGA GCA ACA CCT TTC TC	

Table 1-3. Primers used for the amplification of the nearly complete genome of the NIID-NU1 strain of encephalomyocarditis virus (EMCV). EMCV-specific primers were designed based on complete genome of the GS01 strain (KJ524643.1). DNA fragments corresponding to EMCV NIID-NU1 were amplified and the amplicons were sequenced.

Primer name	Primer sequence (5' → 3')	Position (*)	Amplified fragment (bp)
EMCV-P1 F	TGAATGTCGTGAAGGAAGCAGT	337-349	315 bp
EMCV-P1 R	ACCTCGACTAAACACATGT	633-651	
EMCV-P2 F	AYTRKHTGGRATCTRATCTGGGG	592-614	1189 bp
EMCV-P2 R	ACDGCWATSACCARDGTCCA	1761-1780	
EMCV-P3 F	AARGGNCCDTTYGCYATGG	1611-1629	1278 bp
EMCV-P3 R	NGTYTYYTCATTYCSRTTBCCC	2867-2888	
EMCV-P4 F	AGAACCAAACGAAGGTGGCT	2671-2690	1065 bp
EMCV-P4 R	TCTGAACCAGGGGCAGTCTA	3716-3735	
EMCV-P5 F	SGYYTRACNGARATYTGGGGVAA	2850-2872	1194 bp
EMCV-P5 R	GCATCACTGCTATHGTCATNCC	4122-4143	
EMCV-P6 F	CAACGAGGACGCCCRAAARG	3983-4002	845 bp
EMCV-P6 R	AGCCATCAGGATTTTGCCCT	4808-4827	
EMCV-P7 F	CARYTGATWGCMCCCATGACDAT	4110-4132	710 bp
EMCV-P7 R	GGATTYTGBCCYARATCRTCC	4799-4819	
EMCV-P8 F	AGTCAGGTTATTGCCCAGGC	4683-4702	1859 bp
EMCV-P8 R	GAGGTGTTCYTRTCCATRGG	6522-6541	
EMCV-P9 F	TTCTGCAATGTTGTGTGCTGC	5420-5440	820 bp
EMCV-P9 R	CCCATCTGGCAATCTCTCGA	6220-6239	
EMCV-P10 F	TGWRGTRGCHTTYTCMAARCA	6362-6382	1341 bp
EMCV-P10 R	TACTACTCTRGWYTATCTTG	7683-7702	
oligo-d(T) Anchor primer	GACCACGCGTATCGATGTCGACTT TTTTTTTTTTTTTV		
	GCAAAGACAGGATATAAGAT	7269-7288	449 bp
Anchor primer	GACCACGCGTATCGATGTCGAC		

Table 1.4. Encephalomyocarditis virus isolates used in this study. Multiple sequence alignment based on ORFs and other strains available from the GenBank nucleotide database was completed using the Clustal X program.

Virus designation (Accession number)	Group	Geographic origin	Host species	Nucleotides identitiy	Amino acid identity
EMCV-HB10 (JQ864080.1)	1A	China	Pig	99.75%	99.56%
EMCV-GS01 (KJ524643.1)	1A	China	Pig	99.75%	99.69%
EMCV-GX0601 (FJ604852.1)	1A	China	Pig	99.74%	99.48%
EMCV-GXLC (FJ897755.1)	1A	China	Pig	99.59%	99.17%
EMCV-CBNU (DQ517424.1)	1A	South Korea	Pig	99.77%	99.61%
EMCV-K3 (EU780148.1)	1A	South Korea	Pig	99.59%	99.30%
EMCV-K11 (EU780149.1)	1A	South Korea	Pig	99.59%	99.17%
EMCV-ZM (KF598864.1)	1A	China	Pig	99.48%	99.21%
EMCV BEL-2887A/91 (AF356822.1)	1A	Belgium	Pig	99.75%	99.61%
EMCV-C15 (KU664327.1)	1A	China	Dog	99.62%	99.48%
EMCV-PV21 (X74312.1)	1A	Germany	Pig	99.59%	99.52%
EMCV pEC9 (DQ288856.1)	1A	USA	Pig	99.64%	99.43%
EMC-R (M81861.1)	1A	USA	Chimpanzee	99.49%	99%
EMCV-30 (AY296731.1)	1A	USA	Pig	84.35%	96.42%
EMC-B (M22457.1)	1B	USA	Pig	82.43%	95.64%
EMC-D (M22458.1)	1B	USA	Pig	82.46%	95.81%
EMCV D-variant (M37588.1)	1B	Panama	Pig	82.57%	95.90%
EMCV-PV2 (X87335.1)	1B	Germany	Pig	82.54%	95.90%
Mengo virus (DQ294633.1)		USA	Mouse	80.07%	93.63%

Chapter 2: **Functional analysis of pattern recognition receptors in bat cell line post-viral infection**

Introduction

Chapter 1 has revealed that most bat cell lines had a lower viral replication of EMCV, JEV, and PRV with a different IFNs response than non-bat cell lines. The higher IFNs response might be caused by the higher stimulation from pattern recognition receptors. The main viral RNA sensors (TLR3, RIG-I, and MDA5) and IFN-β have been characterized in 18, 13, 12, and 13 bat species, respectively and are highly conserved than other mammalian species [81–85]. Similar activity of IFNs between bats and other mammalian species is confirmed by up-regulation of some interferon-stimulated genes (ISGs), such as ISG 54 and 56 after treatment with human IFNs in bat cell lines [42, 63]. It suggests that pattern recognition receptors and IFNs in bats have a similar function as other mammalian species. The different innate immune response that was observed in Chapter 1 is probably caused by the higher expression of pattern recognition receptors and IFNs, not by different activity of pattern recognition receptors and IFNs between bats and other mammals.

Previous study by Li et al. [82] and Cowled et al. [85] showed that RIG-I and TLR3 was constitutively expressed in horseshoe bats (*Rhinolophus sinicus* and *Rhinolophus affinis*) and the black flying foxes (*Pteropus alecto*), respectively. However, the significance of these highly expressed pattern recognition receptors for antiviral response has not been elucidated. To confirm the role of pattern recognition receptors in stimulating IFNs response as antiviral response in bat cell lines, the author performed gene knockdown of TLR3, RIG-I, and MDA5 mRNA. By lowering the expression of pattern recognition receptors, there will be insufficient signal for IFN production and supposedly increase viral replication in bat cell lines.

Materials and Methods

Cells and viruses

DEMKT1 (Leschenault's rousette, *Rousettus leschenaultii*, kidney), BKT1 (Greater horseshoe bat, *Rhinolophus ferrumequinum*, kidney), and YUBFKT1 (Eastern bent-wing bats, *Miniopterus fuliginosus*, kidney) cell lines were maintained in Dulbecco's modified eagle medium (DMEM; Nissui, Tokyo, Japan) supplemented with 10% fetal bovine serum (FBS; HyClone, Logan, USA), 2% L-Glutamine (Sigma, Milwaukee, Wisconsin, USA), 0.14% Sodium hydrogen carbonate ($NaHCO_3$; Sigma, Milwaukee, USA), and penicillin-streptomycin (Meiji, Tokyo, Japan) at final concentration of 100 U/mL (penicillin) and 0.1 μg/mL (streptomycin).

The viruses used in this study, encephalomyocarditis virus (EMCV, strain NIID-NU1), the Japanese encephalitis virus (JEV, JEV/sw/Chiba/88/2002), and the pteropine orthoreovirus (PRV, Garut-50) was previously isolated from swine for JEV [66] and large flying fox (*Pteropus vampyrus*) for PRV. Both EMCV and JEV were propagated in BHK-21 cells, while the PRV was propagated in Vero 9013 cells (JCRB number; JCRB9013).

Knockdown of Pattern Recognition Receptors in bat cell lines

Phosphorothioate antisense RNA oligonucleotide (s-oligo) were synthesized using the consensus sequences of TLR3, RIG-I, and MDA5 genes of three bats species (*R. ferrumequinum, M. fuliginosus,* and *R. leschenaultii)* (Figure 1-5, 1-6, and 1-7) at FASMAC Co., Ltd., Kanagawa, Japan. The sequence of s-oligo used in this study were as follows: *TLR3*, 5'-GCACAAUUCUGGCUCCAGUTT-3'; *RIG-I*, 5'-AUCUGAGAAGGCAUUCAACTT-3'; and *MDA5*, 5'-UGACACUUCCUUCUGCCAATT-3'. Bat cell lines (BKT1, DEMKT1, and

YUBFKT1) were transfected with the antisense RNA oligonucleotides (120 pmol) using polyethylenimine [68].

The knockdown was verified by measuring the expression level of TLR3, RIG-I, and MDA5 by qRT-PCR. The knockdown cells were then infected with EMCV and JEV at the MOI of 1.0; and PRV at the MOI of 0.1. RNA extraction and first strand cDNA synthesis using 500 ng of total RNA were performed at 1-day post infection. The expression levels of TLR3, RIG-I, MDA5, IFN-β, and GAPDH genes; and viral genome titers were determined by qRT-PCR. The cell growth was measured using trypan blue dye exclusion test.

Result

The knockdown of pattern recognition receptors (PRRs) was confirmed by qRT-PCR in which only the expression level of PRRs was significantly reduced in BKT1 (Figure 2-1a). Knockdown of PRRs in other bat cell lines (DEMKT1 and YUBFKT1 cells) was not successful, as the expression level of PRRs was not decreased in those cell lines. The expression level of IFN-β was also decreased in BKT1 but it was not as intensive as that of PRRs (Figure 2-1b).

Knockdown of TLR3, RIG-I, and MDA5 caused a total destruction cytopathic effect (CPE) at 1-day post EMCV infection in cells knocked down for RIG-I and MDA5, and at 2 days post EMCV infection in cells knocked down for TLR3. In contrast, no CPE was observed in the BKT1 without knockdown of PRRs (Figure 2-2). The number of live cells in EMCV-infected knockdown cells was significantly lower than uninfected knockdown cells since day 1 of EMCV infection (Figure 2-3a–c). The cells without knocked down for PRRs just showed a significant lower live cell numbers since day 3 of EMCV infection (Figure 2-3d).

After JEV infection, the total destruction CPE in PRRs knockdown cells was observed at 5 days post infection, while no CPE was observed in cells without gene knockdown (Figure 2-4). The numbers of live cells in JEV-infected knockdown cells was significantly lower than uninfected knockdown cells since days 3 of JEV infection (Figure 2-5 a–c). The cells without knocked down for PRRs just showed a significant lower live cell numbers since days 5 of JEV infection (Figure 2-5d).

After PRV infection, the syncytial CPE in PRRs knockdown cells was observed at 1-day post infection in cells knocked down for RIG-I, and at 2 days post infection in cells knocked down for TLR3 and MDA5. In contrast, no CPE was observed in cells

without knocked down for PRRs (Figure 2-6). The number of live cells in PRV-infected cells knocked down for RIG-I was significantly lower than uninfected knockdown cells since days 1 of PRV infection, while the number of live cells in PRV-infected cells knocked down for TLR3 and MDA5 was significantly lower than uninfected knockdown cells since days 2 of PRV infection (Figure 2-7a–c). Cells without knocked down for PRRs just showed a significant lower live cell numbers since day 3 of PRV infection (Figure 2-7d).

Knockdown of TLR3, RIG-I, and MDA5 led to a reduced expression level of IFN-β after EMCV, JEV, and PRV infection (Figure 2-8). The expression of IFN-β was the lowest in the cells knocked down for TLR3 after EMCV infection and RIG-I after PRV infection. After JEV infection, all cells knocked down for either of the three PRRs showed a comparable IFN-β expression level.

All PRRs-knockdown cells showed a significantly higher viral genome titer of EMCV, JEV, and PRV than cells without gene knockdown, except PRV-infected cells knockdown for TLR3 (Figure 2-9). Cells knocked down for MDA5 demonstrated the highest viral genome titer of EMCV and JEV while cells knocked down for RIG-I showed the highest viral genome titer of PRV.

Discussion

Knockdown of TLR3, RIG-I, and MDA5 resulted in decreased expression level of IFN-β, suggesting that these pattern recognition receptors (PRRs) are important for stimulating IFN-β production in horseshoe bat cell line (BKT1). Increased replication level of EMCV, JEV, and PRV after knockdown of PRRs indicates that TLR3, RIG-I, and MDA5 are responsible for suppressing EMCV and JEV replication in BKT1 through IFN-β production. IFN-β is predominantly induced by TLR3 after EMCV infection and RIG-I after PRV infection but comparable IFN-β expression level was shown in all cells knocked down for PRRs after JEV infection. In a previous study, knockdown of PRRs in the big brown bats (*Eptesicus fuscus*) kidney cells also showed that IFN-β is predominantly induced by TLR3 than RIG-I and MDA5 after poly(I:C) transfection [47]. It suggests that bats might use different PRRs to sense viral RNA for producing IFN-β.

IFN-β as the main antiviral response against PRV is confirmed because cells knocked down for RIG-I that had the lowest IFN-β expression level, also had the highest PRV replication level. RIG-I, MDA5, and IFN-β were also highly up-regulated after Nelson Bay orthoreovirus (NBV) infection in bat cell lines derived from the black flying foxes (*Pteropus alecto*), the natural host of PRV and L929 mouse fibroblast cell lines that is resistant against NBV [91].

Knockdown of MDA5 resulted in the highest EMCV and JEV replication level among all cells knocked down for PRRs. Previous studies have shown that MDA5 is the dominant mediator of type I IFN and cytokine response during EMCV infection in mice because of RIG-I degradation by EMCV 3C protease [50, 57]. MDA5 seemed to have a greater role in stimulating antiviral pathway in horseshoe bats because it was highly up-regulated as compared to other PRRs after EMCV infection of BKT1 and was the only

up-regulated PRRs after JEV infection. It is possible that MDA5 stimulates antiviral pathways other than IFNs during EMCV and JEV infection of BKT1. Transcriptome studies in some bats species showed a high proportion of unannotated transcript (88–90), suggesting them as bats-specific transcript that might have an important role in antiviral mechanism [95].

In conclusion, TLR3, RIG-I, and MDA5 play important roles in antiviral response against EMCV, JEV, and PRV infections, at least in horseshoe bats.

Figures

Figure 2-1

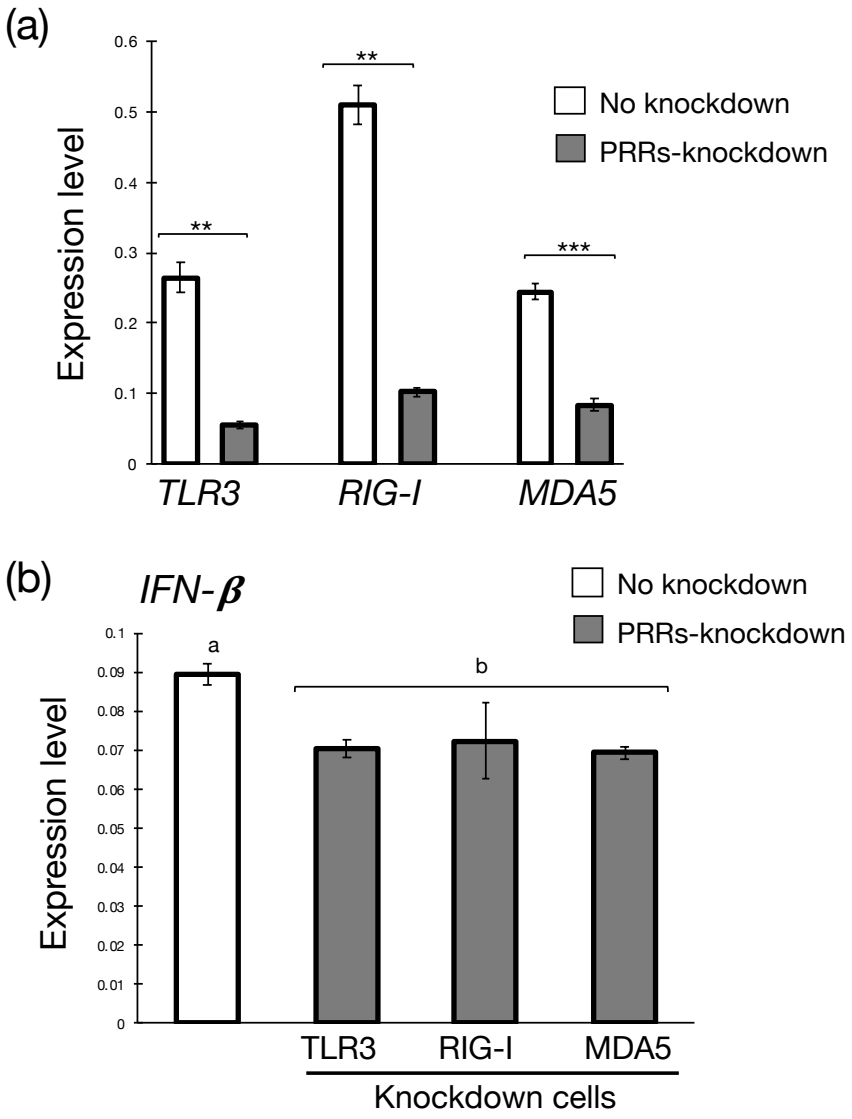

Gene knockdown of TLR3, RIG-I, and MDA5 in BKT1. Expression level of TLR3, RIG-I and MDA5 after knockdown of each pattern recognition receptors (a) (mean ± SD, n = 3). *p < 0.01 vs Not infected, **p < 0.001 vs Not infected. Expression level of IFN-β after knockdown of TLR3, RIG-I, and MDA5 (b) (mean ± SD, n = 3). Differences between groups were analyzed by one-way ANOVA, followed by Tukey's test. Values that do not share a common letter are significantly different ($p<0.05$).

Figure 2-2

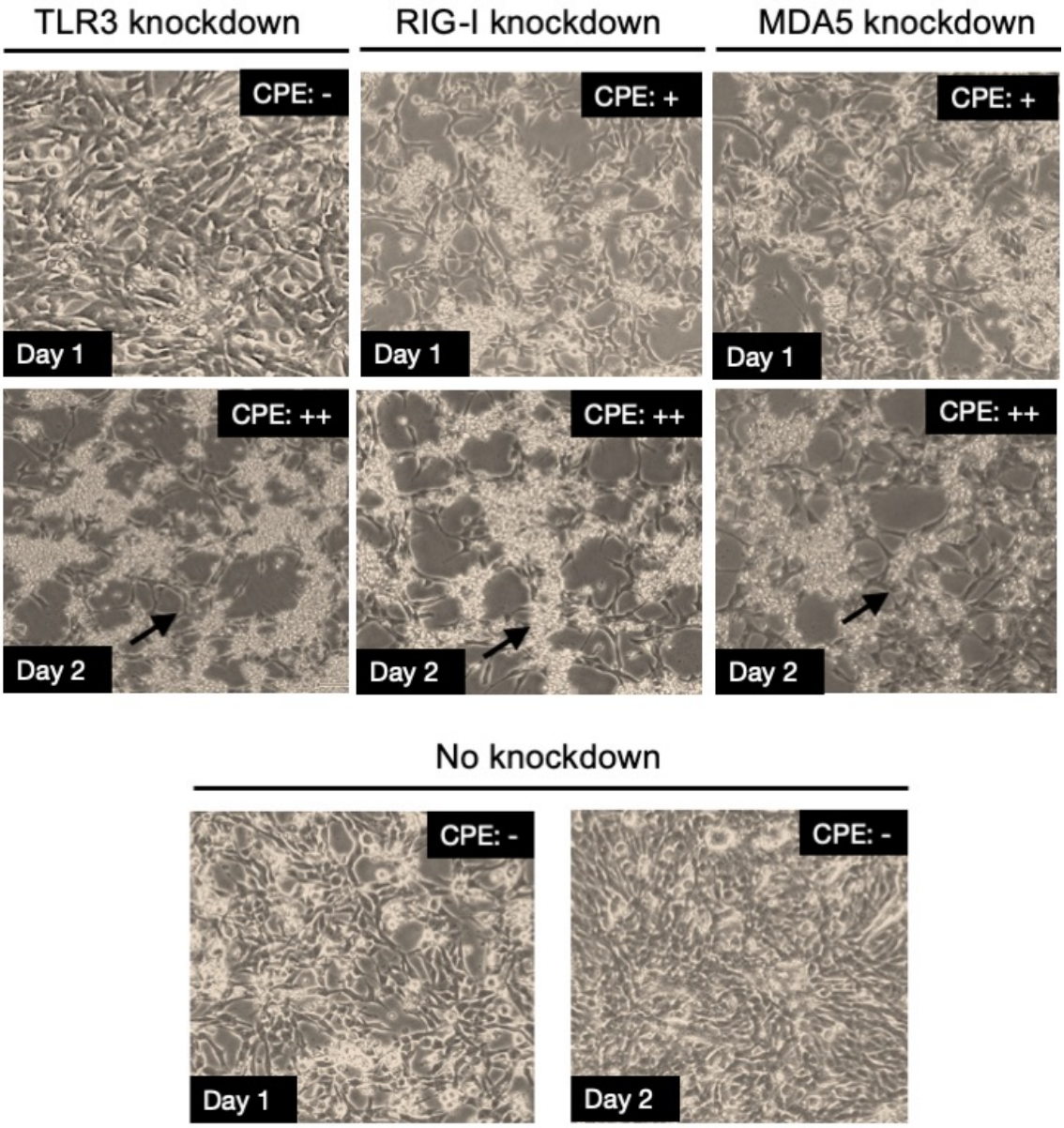

Cytopathic effect (CPE) after EMCV infection in BKT1 knocked down for PRRs. EMCV infection caused fast total destruction CPE in cell knocked down for TLR3, RIG-I and MDA5 at 2 days post EMCV infection. BKT1 without gene knockdown did not show CPE at 2 days post EMCV infection. The total destruction CPE after EMCV infection is indicated by arrow.

Figure 2-3

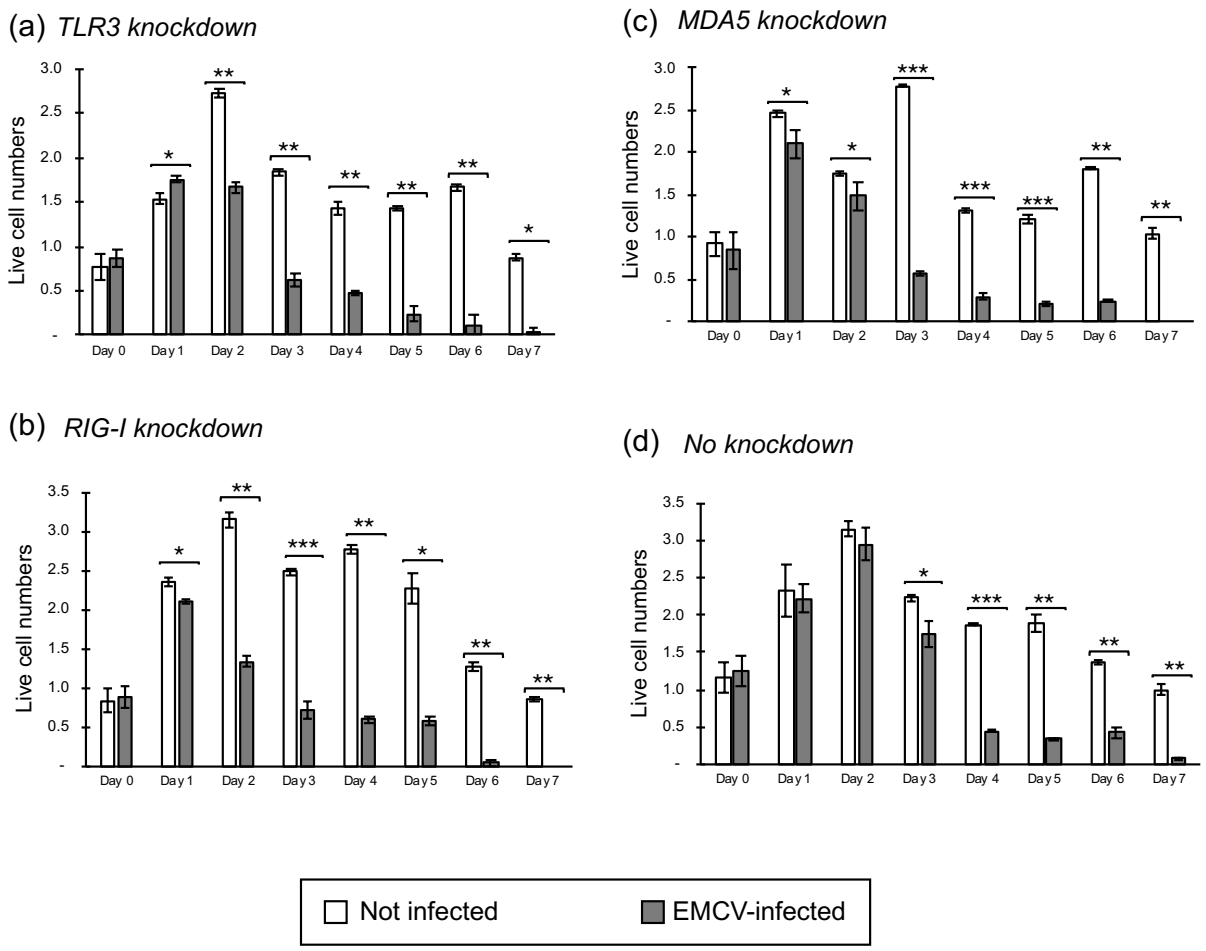

Cell growth after EMCV infection in BKT1 knocked down for PRRs. Live cell numbers in BKT1 knocked down for TLR3 (a), RIG-I (b), MDA5 (c), and without gene knockdown (d) were measured until 7 days post EMCV infection at multiplicity of infection (MOI) of 1.0 (mean ± SD, n = 3). Live cells number is expressed as $x10^5$ cells/mm^3. *$p < 0.05$ vs Not infected, **$p < 0.005$ vs Not infected, ***$p<0.0005$ vs Not infected

Figure 2-4

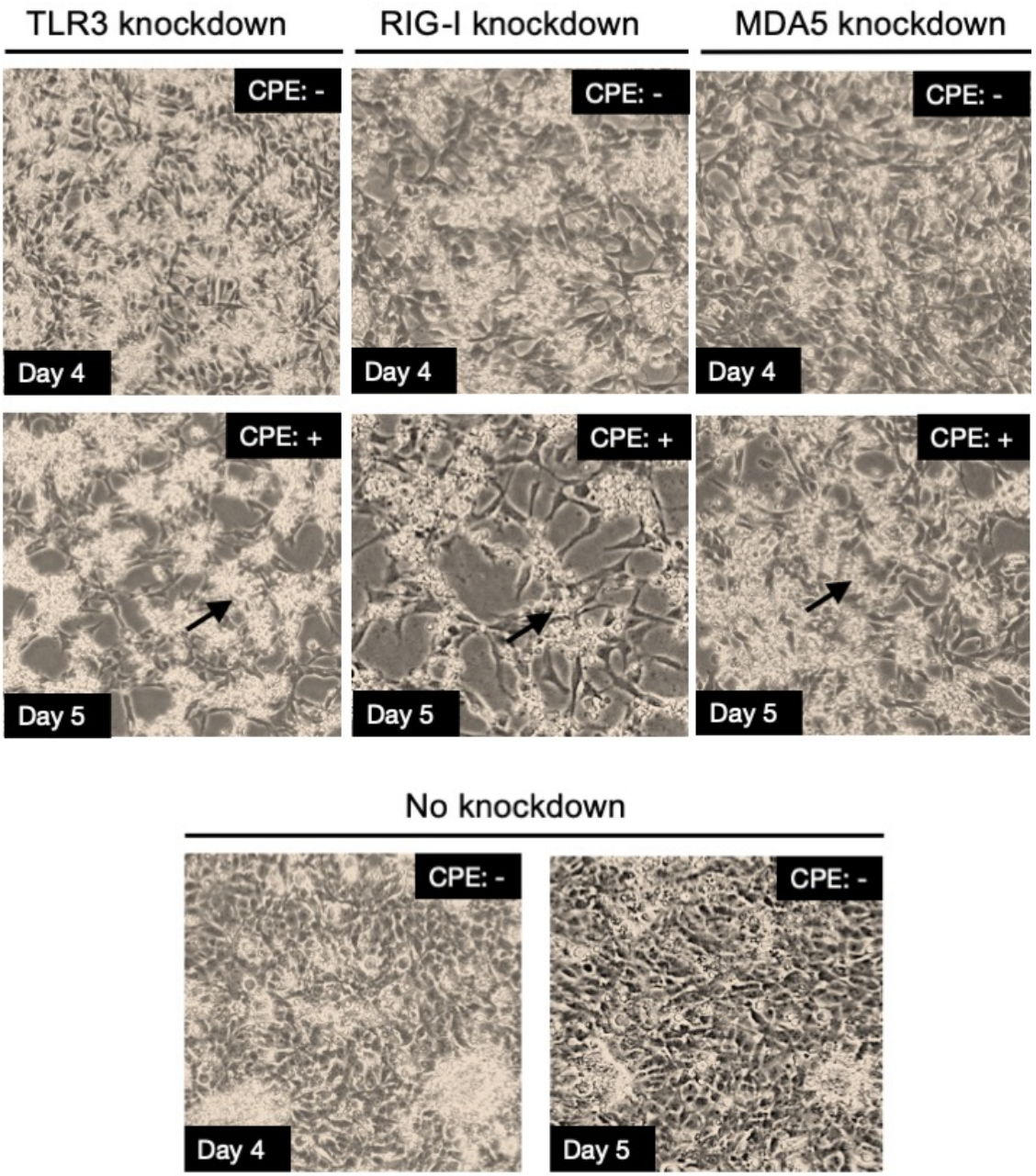

Cytopathic effect (CPE) after JEV infection in BKT1 knocked down for PRRs. JEV infection caused total destruction CPE in BKT1 knocked down for TLR3, RIG-I and MDA5 at 5 days post JEV infection. BKT1 without gene knockdown did not show CPE at 5 days post JEV infection. The total destruction CPE after JEV infection is indicated by arrow.

Figure 2-5

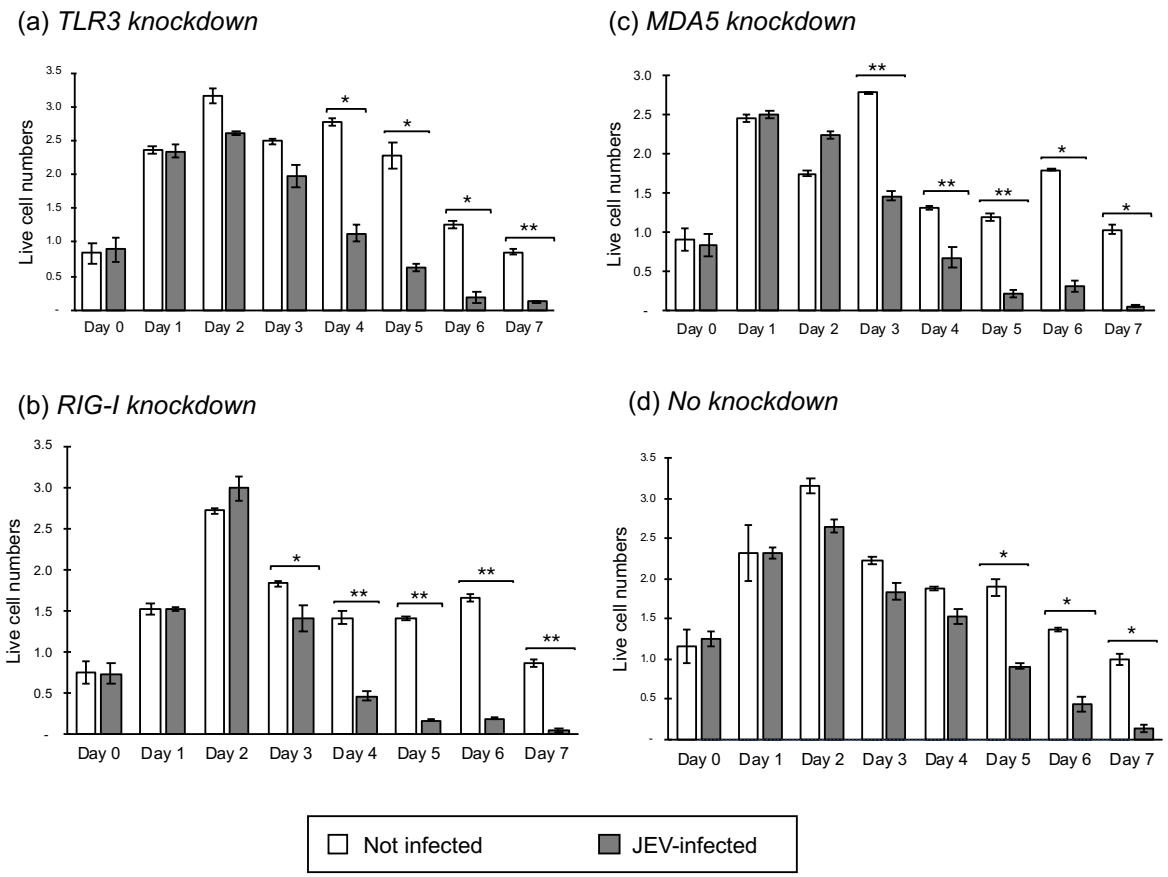

Cell growth after JEV infection in BKT1 knocked down for PRRs. Live cell numbers in BKT1 knocked down for TLR3 (a), RIG-I (b), MDA5 (c), and without gene knockdown (d) were measured until 7 days post JEV infection at multiplicity of infection (MOI) of 1.0 (mean ± SD, n = 3). Live cells number is expressed as $x10^5$ cells/mm^3. *p < 0.05 vs Not infected, **p < 0.01 vs Not infected, ***p<0.001 vs Not infected.

Figure 2-6

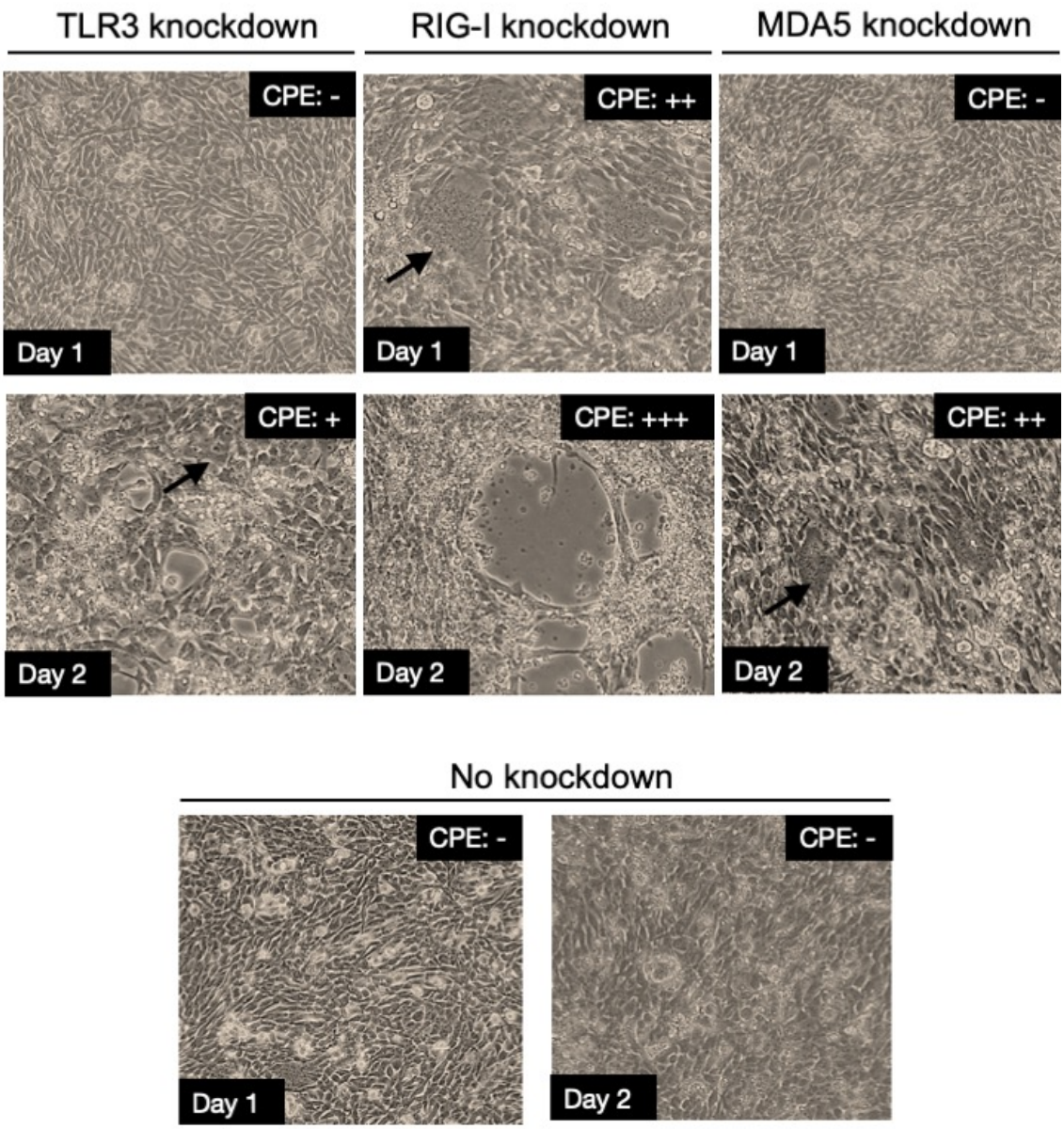

Cytopathic effect (CPE) after PRV infection in BKT1 knocked down for PRRs. PRV infection caused syncytial CPE in BKT1 knocked down for RIG-I at 1-day post infection; and in BKT1 knocked down for TLR3 and MDA5 at 2 days post infection. BKT1 without gene knockdown did not show CPE at 2 days post PRV infection. The syncytial CPE after PRV infection is indicated by arrow.

Figure 2-7

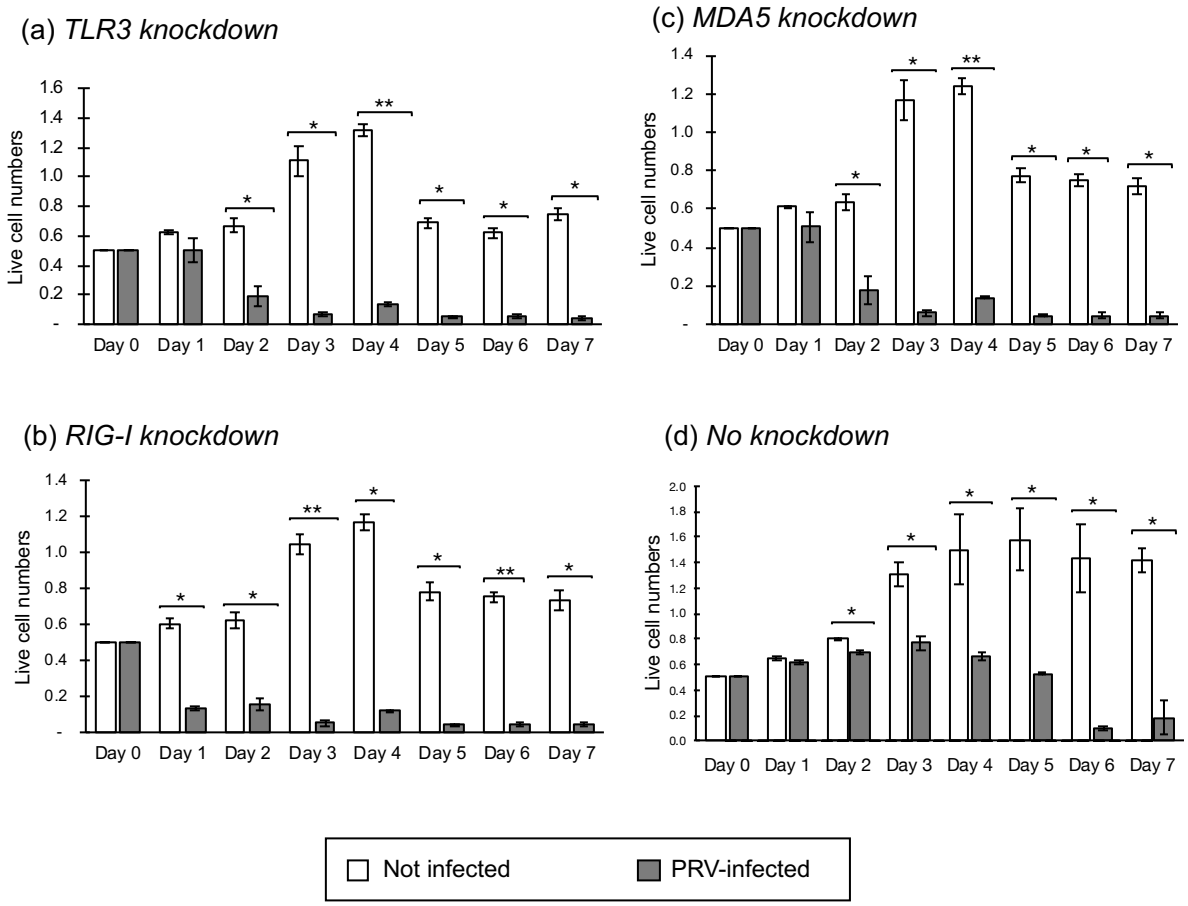

Cell growth after PRV infection in BKT1 knocked down for PRRs. Live cell numbers in BKT1 knocked down for TLR3 (a), RIG-I (b), MDA5 (c), and without gene knockdown (d) were measured until 7 days post PRV infection at multiplicity of infection (MOI) of 0.1 (mean ± SD, n = 3). Live cells number is expressed as $x10^5$ cells/mm^3. *p < 0.05 vs Not infected, **p < 0.005 vs Not infected, ***p<0.0005 vs Not infected.

Figure 2-8

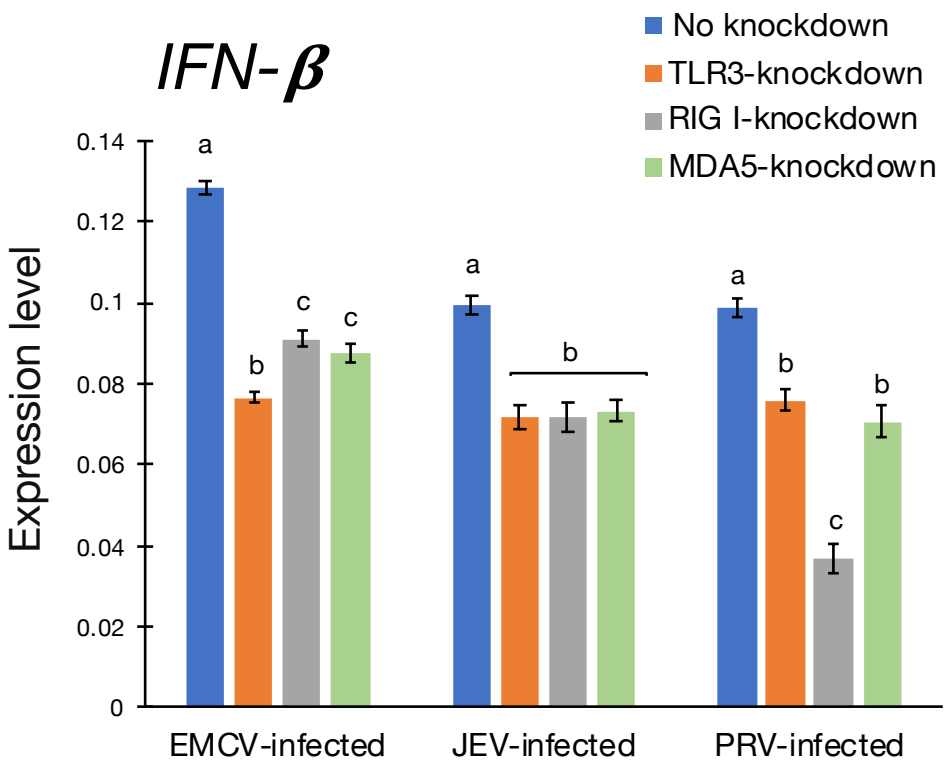

IFN expression in BKT1 knocked down for PRRs. All BKT1 knocked down for PRRs (TLR, RIG-I, and MDA5) had a significantly lower expression of IFN-β than BKT1 without gene knockdown after infection with EMCV, JEV, and PRV (mean ± SD, n = 3). Differences between groups were analyzed by one-way ANOVA, followed by Tukey's test. Values that do not share a common letter are significantly different ($p<0.05$).

Figure 2-9

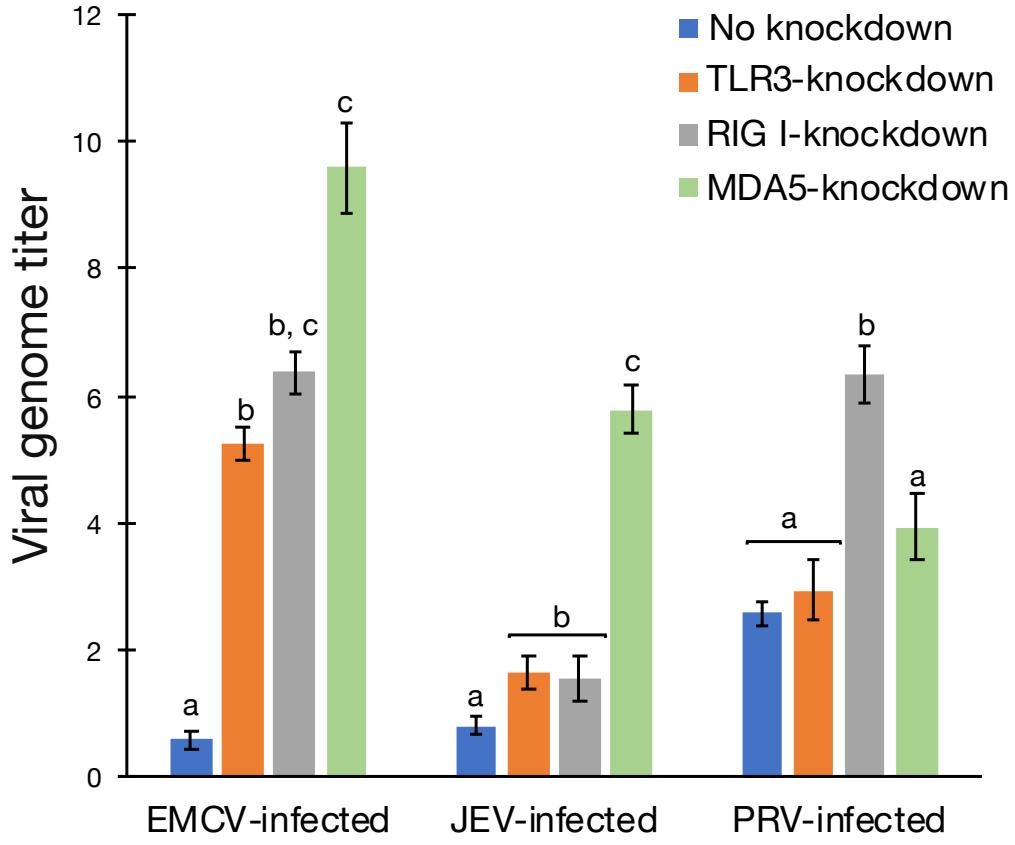

Viral replication in BKT1 knocked down for PRRs. The viral genome titer is significantly higher in BKT1 knocked down for PRRs (TLR3, RIG-I, and MDA5) than BKT1 without gene knockdown after infection with EMCV, JEV, and PRV (b). Viral genome titer is expressed as: $x10^8$ copy numbers/μg total RNA (mean ± SD, n = 3). Differences between groups were analyzed by one-way ANOVA, followed by Tukey's test. Values that do not share a common letter are significantly different ($p<0.05$).

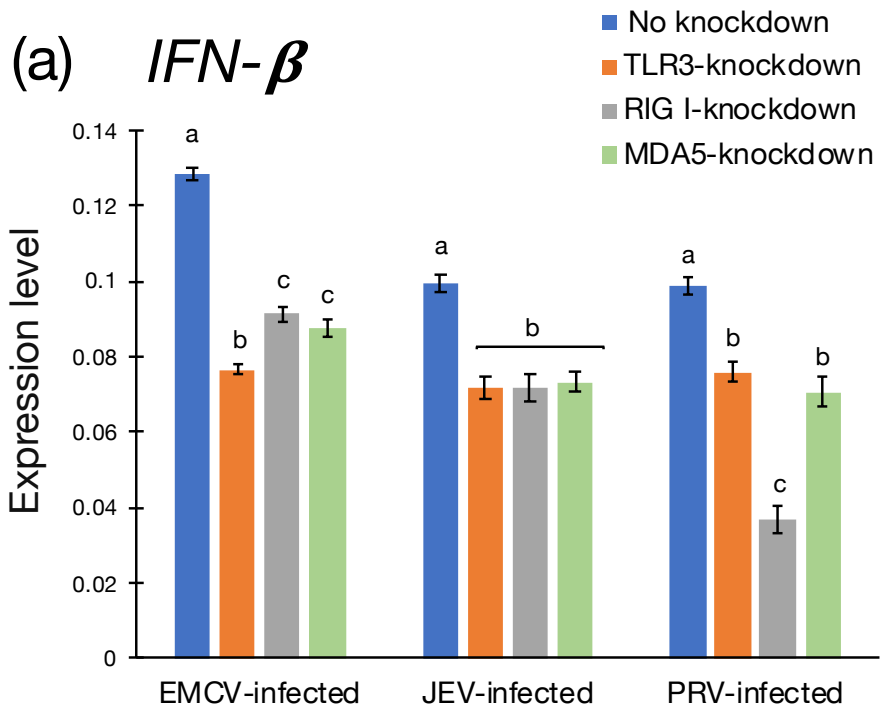
(a) IFN-β
No knockdown
TLR3-knockdown
RIG I-knockdown
MDA5-knockdown
Expression level
0.14
0.12
0.1
0.08
0.06
0.04
0.02
0
a
b
c
c
a
b
a
b
c
b
EMCV-infected
JEV-infected
PRV-infected

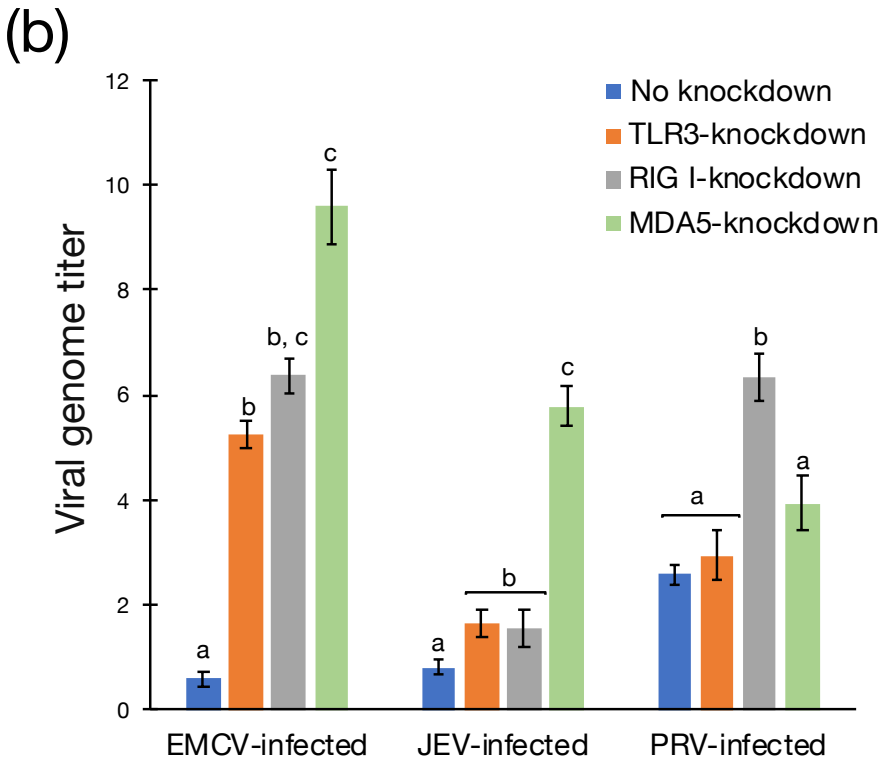
(b)
No knockdown
TLR3-knockdown
RIG I-knockdown
MDA5-knockdown
Viral genome titer
12
10
8
6
4
2
0
a
b
b, c
c
a
b
c
a
a
b
a
EMCV-infected
JEV-infected
PRV-infected

General discussion and conclusion

As the natural hosts of several highly pathogenic viruses, it is important to understand how infection with the same virus could cause different outcome between bats as natural hosts and humans as susceptible host [3, 5, 6, 96–98]. In this study, the author focused on the innate immune response on bats as the first line of defense against invading pathogens. This information is crucial to understand how bats can control viral replication without developing little significant clinical sign. As the model of bats-viruses interaction, the author used four cell lines derived from four bat species that have been identified as natural hosts of highly pathogenic viruses, such as horseshoe bats (SARS-CoV), rousette bats (Marburg virus), and flying foxes (Hendra and Nipah virus). In addition, the viruses used in this study: encephalomyocarditis virus (EMCV), Japanese encephalitis virus (JEV), and pteropine orthoreovirus (PRV), previously have been detected or isolated in bats. Most bat cell lines used in this study are resistant against those viruses, suggesting that the special innate immune response exists in bats (Chapter 1). In contrast, those viruses were highly replicated in human cell line and induced expression of pro-inflammatory cytokine, which suggests a strong self-damaging inflammation and serious diseases in human.

Bats are the only mammals capable of sustainable flight that consequently increase body temperature and metabolic rate, then produce reactive oxygen species that cause bats more susceptible to damaging DNA. To reduce the self-DNA mediated immunopathology generated by flight, the endogenous DNA-sensing pathway has been dampened in bats such as loss of PYHIN gene family [99] and lack activation of STING (stimulator of interferon genes) [100]. STING has dual function in host defense, inhibit protein synthesis of RNA viruses and stimulate interferons (IFNs) to restrict DNA viruses replication [101]. This flight evolution should have consequence for increased

susceptibility against viruses in bats. However, bats remain asymptomatic after infection with highly pathogenic viruses, which suggests that they had a special antiviral mechanism to counteract the dampened DNA-sensing pathway. Firstly, it is hypothesized that bats can control viral replication because of the "always on" IFNs system that is found in the black flying foxes (*Pteropus alecto*). However, this study showed that most bat cell lines had a comparable basal expression of IFN-β compared to other mammalian cell lines. These finding suggests that the "always on" IFNs system is not the general characteristic of bats. Surprisingly, the basal expression of all pattern recognition receptors for viral RNA sensing (TLR3, RIG-I, and MDA5) in bat cell lines are significantly higher than other mammalian cell lines (Chapter 1). These finding suggests that bats have a higher capacity for viral RNA recognition that will produce a higher signal for IFNs production.

EMCV, JEV, and PRV infection stimulated the expression of pattern recognition receptors and IFNs in both bats and other mammalian cell lines. However, two pattern recognition receptors (RIG-I and MDA5) and IFNs (β and λ_1) are more highly up-regulated in bat cell lines than other mammalian cell lines (Chapter 1). Higher expression of RIG-I and MDA5 enable more viral RNA sensing and stimulate more IFNs production in bat cell lines. IFNs also can generate a positive feedback loop to activate more production of RIG-I and MDA5 [102, 103]. Another possibility is the RNaseL that is induced by IFNs in the black flying foxes (*Pteropus alecto*), can produce shorter viral RNA fragments to potentiate the IFNs response by activating the cytosolic RNA sensor, such as RIG-I and MDA5 [42]. Chapter 1 provides evidences about the importance of IFNs response in bats, however the IFNs response in bats showed species variation. Type I IFNs gene cluster was varied among bats species, type I IFNs locus has contracted in

P.alecto but expanded in the little brown bats (*Myotis lucifugus*) and the Egyptian fruit bats (*Rousettus aegypticus*) [18, 104, 105]. A study performed by Wu et al. [106] showed a different viral diversity among 40 major bat species across China. It will be a great interest to determine whether the different viral diversity among bats is related to different IFNs response.

Chapter 1 provides significant data about unique innate immune system in bats that inhibit viral infection in bats. However, how viral spillover from bats to humans or domestic mammals occur since viruses inefficiently replicate in bats remain unclear. One critical factor for viral spillover from bats is a high viral shedding from bats [107]. Chapter 2 demonstrate that viral replication was increased after suppression of innate immune response by means of decreasing the expression of pattern recognition receptors and IFNs. In nature, suppression to the immune system in bats resulting in failing to inhibit viral replication occurs during reproductive cycle (parturition and lactation) and starvation [108–110]. High number of viruses shed from such immune-suppressed bats might increase the possibility of the emergence of bat-borne viruses in human population. High seroprevalence and seasonal spillover of Hendra virus [111–113], Nipah virus [114], and ebola virus [115] have been noted to coincide with food shortage and breeding season of bats. One study reported the recrudescence of Nipah virus in captive bats is triggered by increased level of stress due to a combination of factors such as confinement in the cage, and physiological and behavioral changes during the breeding season [116].

"With the advent of truly global travel, the last five centuries have seen more new diseases than ever before become potential pandemic" —Arno Karlen [8]. The threat of emerging infectious diseases in the twenty-first century is real. Population growth in many developing countries have compelled massive deforestation in order to provide land

for settlement, agriculture, and plantation. This massive deforestation has caused shrinking or loss of habitat for bats. Consequently, bats migrated to new places adjacent to human settlement. Colonization of bat near human settlement greatly increases the chance of viral spillover from bats to human, either directly or indirectly through intermediate host. Once the virus adapted and transmitted efficiently among the human population, it may rapidly cause a severe outbreak or even pandemic due to frequent international travel in this globalization era. Bats (order Chiroptera) pose a considerable threat to human health because hold the highest viral diversity among mammals [117].

My study reveals the importance of innate immune system for suppressing viral replication in bats. In nature, reproductive cycle and environmental change often suppress the immune system of bats with a consequence of increasing viruses number in bat population [108–110]. The most crucial effort would be preventing deforestation as the major driver of immunosuppression in bats. Protection of native bat habitats will restrict viruses inside the bat population and prevent the emergence of bat-borne viruses in the human population.

Ackowledgements

I would like to express my sincere gratitude and deepest appreciation to the following peoples who have contributed to the success of this thesis.

To Professor Eiichi Hondo, for his generosity in providing me an opportunity to study with him, for his creative and interesting ideas, always encourage to be enthusiasm with sciences; and teaches me about logical thinking and how to be a good scientist.

To Assistant Professor Atsuo Iida, for his helpful direction and constructive advices in my study.

To Dr. Hitoshi Takemae, for kindly teach me how to do experiment properly since I was involved in the SATREPS project, and providing some materials for my research.

To Professor Ken Maeda and Dr Hiroshi Shimoda, for sharing their knowledge and constructive advices for the improvement of my study, and for providing some materials for my research.

To the past and present members of Laboratory of Animal Morphology for their friendship and their generous support.

To MEXT (The Japanese Ministry of Education, Culture, Sports, Science, and Technology) and SATREPS project: Ecological studies on flying foxes and their involvement in rabies-related and other viral infectious diseases, for providing me the scholarship that enable me to study in PhD course.

To the Ministry of Research, Technology, and Higher Education of Republic Indonesia and IPB University for giving me permission to study PhD course.

In the end I would like to express my gratitude to my wife, Monika Danaparamitha Andriani, my parents and sister for their support and understanding.

References

1. Zhu N, Zhang D, Wang W, Li X, Yang B, Song J, Zhao X, Huang B, Shi W, Lu R, Niu P, Zhan F, Ma X, Wang D, Xu W, Wu G, Gao G.F, Tan W (2020) A novel coronavirus from patients with pneumonia in China, 2019. *N Engl J Med* 382(8): 727–733.

2. Leroy E.M, Kumulungui B, Pourrut X, Rouquet P, Hassanin A, Yaba P, Délicat A, Paweska J.T, Gonzalez J.P, Swanepoel R (2005) Fruit bats as reservoirs of Ebola virus. *Nature* 438(7068): 575–576.

3. Hu B, Ge X, Wang L.F, Shi Z (2015) Bat origin of human coronaviruses. *Virol J* 12(221): 1–10.

4. Pillai V.S, Krishna G, Veettil M.V (2020) Nipah Virus: Past Outbreaks and Future Containment. *Viruses* 12(4): 465–480.

5. Towner J.S, Amman B.R, Sealy T.K, Carroll S.A.R, Comer J.A, Kemp A, Swanepoel R, Paddock C.D, Balinandi S, Khristova M.L (2009) Isolation of genetically diverse Marburg viruses from Egyptian fruit bats. *PLoS Pathog* 5(7): e1000536.

6. Halpin K, Young P.L, Field H.E, Mackenzie J.S (2000) Isolation of Hendra virus from pteropid bats: a natural reservoir of Hendra virus. *J Gen Virol* 81(8): 1927–1932.

7. Hayman D.T (2016) Bats as viral reservoirs. *Annu Rev Virol* 3: 77–99.

8. Karlen A (1996) Man and microbes: Disease and Plagues in History and Modern Times. Simon and Schuster Paperbacks.

9. O'Shea T.J, Cryan P.M, Cunningham A.A, Fooks A.R, Hayman D.T, Luis A.D, Peel A.J, Plowright R.K, Wood J.L (2014) Bat flight and zoonotic viruses. *Emerg Infect Dis* 20(5): 741–745.

10. Field H, McCall B, Barrett J (1999) Australian bat lyssavirus infection in a captive juvenile black flying fox. *Emerg Infect Dis* 5(3): 438–440.

11. McColl K.A, Chamberlain T, Lunt R.A, Newberry K.M, Middleton D, Westbury H.A (2002) Pathogenesis studies with Australian bat lyssavirus in grey-headed flying foxes (*Pteropus poliocephalus*). *Aust Vet J* 80(10): 636–641.

12. Middleton D.J, Morrissy C.J, Van Der Heide B.M, Russell G.M, Braun M.A, Westbury H.A, Halpin K, and Daniels P.W (2007) Experimental Nipah virus infection in pteropid bats (*Pteropus poliocephalus*). *J. Comp. Pathol.* 136(4): 266–272.

13. Munster V. J, Adney D.R, Van Doremalen N, Brown V.R, Miazgowicz K.L, Milne-Price S, Bushmaker T, Rosenke R, Scott D, Hawkinson A (2016) Replication and shedding of MERS-CoV in Jamaican fruit bats (*Artibeus jamaicensis*). *Sci. Rep.* 6(1): 1–10.

14. Paweska J.T, Storm N, Grobbelaar A, Markotter W, Kemp A, Van Vuren P.J (2016) Experimental inoculation of Egyptian fruit bats (*Rousettus aegyptiacus*) with Ebola virus. *Viruses* 8(2): 29-40.

15. Blatteis C.M (2003) Fever: pathological or physiological, injurious or beneficial? *J Therm Biol* 28(1): 1–13.

16. Chionh Y.T, Cui J, Koh J, Mendenhall I.H, Ng J.H, Low D, Itahana K, Irving A.T, Wang L.F (2019) High basal heat-shock protein expression in bats confers resistance to cellular heat/oxidative stress. *Cell Stress Chaperones* 24(4): 835–849.

17. Baker M.L, Schountz T, Wang L.F (2013) Antiviral immune responses of bats: a review. *Zoonoses Public Health* 60(1): 104–116.

18. Zhou P, Tachedjian M, Wynne J.W, Boyd V, Cui J, Smith I, Cowled C, Ng J.H, Mok L, Michalski W.P (2016) Contraction of the type I IFN locus and unusual constitutive expression of IFN-α in bats. *Proc Natl Acad Sci* 113(10): 2696–2701.

19. Reikine S, Nguyen J.B, Modis Y (2014) Pattern recognition and signaling mechanisms of RIG-I and MDA5. *Front Immunol* 5(342): 1–7.

20. Doysabas K.C.C, Oba M, Furuta M, Iida K, Omatsu T, Furuya T, Okada T, Sutummaporn K, Shimoda H, Wong M.L, Wu C.H, Ohmori Y, Kobayashi R, Hengjan Y, Yonemitsu K, Kuwata R, Kim Y.K, Han S.H, Sohn J.H, Han S.H, Suzuki K, Kimura J, Maeda K, Oh H.S, Endoh D, Mizutani T, Hondo E (2019) Encephalomyocarditis virus is potentially derived from eastern bent-wing bats living in East Asian countries. *Virus Res* 259: 62–67.

21. Fagre A.C, Kading R.C (2019) Can bats serve as reservoirs for arboviruses? *Viruses* 11(3): 215–242.

22. Wang J.L, Pan X.L, Zhang H.L, Fu S.H, Wang H.Y, Tang Q, Wang L.F, Liang G.D (2009) Japanese encephalitis viruses from bats in Yunnan, China. *Emerg Infect Dis* 15(6): 939–942.

23. Takemae H, Basri C, Mayasari N.L.P.I, Tarigan R, Shimoda H, Omatsu T, Pramono D, Cahyadi D.D, Kobayashi R, Iida K, Mizutani T, Maeda K, Agungpriyono S, Hondo E. 2018. Isolation of Pteropine orthoreovirus from *Pteropus vampyrus* in Garut, Indonesia. *Virus Genes* 54(6): 823–827.

24. Taniguchi S, Maeda K, Horimoto T, Masangkay J.S, Puentespina R, Alvarez J, Eres E, Cosico E, Nagata N, Egawa K, Singh H, Fukuma A, Yoshikawa T, Tani H, Fukushi S, Tsuchiaka S, Omatsu T, Mizutani T, Une Y, Yoshikawa Y, Shimojima M, Saijo M, Kyuwa S (2017) First isolation and characterization of pteropine orthoreoviruses in fruit bats in the Philippines. *Arch Virol* 162(6): 1529–1539.

25. Carocci M, Bakkali-Kassimi L (2012) The encephalomyocarditis virus. *Virulence* 3(4): 351–367.

26. Oberste M.S, Gotuzzo E, Blair P, Nix W.A, Ksiazek T.G, Comer J.A, Rollin P, Goldsmith C.S, Olson J, Kochel T.J (2009) Human febrile illness caused by encephalomyocarditis virus infection, Peru. *Emerg Infect Dis* 15(4): 640–646.

27. Hirasawa K, Takeda M, Matsuzaki H, Doi K (1991) Encephalomyocarditis (EMC) virus-induced orchitis in Syrian hamsters. *Int J Exp Pathol* 72(6): 640–646.

28. Shigesato M, Hirasawa K, Takeda M, Doi K (1994) Encephalomyocarditis (EMC) virus-induced testicular lesion in BALB/c mice. *Lab Anim* 28(4): 330–334.

29. Anirban B, Kallol D (2017) Recent advances in Japanese encephalitis. *F1000Research* 6(259): 1–9.

30. World Health Organization (2015). Japanese encephalitis. available from https://www.who.int/immunization/diseases/japanese_encephalitis/en/.

31. Campbell G.L, Hills S.L, Fischer M, Jacobson J.A, Hoke C.H, Hombach J.M, Marfin A.A, Solomon T, Tsai T.F, Tsu V.D (2011) Estimated global incidence of Japanese encephalitis: a systematic review. *Bull World Health Organ* 89: 766–774.

32. Pritchard L.I, Chua K.B, Cummins D, Hyatt A, Crameri G, Eaton B.T, Wang L.F (2006) Pulau virus; a new member of the Nelson Bay orthoreovirus species isolated from fruit bats in Malaysia. *Arch Virol* 151(2): 229–239.

33. Gard G, Compans R.W (1970) Structure and cytopathic effects of Nelson Bay virus. *J Virol* 6(1): 100–106.

34. Hu T, Qiu W, He B, Zhang Y, Yu J, Liang X, Zhang W, Chen G, Zhang Y, Wang Y (2014) Characterization of a novel orthoreovirus isolated from fruit bat, China. *BMC Microbiol* 14(1): 293–301.

35. Chua K.B, Crameri G, Hyatt A, Yu M, Tompang M.R, Rosli J, McEachern J, Crameri S, Kumarasamy V, Eaton B.T (2007) A previously unknown reovirus of bat origin is associated with an acute respiratory disease in humans. *Proc Natl Acad Sci* 104(27): 11424–11429.

36. Voon K, Tan Y.F, Leong P.P, Teng C.L, Gunnasekaran R, Ujang K, Chua K.B, Wang L.F (2015) Pteropine orthoreovirus infection among out-patients with acute upper respiratory tract infection in Malaysia. *J Med Virol* 87(12): 2149–2153.

37. Singh H, Shimojima M, Ngoc T.C, Quoc Huy N.V, Chuong T.X, Le Van A, Saijo M, Yang M, Sugamata M (2015) Serological evidence of human infection with Pteropine orthoreovirus in Central Vietnam. *J Med Virol* 87(12): 2145–2148.

38. Uehara A, Tan C.W, Mani S, Chua K.B, Leo Y.S, Anderson D.E, Wang L.F (2019) Serological evidence of human infection by bat orthoreovirus in Singapore. *J Med Virol* 91(4): 707–710.

39. Yamanaka A, Iwakiri A, Yoshikawa T, Sakai K, Singh H, Himeji D, Kikuchi I, Ueda A, Yamamoto S, Miura M (2014) Imported case of acute respiratory tract infection

associated with a member of species nelson bay orthoreovirus. *PloS One* 9(3): e92777.

40. Cheng P, Lau C, Lai A, Ho E, Leung P, Chan F, Wong A, Lim W (2009) A novel reovirus isolated from a patient with acute respiratory disease. *J Clin Virol* 45(1): 79–80.

41. Kawagishi T, Kanai Y, Tani H, Shimojima M, Saijo M, Matsuura Y, Kobayashi T (2016) Reverse genetics for fusogenic bat-borne orthoreovirus associated with acute respiratory tract infections in humans: Role of outer capsid protein σC in viral replication and pathogenesis. *PLoS Pathog* 12(2): e1005455.

42. Pamela C, Kanchwala M, Liang H, Kumar A, Wang L.F, Xing C, Schoggins J.W (2018) The IFN response in bats displays distinctive IFN-stimulated gene expression kinetics with atypical RNASEL induction. *J Immunol* 200(1): 209–217.

43. Schountz T, Baker M.L, Butler J, Munster V (2017) Immunological control of viral infections in bats and the emergence of viruses highly pathogenic to humans. *Front Immunol* 8: 1098–1107.

44. Hölzer M, Schoen A, Wulle J, Müller M.A, Drosten C, Marz M, Weber F (2019) Virus-and interferon alpha-induced transcriptomes of cells from the microbat. *iScience* 19:647–661.

45. Kuzmin I.V, Schwarz T.M, Ilinykh P.A, Jordan I, Ksiazek T.G, Sachidanandam R, Basler C.F, Bukreyev A (2017) Innate immune responses of bat and human cells to filoviruses: commonalities and distinctions. *J Virol* 91(8): e02471–e02516.

46. Ahn M, Anderson D.E, Zhang Q, Tan C.W, Lim B.L, Luko K, Wen M, Chia W.N, Mani S, Wang L.C (2019) Dampened NLRP3-mediated inflammation in bats and implications for a special viral reservoir host. *Nat Microbiol* 4(5): 789–799.

47. Banerjee A, Rapin N, Bollinger T, Misra V (2017) Lack of inflammatory gene expression in bats: a unique role for a transcription repressor. *Sci Rep* 7(1): 1–15.

48. Ghosh D, Basu A (2009) Japanese encephalitis: a pathological and clinical perspective. *PLoS Negl Trop Dis* 3(9): e437.

49. Meylan E, Tschopp J (2006) Toll-like receptors and RNA helicases: two parallel ways to trigger antiviral responses. *Mol Cell* 22(5): 561–569.

50. Gitlin L, Barchet W, Gilfillan S, Cella M, Beutler B, Flavell R.A, Diamond M.S, Colonna M. 2006. Essential role of MDA-5 in type I IFN responses to polyriboinosinic: polyribocytidylic acid and encephalomyocarditis picornavirus. *Proc. Natl. Acad. Sci.* 103(22): 8459–8464.

51. Hardarson H.S, Baker J.S, Yang Z, Purevjav E, Huang C.H, Alexopoulou L, Li N, Flavell R.A, Bowles N.E, Vallejo J.G (2007) Toll-like receptor 3 is an essential component of the innate stress response in virus-induced cardiac injury. *Am J Physiol-Heart Circ Physiol* 292(1): H251–H258.

52. Jiang R, Ye J, Zhu B, Song Y, Chen H, Cao S (2014) Roles of TLR3 and RIG-I in mediating the inflammatory response in mouse microglia following Japanese encephalitis virus infection. *J Immunol Res* 2014:1–11.

53. Kato H, Takeuchi O, Sato S, Yoneyama M, Yamamoto M, Matsui K, Uematsu S, Jung A, Kawai T, Ishii K.J (2006) Differential roles of MDA5 and RIG-I helicases in the recognition of RNA viruses. *Nature* 441(7089): 101–105.

54. Mok L, Wynne J.W, Grimley S, Shiell B, Green D, Monaghan P, Pallister J, Bacic A, Michalski W.P (2015) Mouse fibroblast L929 cells are less permissive to infection by Nelson Bay orthoreovirus compared to other mammalian cell lines. *J Gen Virol* 96(7): 1787–1794.

55. Nazmi A, Dutta K, Basu A (2011) RIG-I mediates innate immune response in mouse neurons following Japanese encephalitis virus infection. *PLoS One* 6(6): e21761.

56. Li L, Fan H, Song Z, Liu X, Bai J, Jiang P (2019) Encephalomyocarditis virus 2C protein antagonizes interferon-β signaling pathway through interaction with MDA5. *Antiviral Res* 161: 70–84.

57. Papon L, Oteiza A, Imaizumi T, Kato H, Brocchi E, Lawson T.G, Akira S, Mechti N (2009) The viral RNA recognition sensor RIG-I is degraded during encephalomyocarditis virus (EMCV) infection. *Virology* 393(2): 311–318.

58. Huang L, Xiong T, Yu H, Zhang Q, Zhang K, Li C, Hu L, Zhang Y, Zhang L, Liu Q (2017) Encephalomyocarditis virus 3C protease attenuates type I interferon production through disrupting the TANK–TBK1–IKKε–IRF3 complex. *Biochem J* 474(12): 2051–2065.

59. Zhou D, Jia F, Li Q, Zhang L, Chen Z, Zhao Z, Cui M, Song Y, Chen H, Cao S (2018) Japanese Encephalitis Virus NS1′ Protein Antagonizes Interferon Beta Production. *Virol Sin* 33(6): 515–523.

60. Zhang H.L, Ye H.Q, Liu S.Q, Deng C.L, Li X.D, Shi P.Y, Zhang B (2017) West Nile virus NS1 antagonizes interferon beta production by targeting RIG-I and MDA5. *J Virol* 91(18): e02396–e02416.

61. Sherry B (2009) Rotavirus and reovirus modulation of the interferon response. *J Interferon Cytokine Res* 29(9): 559–567

62. Banerjee A, Falzarano D, Rapin N, Lew J, Misra V (2019) Interferon regulatory factor 3-mediated signaling limits Middle-East respiratory syndrome (MERS) coronavirus propagation in cells from an insectivorous bat. *Viruses* 11(2): 152–173.

63. Virtue E.R, Marsh G.A, Baker M.L, Wang L.F (2011) Interferon production and signaling pathways are antagonized during henipavirus infection of fruit bat cell lines. *PloS One* 6(7): e22488.

64. Maeda K, Hondo E, Terakawa J, Kiso Y, Nakaichi N, Endoh D, Sakai K, Morikawa S, Mizutani T. 2008. Isolation of novel adenovirus from fruit bat (*Pteropus dasymallus yayeyamae*). *Emerg. Infect. Dis.* 14(2): 347-349.

65. Maruyama J, Miyamoto H, Kajihara M, Ogawa H, Maeda K, Sakoda Y, Yoshida R, Takada A (2014) Characterization of the envelope glycoprotein of a novel filovirus, lloviu virus. *J Virol* 88(1): 99–109.

66. Nerome R, Tajima S, Takasaki T, Yoshida T, Kotaki A, Lim C.K, Ito M, Sugiyama A, Yamauchi A, Yano T (2007) Molecular epidemiological analyses of Japanese encephalitis virus isolates from swine in Japan from 2002 to 2004. *J Gen Virol* 88(10): 2762–2768.

67. Subramanya S, Kim S.S, Abraham S, Yao J, Kumar M, Kumar P, Haridas V, Lee S.K, Shultz L.D, Greiner D (2010) Targeted delivery of small interfering RNA to human dendritic cells to suppress dengue virus infection and associated proinflammatory cytokine production. *J Virol* 84(5): 2490–2501.

68. Höbel S, Aigner A (2010) Polyethylenimine (PEI)/siRNA-mediated gene knockdown in vitro and in vivo. In: RNA Interf. Springer, pp 283–297.

69. Liu W.J, Wang X.J, Clark D.C, Lobigs M, Hall R.A, Khromykh A.A (2006) A single amino acid substitution in the West Nile virus nonstructural protein NS2A disables its ability to inhibit alpha/beta interferon induction and attenuates virus virulence in mice. *J Virol* 80(5): 2396–2404.

70. Hemann E.A, Gale J.M, Savan R (2017) Interferon lambda genetics and biology in regulation of viral control. *Front Immunol* 8: 1–12.

71. Adachi M, Amsterdam D, Brooks S.E, Volk B.W (1975) Ultrastructural alterations of tissue cultures from human fetal brain infected with the E variant of EMC virus. *Acta Neuropathol (Berl)* 32(2): 133–142.

72. Wellmann K.F, Amsterdam D, Volk B.W (1975) EMC virus and cultured human fetal pancreatic cells. Ultrastructural observations. *Arch Pathol* 99(8): 424–429.

73. Sandekian V, Lim D, Prud'homme P, Lemay G (2013) Transient high level mammalian reovirus replication in a bat epithelial cell line occurs without cytopathic effect. *Virus Res* 173(2): 327–335.

74. Lee G.C.Y, Grayston J.T, Kenny G.E (1965) Growth of Japanese encephalitis virus in cell culture. *J Infect Dis* 115(4): 321–329.

75. Lee C.J, Liao C.L, Lin Y.L (2005) Flavivirus activates phosphatidylinositol 3-kinase signaling to block caspase-dependent apoptotic cell death at the early stage of virus infection. *J Virol* 79(13): 8388–8399.

76. Okamoto T, Suzuki T, Kusakabe S, Tokunaga M, Hirano J, Miyata Y, Matsuura Y (2017) Regulation of apoptosis during flavivirus infection. *Viruses* 9(9) :243–255.

77. Omatsu T, Watanabe S, Akashi H, Yoshikawa Y (2007) Biological characters of bats in relation to natural reservoir of emerging viruses. *Comp Immunol Microbiol Infect Dis* 30(5-6): 357–374.

78. Cui J, Counor D, Shen D, Sun G, He H, Deubel V, Zhang S (2008) Detection of Japanese encephalitis virus antibodies in bats in Southern China. *Am J Trop Med Hyg* 78(6): 1007–1011.

79. Van den Hurk A.F, Smith C.S, Field H.E, Smith I.L, Northill J.A, Taylor C.T, Jansen C.C, Smith G.A, Mackenzie J.S (2009) Transmission of Japanese encephalitis virus from the black flying fox, *Pteropus alecto*, to *Culex annulirostris* mosquitoes, despite the absence of detectable viremia. *Am. J. Trop. Med. Hyg.* 81(3): 457–462.

80. Lorusso A, Teodori L, Leone A, Marcacci M, Mangone I, Orsini M, Capobianco-Dondona A, Monaco F, Savini G (2015) A new member of the Pteropine Orthoreovirus species isolated from fruit bats imported to Italy. *Infect Genet Evol* 30: 55–58.

81. Iha K, Omatsu T, Watanabe S, Ueda N, Taniguchi S, Fujii H, Ishii Y, Kyuwa S, Akashi H, Yoshikawa Y (2010) Molecular cloning and expression analysis of bat toll-like receptors 3, 7 and 9. *J Vet Med Sci* 72(2): 217–220.

82. Li J, Zhang G, Cheng D, Ren H, Qian M, Du B (2015) Molecular characterization of RIG-I, STAT-1 and IFN-beta in the horseshoe bat. *Gene* 561(1) :115–123.

83. Sarkis S, Lise M.C, Darcissac E, Dabo S, Falk M, Chaulet L, Neuveut C, Meurs E.F, Lavergne A, Lacoste V (2018) Development of molecular and cellular tools to decipher the type I IFN pathway of the common vampire bat. *Dev Comp Immunol* 81: 1–7.

84. Cowled C, Baker M.L, Zhou P, Tachedjian M, Wang L.F (2012) Molecular characterisation of RIG-I-like helicases in the black flying fox, *Pteropus alecto*. *Dev. Comp. Immunol.* 36(4): 657–664.

85. Cowled C, Baker M.L, Tachedjian M, Zhou P, Bulach D, and Wang L.F (2011) Molecular characterisation of Toll-like receptors in the black flying fox *Pteropus alecto*. *Dev. Comp. Immunol.* 35: 7–18.

86. Taniguchi T, Takaoka A (2001) A weak signal for strong responses: interferon-alpha/beta revisited. *Nat Rev Mol Cell Biol* 2(5): 378–386.

87. Ramakrishnan P, de Jesus T, Shukla S (2018) NF-kB c-Rel Dictates the Inflammatory Threshold by Acting as a Transcriptional Repressor. *Iscience* 23:1-18.

88. Farone A.L, O'Brien P.C, Cox D.C (1993) Tumor necrosis factor-α induction by reovirus serotype 3. *J Leukoc Biol* 53(2): 133–137.

89. Shwetank O.S, Kim K.S, Manjunath R (2013) Infection of human endothelial cells by Japanese encephalitis virus: increased expression and release of soluble HLA-E. *PLoS One* 8(11): e79197.

90. Schwarz E.M, Badorff C, Hiura T.S, Wessely R, Badorff A, Verma I.M, Knowlton K.U (1998) NF-κB-mediated inhibition of apoptosis is required for encephalomyocarditis virus virulence: a mechanism of resistance in p50 knockout mice. *J Virol* 72(7): 5654–5660.

91. Mok L, Wynne J.W, Tachedjian M, Shiell B, Ford K, Matthews D.A, Bacic A, Michalski W.P (2017) Proteomics informed by transcriptomics for characterising differential cellular susceptibility to Nelson Bay orthoreovirus infection. *BMC Genomics* 18(1): 1–17.

92. Lee A.K, Kulcsar K.A, Elliott O, Khiabanian H, Nagle E.R, Jones M.E, Amman B.R, Sanchez-Lockhart M, Towner J.S, Palacios G (2015) De novo transcriptome reconstruction and annotation of the Egyptian rousette bat. *BMC Genomics* 16(1): 1–11.

93. Papenfuss A.T, Baker M.L, Feng Z.P, Tachedjian M, Crameri G, Cowled C, Ng J, Janardhana V, Field H.E, Wang L.F (2012) The immune gene repertoire of an important viral reservoir, the Australian black flying fox. *BMC Genomics* 13(1): 1–17.

94. Shaw T.I, Srivastava A, Chou W.C, Liu L, Hawkinson A, Glenn T.C, Adams R, Schountz T (2012) Transcriptome sequencing and annotation for the Jamaican fruit bat (*Artibeus jamaicensis*). *PloS One* 7(11): e48472.

95. Banerjee A, Baker M.L, Kulcsar K, Misra V, Plowright R, Mossman K (2020) Novel insights into immune systems of bats. *Front Immunol* 11: 1–15.

96. Chua K.B, Koh C.L, Hooi P.S, Wee K.F, Khong J.H, Chua B.H, Chan Y.P, Lim M.E, Lam S.K (2002) Isolation of Nipah virus from Malaysian Island flying-foxes. *Microbes Infect* 4(2): 145–151.

97. Banyard A.C, Evans J.S, Luo T.R, Fooks A.R (2014) Lyssaviruses and bats: emergence and zoonotic threat. *Viruses* 6(8): 2974–2990.

98. Bean A.G, Baker M.L, Stewart C.R, Cowled C, Deffrasnes C, Wang L.F, Lowenthal J.W (2013) Studying immunity to zoonotic diseases in the natural host: keeping it real. *Nat Rev Immunol* 13(12): 851–861.

99. Ahn M, Cui J, Irving A.T, Wang L.F (2016) Unique loss of the PYHIN gene family in bats amongst mammals: implications for inflammasome sensing. *Sci Rep* 6(1): 1–7.

100. Xie J, Li Y, Shen X, Goh G, Zhu Y, Cui J, Wang L.F, Shi Z.L, Zhou P (2018) Dampened STING-dependent interferon activation in bats. *Cell Host Microbe* 23(3): 297–301.

101. Franz K.M, Neidermyer W.J, Tan Y.J, Whelan S.P, Kagan J.C (2018) STING-dependent translation inhibition restricts RNA virus replication. *Proc Natl Acad Sci* 115(9): E2058–E2067.

102. Kim M.J, Hwang S.Y, Imaizumi T, Yoo J.Y (2008) Negative feedback regulation of RIG-I-mediated antiviral signaling by interferon-induced ISG15 conjugation. *J Virol* 82(3): 1474–1483.

103. Takahashi T, Ui T.K (2020) Mutual Regulation of RNA Silencing and the IFN Response as an Antiviral Defense System in Mammalian Cells. *Int J Mol Sci* 21(4): 1348–1362.

104. Kepler T.B, Sample C, Hudak K, Roach J, Haines A, Walsh A, Ramsburg E.A (2010) Chiropteran types I and II interferon genes inferred from genome sequencing traces by a statistical gene-family assembler. *BMC Genomics* 11(1): 444–456.

105. Pavlovich S.S, Lovett S.P, Koroleva G, Guito J.C, Arnold C.E, Nagle E.R, Kulcsar K, Lee A, Thibaud-Nissen F, Hume A.J (2018) The Egyptian rousette genome reveals unexpected features of bat antiviral immunity. *Cell* 173(5): 1098–1110.

106. Wu Z, Yang L, Ren X, He G, Zhang J, Yang J, Qian Z, Dong J, Sun L, Zhu Y (2016) Deciphering the bat virome catalog to better understand the ecological diversity of bat viruses and the bat origin of emerging infectious diseases. *ISME J* 10(3): 609–620.

107. Plowright R.K, Peel A.J, Streicker D.G, Gilbert A.T, McCallum H, Wood J, Baker M.L, Restif O (2016) Transmission or within-host dynamics driving pulses of zoonotic viruses in reservoir–host populations. *PLoS Negl Trop Dis* 10(8): e0004796.

108. Subudhi S, Rapin N, Misra V (2019) Immune system modulation and viral persistence in bats: Understanding viral spillover. *Viruses* 11(2): 192–203.

109. Plowright R.K, Eby P, Hudson P.J, Smith I.L, Westcott D, Bryden W.L, Middleton D, Reid P.A, McFarlane R.A, Martin G (2015) Ecological dynamics of emerging bat virus spillover. *Proc R Soc B Biol Sci* 282(1798): 1–9.

110. Hengjan Y, Sae K.N, Phichitrasilp T, Ohmori Y, Fujinami H, Hondo E (2018) Seasonal variation in the number of deaths in Pteropus lylei at Wat Pho Bang Khla temple, Thailand. *J Vet Med Sci* 80(8): 1364–1367.

111. Plowright R.K, Field H.E, Smith C, Divljan A, Palmer C, Tabor G, Daszak P, Foley J.E (2008) Reproduction and nutritional stress are risk factors for Hendra virus infection in little red flying foxes (*Pteropus scapulatus*). *Proc R Soc B Biol Sci* 275(1636): 861–869.

112. Breed A.C, Breed M.F, Meers J, Field H.E (2011) Evidence of endemic Hendra virus infection in flying-foxes (*Pteropus conspicillatus*): implications for disease risk management. *PLoS One* 6(12): e28816.

113. Plowright R.K, Foley P, Field H.E, Dobson A.P, Foley J.E, Eby P, Daszak P (2011) Urban habituation, ecological connectivity and epidemic dampening: the

emergence of Hendra virus from flying foxes (*Pteropus* spp.). *Proc R Soc B Biol Sci* 278(1725): 3703–3712.

114. Rahman SA, Hassan L, Epstein J.H, Mamat Z.C, Yatim A.M, Hassan S.S, Field H.E, Hughes T, Westrum J, Naim M.S (2013) Risk factors for Nipah virus infection among pteropid bats, Peninsular Malaysia. *Emerg Infect Dis* 19(1): 51–60.

115. Pourrut X, Delicat A, Rollin P.E, Ksiazek T.G, Gonzalez J.P, Leroy E.M (2007) Spatial and temporal patterns of Zaire ebolavirus antibody prevalence in the possible reservoir bat species. *J Infect Dis* 196: S176–S183.

116. Sohayati A.R, Hassan L, Sharifah S.H, Lazarus K, Zaini C.M, Epstein J.H, Naim N.S, Field H.E, Arshad S.S, Aziz J.A (2011) Evidence for Nipah virus recrudescence and serological patterns of captive *Pteropus vampyrus. Epidemiol. Infect.* 139(10): 1570–1579.

117. Luis A.D, Hayman D.T, O'Shea T.J, Cryan P.M, Gilbert A.T, Pulliam J.R, Mills J.N, Timonin M.E, Willis C.K, Cunningham A.A (2013) A comparison of bats and rodents as reservoirs of zoonotic viruses: are bats special? *Proc R Soc B Biol Sci* 280(1756): 1-9.